AD-A230 310

NPS61-90-005PR

NAVAL POSTGRADUATE SCHOOL

Monterey, California

DTIC
ELECTE
JAN 03 1991
S
D
E

OPTICAL TURBULENCE AND RAWINSONDE MEASUREMENTS FOR 17-28 SEPTEMBER 1989 AT ANDERSON MESA/ UNITED STATES NAVAL OBSERVATORY, FLAGSTAFF, ARIZONA

by

G.Tirrell Vaucher, C.A. Vaucher,
and D.L. Walters

Approved for public release; distribution unlimited

Prepared for: Naval Research Laboratory
Washington, D.C. 20375

91 1 2 027

NAVAL POSTGRADUATE SCHOOL
Monterey, California

Rear Admiral R.W. West, Jr.
Superintendent

H. Shull
Provost

The work reported herein was supported in part by the Naval Research Laboratory Program at the Naval Postgraduate School with funds provided by the Naval Research Laboratory.

Reproduction of all or part of this report is authorized.

This report was prepared by:

Gail Tirrell Vaucher
GAIL TIRRELL VAUCHER
Physical Scientist

Christopher A. Vaucher
CHRISTOPHER A. VAUCHER
Visiting Scientist,
Universities Space
Research Association

Donald Walters
DONALD L. WALTERS
Associate Professor
of Physics

Approved by:

K. Woehler
KARLHEINZ E. WOEHLER
Chairman of Physics

Released by:

G. E. Schacher
GORDON E. SCHACHER
Dean of Faculty and
Graduate Studies

Unclassified
SECURITY CLASSIFICATION OF THIS PAGE

REPORT DOCUMENTATION PAGE

1a REPORT SECURITY CLASSIFICATION: Unclassified	1b RESTRICTIVE MARKINGS
2a SECURITY CLASSIFICATION AUTHORITY	3 DISTRIBUTION / AVAILABILITY OF REPORT: Approved for public release; distribution is unlimited.
2b DECLASSIFICATION / DOWNGRADING SCHEDULE	
4 PERFORMING ORGANIZATION REPORT NUMBER(S): NPS61-90-005PR	5 MONITORING ORGANIZATION REPORT NUMBER(S): NPS61-90-005PR
6a NAME OF PERFORMING ORGANIZATION: Naval Postgraduate School; 6b OFFICE SYMBOL (If applicable): PH	7a NAME OF MONITORING ORGANIZATION: Naval Research Laboratory
6c ADDRESS (City, State, and ZIP Code): Monterey, CA 93943-5000	7b ADDRESS (City, State, and ZIP Code): Washington, D.C. 20375
8a NAME OF FUNDING / SPONSORING ORGANIZATION: Naval Research Lab. (Attn. Dr. Ken Johnston); 8b OFFICE SYMBOL (If applicable): Code 4130	9 PROCUREMENT INSTRUMENT IDENTIFICATION NUMBER: N0017389WR90059
8c ADDRESS (City, State, and ZIP Code): Washington, D.C. 20375	10 SOURCE OF FUNDING NUMBERS: PROGRAM ELEMENT NO. / PROJECT NO. / TASK NO / WORK UNIT ACCESSION NO.

11 TITLE (Include Security Classification)
OPTICAL TURBULENCE AND RAWINSONDE MEASUREMENTS FOR 17-28 SEPTEMBER 1989 AT ANDERSON MESA/UNITED STATES NAVAL OBSERVATORY, FLAGSTAFF, ARIZONA (Unclassified)

12 PERSONAL AUTHOR(S)
Gail Tirrell Vaucher, Christopher A.Vaucher, Donald L. Walters

13a TYPE OF REPORT	13b TIME COVERED	14 DATE OF REPORT (Year, Month, Day)	15 PAGE COUNT
Technical Report	FROM _____ TO _____	1990 June 27	105

16 SUPPLEMENTARY NOTATION The views expressed in this technical report are those of the authors and do not reflect the official policy or position of the Dept of Defense or the US Government

17 COSATI CODES		
FIELD	GROUP	SUB-GROUP

18 SUBJECT TERMS (Continue on reverse if necessary and identify by block number)
atmospheric optical turbulence, transverse coherence length, isoplanatic angle, rawinsonde, (TAC)

19 ABSTRACT (Continue on reverse if necessary and identify by block number)
The Naval Postgraduate School Atmospheric Optics Group acquired atmospheric optical turbulence and navaid radiosonde (rawinsonde) data in the Flagstaff, Arizona region as part of a site survey for a large-scale, ground-based, synothetic aperture system (100-300 m baseline stellar interferometer). From 17 to 25 September 1989, measurements were taken from the Lowell Observatory 31-inch telescope dome facility on Anderson Mesa, 16 km southeast of Flagstaff. Further sampling occurred 26-28 September 1989 from the United States Naval Observatory's (USNO) 61-inch telescope dome, approximately 8 km west of Flagstaff. The parameters measured consisted of transverse coherence lengths, isoplanatic angles, and various meteorological surface and upper-air variables measured from a high resolution, instrumented balloon (rawinsonde) system. This report compiles, analyses and summarizes the acquired data. A summary of the synoptic scale activities occurring simultaneously over the data acquisition sites is also presented.

20 DISTRIBUTION / AVAILABILITY OF ABSTRACT	21 ABSTRACT SECURITY CLASSIFICATION
☒ UNCLASSIFIED/UNLIMITED ☐ SAME AS RPT ☐ DTIC USERS	Unclassified
22a NAME OF RESPONSIBLE INDIVIDUAL: Gail Tirrell Vaucher	22b TELEPHONE (Include Area Code): (408)-646-3207; 22c OFFICE SYMBOL: PH/We

DD FORM 1473, 84 MAR — 83 APR edition may be used until exhausted. All other editions are obsolete.

SECURITY CLASSIFICATION OF THIS PAGE

U.S. Government Printing Office: 1986—606-24

Unclassified

OPTICAL TURBULENCE AND RAWINSONDE MEASUREMENTS FOR 17-28 SEPTEMBER 1989 AT ANDERSON MESA/UNITED STATES NAVAL OBSERVATORY, FLAGSTAFF, ARIZONA

by

G.Tirrell Vaucher, C.A. Vaucher, and D.L. Walters

Atmospheric Optics Group
Department of Physics
Naval Postgraduate School
Monterey, California 93943-5000

FORWARD

The acquisition of data was performed by the Naval Postgraduate School Atmospheric Optics Group for the Naval Research Lab, Dr. Kenneth Johnston, project monitor.

ABSTRACT

The Naval Postgraduate School Atmospheric Optics Group acquired atmospheric optical turbulence and navaid radiosonde (rawinsonde) data in the Flagstaff, Arizona region as part of a site survey for a large-scale, ground-based, synthetic aperture system (100-300 m baseline stellar interferometer). From 17 to 25 September 1989, measurements were taken from the Lowell Observatory 31-inch telescope dome facility on Anderson Mesa, 16 km southeast of Flagstaff. Further sampling occurred 26-28 September 1989 from the United States Naval Observatory's (USNO) 61-inch telescope dome, approximately 8 km west of Flagstaff. The parameters measured consisted of transverse coherence lengths, isoplanatic angles, and various meteorological surface and upper-air variables measured from a high resolution, instrumented balloon (rawinsonde) system. This report compiles, analyses and summarizes the acquired data. A summary of the synoptic scale activities occurring simultaneously over the data acquisition sites is also presented.

Accession For
NTIS GRA&I
DTIC TAB
Unannounced
Justification
By
Distribution/
Availability Codes
Dist | Avail and/or Special
A-1

QUALITY INSPECTED 4

TABLE OF CONTENTS

I. INTRODUCTION 1

II. EXPERIMENT OVERVIEW 3

A. SITE TOPOGRAPHY 3
B. DATA ACQUISITION 3

III. INSTRUMENTATION AND MEASUREMENTS 6

A. OPTICAL DATA 6

1. Transverse Coherence Length Sensor 6
2. Isoplanatic Angle Sensor, Isoplanometer..... 6

B. METEOROLOGICAL DATA 7

1. Upper-Air System and Measurement Procedures. 7

a. Navaid-Radiosonde Ground Processor..... 7
b. Balloon Measurements 8

2. Surface Data Sampling 9
3. Synoptic Weather Information 10

IV. DATA ANALYSIS 12

A. OPTICAL DATA ANALYSIS 12

1. Transverse Coherence Length Data 12
2. Isoplanatic Angle Data 15

B. RAWINSONDE DATA ANALYSIS 18
C. GENERAL SYNOPTIC WEATHER REVIEW 21

1. Anderson Mesa, Arizona 21
2. USNO, Arizona 23

V. DATA SUMMARY 24

VI. RECOMMENDATIONS 28

APPENDIX A. OPTICAL VARIABLES DEFINED 29

A. Transverse Coherence Length 29
B. Isoplanatic Angle 30

APPENDIX B. DAILY SYNOPTIC WEATHER SUMMARY-ANDERSON MESA, AZ..... 31

APPENDIX C. DAILY SYNOPTIC WEATHER SUMMARY-USNO, AZ.... 34

APPENDIX D. RAW OPTICAL DATA (1989 SEPTEMBER 17-28) ... 36

APPENDIX E. TRANSVERSE COHERENCE LENGTH STATISTICS 46

APPENDIX F. ISOPLANATIC ANGLE STATISTICS 55

APPENDIX G. RAWINSONDE THERMODYNAMIC PROFILES (Entire Sounding) 65

APPENDIX H. RAWINSONDE THERMODYNAMIC PROFILES (First 3 km Only) 80

LIST OF REFERENCES 93

INITIAL DISTRIBUTION LIST 94

List of Tables

Table 1. MARK II MICROSONDE SENSOR ACCURACIES 8

Table 2. TRANSVERSE COHERENCE LENGTH STATISTICS 12

Table 3. ISOPLANATIC ANGLE STATISTICS 17

Table 4. THERMODYNAMIC INFORMATION-ANDERSON MESA/USNO.. 22

Table 5. SUMMARY OF OPTICAL/METEOROLOGICAL DATA - ANDERSON MESA (1989 Sept 17-25)/ USNO (1989 Sept 26-28) 25

Table 6. BALLOON LAUNCH SCHEDULE - ANDERSON MESA/USNO . 66

Table 7. LAUNCH SPECIFICATIONS - ANDERSON MESA/USNO ... 67

List of Figures

Fig 1. Topographical Views of the Anderson Mesa, Az Region 4
Fig 2. Topographical Views of the USNO-Flagstaff, Az Region 5
Fig 3. Average Transverse Coherence Lengths (89 Sept 20-28) 13
Fig 4. Normalized Transverse Coherency Length Frequency Distribution 14
Fig 5. Cumulative Normalized r_o Frequency Distribution 16
Fig 6. Average Isoplanatic Angle (89 Sept 17-28) 17
Fig 7. Normalized Isoplanatic Angle Frequency Distribution 19
Fig 8. Cumulative Normalized θ_o Frequency Distribution 20
Fig 9. Rawinsonde Freezing Levels and Pressure Surface Heights 27
Fig 10. Anderson Mesa, Az Optical Data: 1989 Sept 17 .. 37
Fig 11. Anderson Mesa, Az Optical Data: 1989 Sept 20 .. 38
Fig 12. Anderson Mesa, Az Optical Data: 1989 Sept 21 .. 39
Fig 13. Anderson Mesa, Az Optical Data: 1989 Sept 22 .. 40
Fig 14. Anderson Mesa, Az Optical Data: 1989 Sept 23 .. 41
Fig 15. Anderson Mesa, Az Optical Data: 1989 Sept 25 .. 42
Fig 16. USNO, Az Optical Data: 1989 Sept 26 43
Fig 17. USNO, Az Optical Data: 1989 Sept 27 44
Fig 18. USNO, Az Optical Data: 1989 Sept 28 45
Fig 19. Anderson Mesa, Az r_o Statistics: 1989 Sept 20 . 47
Fig 20. Anderson Mesa, Az r_o Statistics: 1989 Sept 21 . 48
Fig 21. Anderson Mesa, Az r_o Statistics: 1989 Sept 22 . 49
Fig 22. Anderson Mesa, Az r_o Statistics: 1989 Sept 23 . 50
Fig 23. Anderson Mesa, Az r_o Statistics: 1989 Sept 25 . 51
Fig 24. USNO, Az r_o Statistics: 1989 Sept 26 52
Fig 25. USNO, Az r_o Statistics: 1989 Sept 27 53
Fig 26. USNO, Az r_o Statistics: 1989 Sept 28 54
Fig 27. Anderson Mesa, Az θ_o Statistics: 1989 Sept 17 . 56
Fig 28. Anderson Mesa, Az θ_o Statistics: 1989 Sept 20 . 57
Fig 29. Anderson Mesa, Az θ_o Statistics: 1989 Sept 21 . 58
Fig 30. Anderson Mesa, Az θ_o Statistics: 1989 Sept 22 . 59
Fig 31. Anderson Mesa, Az θ_o Statistics: 1989 Sept 23 . 60
Fig 32. Anderson Mesa, Az θ_o Statistics: 1989 Sept 25 . 61
Fig 33. USNO, Az θ_o Statistics: 1989 Sept 26 62
Fig 34. USNO, Az θ_o Statistics: 1989 Sept 27 63
Fig 35. USNO, Az θ_o Statistics: 1989 Sept 28 64
Fig 36. Entire Rawinsonde Profile: 89 Sept 19, 2100 MST 68
Fig 37. Entire Rawinsonde Profile: 89 Sept 20, 2033 MST 69
Fig 38. Entire Rawinsonde Profile: 89 Sept 21, 0355 MST 70
Fig 39. Entire Rawinsonde Profile: 89 Sept 21, 1957 MST 71

Fig 40. Entire Rawinsonde Profile: 89 Sept 22, 0348 MST 72
Fig 41. Entire Rawinsonde Profile: 89 Sept 22, 2004 MST 73
Fig 42. Entire Rawinsonde Profile: 89 Sept 23, 0340 MST 74
Fig 43. Entire Rawinsonde Profile: 89 Sept 25, 0341 MST 75
Fig 44. Entire Rawinsonde Profile: 89 Sept 25, 2220 MST 76
Fig 45. Entire Rawinsonde Profile: 89 Sept 26, 2029 MST 77
Fig 46. Entire Rawinsonde Profile: 89 Sept 27, 0246 MST 78
Fig 47. Entire Rawinsonde Profile: 89 Sept 27, 2006 MST 79
Fig 48. Rawinsonde Profile First 3-km: 89 Sept 19, 2100 MST 81
Fig 49. Rawinsonde Profile First 3-km: 89 Sept 20, 2033 MST 82
Fig 50. Rawinsonde Profile First 3-km: 89 Sept 21, 0355 MST 83
Fig 51. Rawinsonde Profile First 3-km: 89 Sept 21, 1957 MST 84
Fig 52. Rawinsonde Profile First 3-km: 89 Sept 22, 0348 MST 85
Fig 53. Rawinsonde Profile First 3-km: 89 Sept 22, 2004 MST 86
Fig 54. Rawinsonde Profile First 3-km: 89 Sept 23, 0340 MST 87
Fig 55. Rawinsonde Profile First 3-km: 89 Sept 25, 0341 MST 88
Fig 56. Rawinsonde Profile First 3-km: 89 Sept 25, 2220 MST 89
Fig 57. Rawinsonde Profile First 3-km: 89 Sept 26, 2029 MST 90
Fig 58. Rawinsonde Profile First 3-km: 89 Sept 27, 0246 MST 91
Fig 59. Rawinsonde Profile First 3-km: 89 Sept 27, 2006 MST 92

ACKNOWLEDGEMENTS

We would like to express our sincere appreciation to the Lowell Observatory, particularly Drs. Nat White and Bob Millis (Director), for their assistance in the data acquisition and use of their 31" telescope dome facility on Anderson Mesa. Also, a thank you to the Flagstaff Naval Observatory Director, Dr. Harold Ables, for the support personnel that assisted during the 26-28 September measurement sessions. And finally, a special thanks to Nancy Alexander from Technical and Business Systems, for her outstanding skills and dedication in the areas of field measurements and business management.

I. INTRODUCTION

The atmospheric optical turbulence and navaid radiosonde (rawinsonde) data acquired by the Naval Postgraduate School (NPS) Atmospheric Optics Group in the Flagstaff, Arizona region are part of a site survey for a Naval Research Laboratory (NRL) large-scale, ground-based, synthetic aperture system (100-300 m baseline stellar interferometer). Between 17 and 25 September 1989, measurements were taken from the Lowell Observatory's 31-inch telescope dome on Anderson Mesa, 16 km southeast of Flagstaff. Further sampling occurred 26-28 September 1989 from the United States Naval Observatory's (USNO) 61-inch telescope dome, 8 km west of Flagstaff. The data acquired during the Naval Observatory measurement session were taken in the hopes of deriving an algorithm linking the USNO stellar full-width half-maximum and NPS transverse coherence length measurements. Because the Naval Observatory is located within 30 km of Anderson Mesa, the optical and meteorological analyses for USNO are also included in this report.

The purpose of this report is to document the September 1989 measurements and provide a summary of the findings. Supplementing the report text are eight appendices. The first, Appendix A, provides a brief description of the two optical turbulence parameters measured (transverse coherence length, r_o and isoplanatic angle, θ_o). Appendices B and C are summaries of the general synoptic weather conditions coincident with the data acquisition over and around the sites, Anderson Mesa and USNO, respectively.

Appendix D displays all the processed optical data sampled between 17-28 September 1989. Each figure shows the individual points per night.

Appendix E presents the transverse coherence length unnormalized percent frequency distribution (bin interval 10 mm) and empirical seeing quality histogram for each observing night. The bin intervals selected for the latter qualitative interpretation are a product of approximately 50 site surveys spanning 18-40 degrees of latitude and 65-156 degrees of longitude. Specific empirical seeing quality intervals are listed in Appendix E.

Appendix F displays the isoplanatic angle un-normalized percent frequency distribution (bin interval 1 urad) and empirical seeing quality plots for each sampling session. Also included is a list of the specific empirically-derived seeing quality bin intervals.

Rawinsonde launches were made - usually twice a night - at the two northern Arizona sites. These soundings assist in identifying atmospheric layers responsible for producing the integrated optical turbulence viewed by the telescope-mounted sensors. Appendix G catalogs balloon launch schedules and specifications for both locations. Appendices G (Entire Sounding) and H (First 3 km Only) present the thermodynamic information in the form of vertical atmospheric profiles. The total number of plots per balloon launch is four:

1. Temperature/Dewpoint - entire sounding,
2. Relative Humidity - entire sounding,
3. Temperature/Dewpoint - first 3 km above site, and
4. Relative Humidity - first 3 km above site.

In both Appendices, the complete series of Anderson Mesa profiles precede the USNO plots. Although collected, no navaid-wind results appear in this report. The protracted effort required to recondition the poor signal-to-noise ratio data exceeds practical time limits for this project.

II. EXPERIMENT OVERVIEW

A. SITE TOPOGRAPHY

The initial site, Anderson Mesa, is an 125 m high plateau situated in the ponderosa pine and lake mesa-country 16 km southeast of Flagstaff and 18 km west of the high desert floor. The 31-inch telescope dome used for optical data gathering (rawinsonde launches were made just outside the dome) is 2.2 km above sea level and located on the southwest edge of the mesa. Figure 1 displays a 3-dimensional topographical view of Anderson Mesa, showing the location of the 31-inch site, as well as major features of interest.

The second site, USNO, from which the 26-28 September series of observations were made, is 8 km west of Flagstaff. The site is on a small, rounded hill, 80 m above the forested plain. The building structure is 2.3 km above sea level. Optical measurements were taken along side of the 61-inch telescope mounted on the third story of the observatory. The rawinsonde launches were made from local ground level. Figure 2 presents a 3-dimensional view of the terrain around the USNO site, along with major features of interest.

B. DATA ACQUISITION

All data acquisition sessions commenced at local sunset and terminated with the onset of local sunrise twilight. Total data collection time was approximately 10-11 hours per night. Intermittent cloud-cover often disrupted the ability to sample data, providing both gaps in the optical record on individual nights as well as over some entire nights. Due to logistical hurtles, the cessation of the last USNO session was at local midnight.

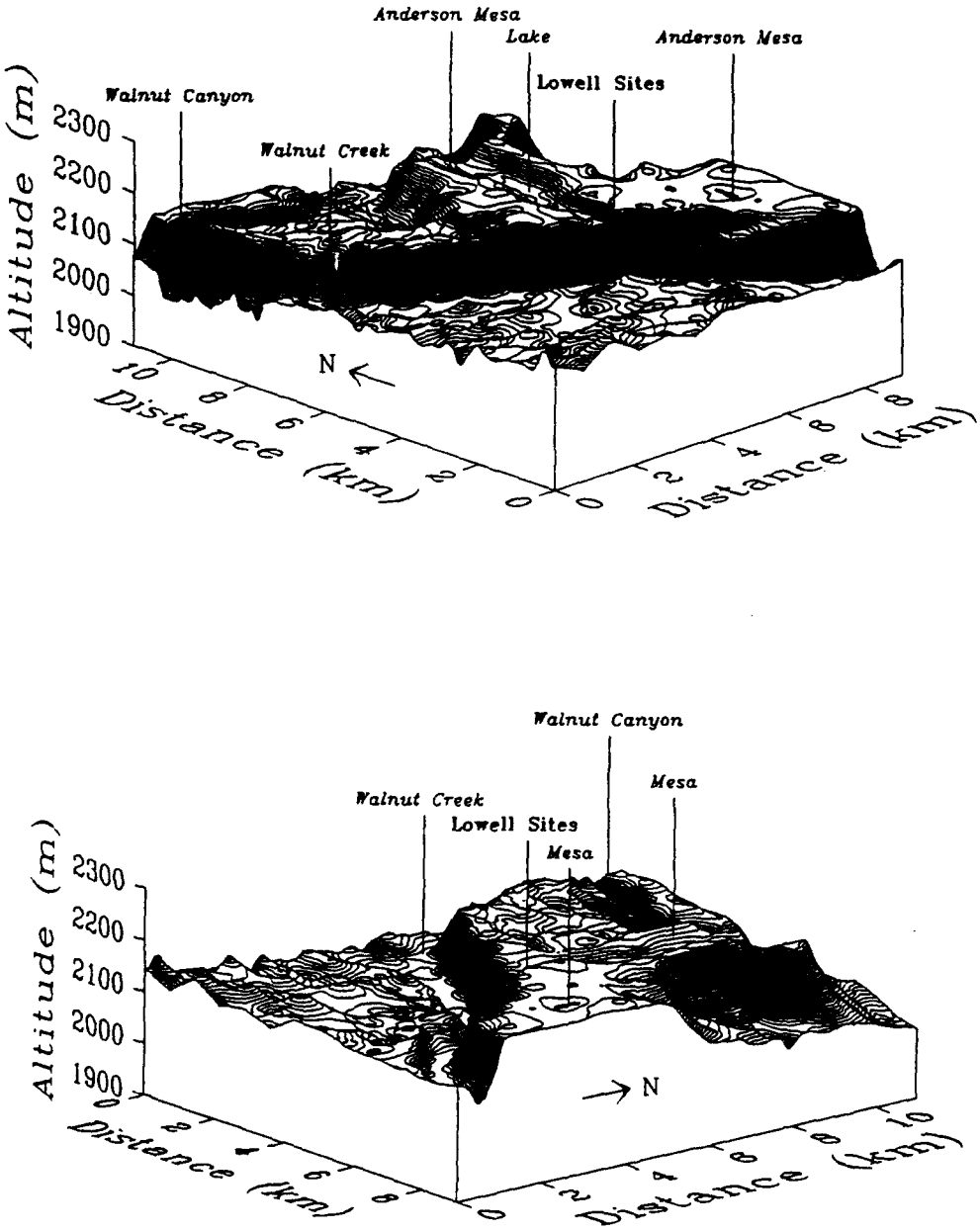

Fig 1. Topographical Views of the Anderson Mesa, Az Region

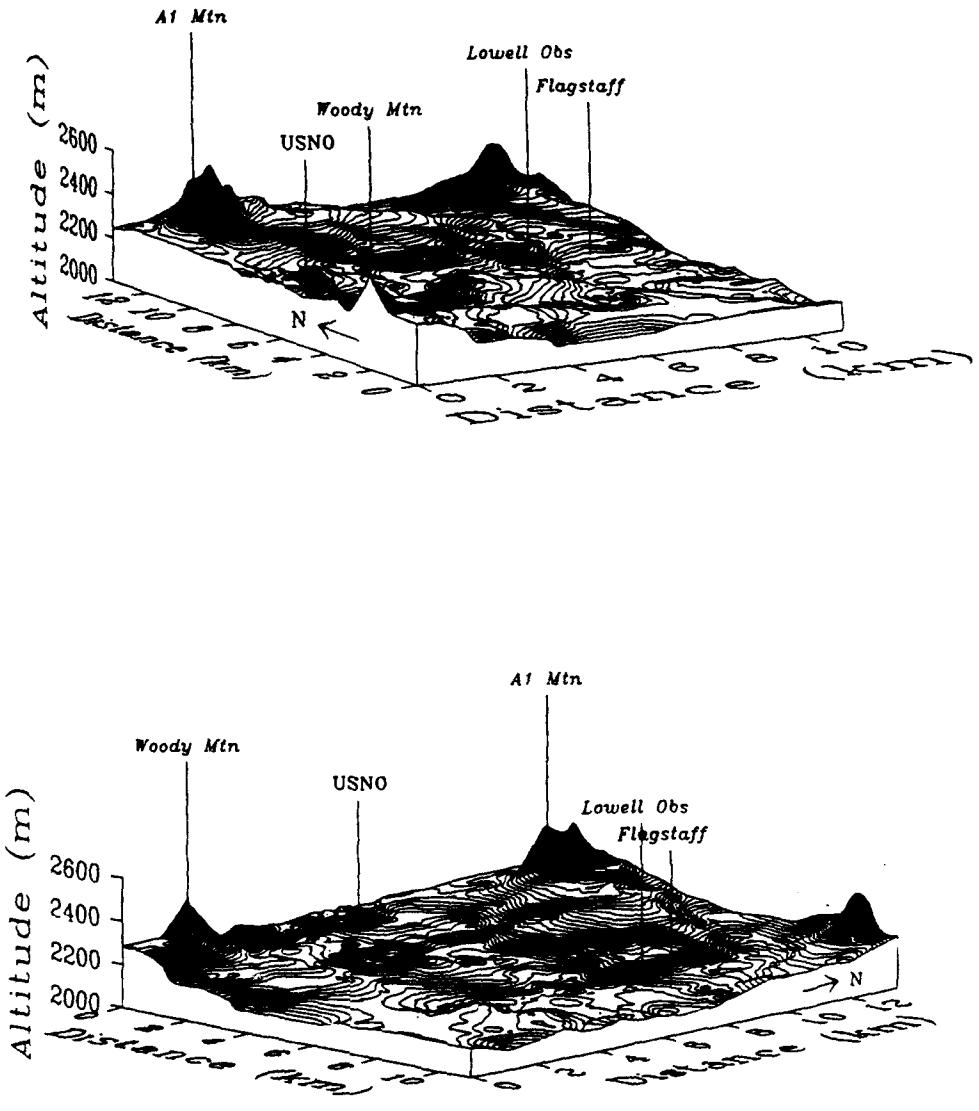

Fig 2. Topographical Views of the USNO-Flagstaff, Az Region

III. INSTRUMENTATION AND MEASUREMENTS

A. OPTICAL DATA

The optical turbulence parameters gathered throughout the experiment include the transverse coherence length and the isoplanatic angle. Appendix A provides a brief description of these parameters.

An isoplanometer and transverse coherence length sensor, designed and built by Dr. D.L. Walters, measured the optical data. Stevens (1985) and Walters, Favier, and Hines (1979) describe specific details for each instrument, respectively.

All optical data is referenced in Universal Time Coordinated (UTC). The conversion from local Mountain Standard Time (MST) to UTC is:

$$\text{Time(UTC)} = \text{Time(MST)} + 7 \text{ hours.}$$

1. Transverse Coherence Length Sensor

The transverse coherence length sensor was mounted on the tailplate of a portable 14-inch (356 mm) Celestron telescope. A researcher interacted with software designed for real-time data collection. This additional interface served to suppress instrumental artifacts. The average sampling rate was between 1-2 minutes per sample. An HP 300 series computer stored the processed data on its hard disc. All data files were later transferred serially to an IBM-class personal computer for statistical evaluation.

2. Isoplanatic Angle Sensor, Isoplanometer

An isoplanometer mounted onto the tailplate of a portable, apodized, 8-inch (203 mm) Celestron telescope measured the isoplanatic angles. An HP 217 computer ran the isoplanometer software. Automated sampling at a rate of 1 per second complimented a real-time, graphics display of Time(UTC) verses Raw Isoplanatic Angle(urad). Samples were converted into 10-second averages before being stored. Providing the polar alignment was good and the chosen star's zenith angle did not exceed 40 degrees, the isoplanatic angle system operated independent of human interaction for 1-2 hours. Post-experiment processing for this report consisted of transferring the data files

serially to an IBM-class personal computer, calculating the zenith angle correction, and submitting the data to a basic statistical analysis.

B. METEOROLOGICAL DATA

1. Upper-Air System and Measurement Procedures

Rawinsonde launches at both sites helped to identify layers in the earth's atmosphere which produced the integrated optical turbulence viewed simultaneously by our telescope mounted sensors. Although the rawinsonde system measured both the atmospheric thermodynamic and horizontal wind variables at discrete elevations in each sounding, this report presents only the thermodynamic results. Problems with the Loran-C signal acquisition and processing have made further filtering and conditioning mandatory before any wind information can be properly extracted.

a. Navaid-Radiosonde Ground Processor

The navaid-radiosonde (rawinsonde) upper-air system package is a portable, light-weight, solid-state, automatic instrument capable of real-time collection and final processing of various meteorological variables. The variables include: pressure, temperature, relative humidity, dewpoint, wind speed, and wind direction. The total system, constructed by VIZ and named "ZEEMET", has two major components: a W-9000 P90 BUS (receiving station) and a data gathering, real-time processing, Dell-300, 16-MHz, 80386 microcomputer (ground processor).

The instrumented balloon package - also made by VIZ and termed Mark II Microsonde - is activated and powered by two 9-volt lithium batteries. The Mark II microsonde provided three channels allowing measurement of pressure, temperature, and humidity. The three thermodynamic sensors mounted on each sonde include: a fast-response rod thermister coated with a white, water-repellent material to measure temperature; a fast-response carbon-gel element mounted on a glass-plate to measure humidity; and, a high-accuracy aneroid barometer-capacitor to measure the pressure. Table 1 lists the Mark II RMS sensor accuracy specifications, as provided by VIZ (Bell, 1989).

TABLE 1. MARK II MICROSONDE SENSOR ACCURACIES

SENSOR TYPE	ACCURACY (RMS)	RANGE OF VALIDITY
Pressure (capacitor/resistor)	< 2 mb	1080-5 mb (temperature compensated from +40C to -70C)
Temperature (rod thermistor)	< 0.4C	+50C to -90C
Humidity (carbon coated glass)	< 4% RH	+5% to 100% RH (temperature compensated from +40C to -60C)

VIZ pre-calibrates all Microsonde sensors at the factory. The rawinsonde ground processor uses these calibration values for all real-time data reduction. Navigational timing signals, transmitted by the Loran-C West Coast (USA) chain, provide the calculation base for obtaining the horizontal winds. The microsonde receives the Loran times and superimposes these signals on top of the digital thermodynamic data signal. All sensor information is then transmitted to the ground system as a 400-406 MHz signal for nearly real-time processing and reduction. During a launch, the researcher has the option to review either the processed thermodynamic or wind profiles as a function of time or height. A set of binary files on the microcomputer's hard disc store all sounding data. A binary to ASCII conversion utility permits post-launch review and analysis of selected files.

The ZEEMET ground system is capable of logging and processing up to two hours of data, allowing the microsonde to reach altitudes of up to 25 km. Should the balloon burst prior to this time, data collecting will continue uninterrupted.

b. Balloon Measurements

A total of 12 Navaid (Loran-based) balloon launches were successfully completed at both Anderson Mesa (19-25 September 1989) and USNO (26-28 September 1989). The

datasets generated by the ascending instrumented packages created vertical atmospheric profiles of thermodynamic and wind variables at selected height levels above each site. Table 6 (Appendix G) includes a complete listing of all the individual dates and times of balloon launches.

Table 7 (Appendix G), which summarizes the atmospheric balloon soundings, includes the launch time, duration, maximum vertical height obtained, and vertical resolution (sample rate) of every balloon flight. Here, the vertical resolution is an average estimated from differencing each height level, summing the differences, then dividing by their total number. All heights referenced in any of the tables are with respect to mean sea level (MSL). The following site elevations will allow the conversion to local ground level (relative height):

ANDERSON MESA(31" telescope dome): 7210 feet or 2198 meters,
USNO(61" telescope dome): 7560 feet or 2304 meters.

To facilitate quick inspection, Appendices G and H plot all sounding profiles with respect to local ground level.

As can be seen from Table 7 (Appendix G), the average height resolution varied between 2-5 meters (typically 4 m), with soundings reaching a maximum altitude of 14-21 km above their launch points, into the Arizona stratosphere in most cases. (Sounding ANM92504 is an exception. The ascent rate was purposefully kept slow, allowing a much higher vertical resolution in that profile.)

It should be emphasized that all rawinsonde information and plots are referenced in Mountain Standard Time (MST). This allows review between the sounding information and known diurnal atmospheric effects. There is a seven hour additive correction to go from MST to UTC (Arizona retains MST throughout the year).

2. Surface Data Sampling

Prior to a launch, surface data probes measured the temperature, humidity, and pressure to calibrate the rawinsonde ground processor's thermodynamic arrays. These intermittently monitored the multiple weather changes and potentially hazardous (extreme cold) environments during data collection.

The surface data probes include a Vaisala Digital Barometer Model PA 11 and a WeatherMeasure WEATHERtronics Humidity/Temperature Indicator Model 5165-A. The digital barometer has three independent aneroid capsules, each with a vacuum sealed capacitive element. A microprocessor controls the three transducer units (pressure-frequency converters). Continuous measurements of the capsule temperature compensates for temperature drift of the aneroid capsules and electronics.

The Model 5165-A Humidity/Temperature Indicator uses two 9-volt, nickel cadmium batteries for power. The humidity sensor is a thin film capacitor with a one second response time. The published measuring range is 0-100 % Relative Humidity. The temperature sensor has a two element, composite thermistor with an accuracy of +/- 0.15 Celsius. The measuring range is -5 to 45 degrees Celsius. (WeatherMeasure, 1987)

3. Synoptic Weather Information

GOES-WEST Satellite Images (Visible) as well as surface, 500 mb, and 200 mb National Weather Service charts provided on-site evaluation of synoptic weather conditions. These also detected trends and potential sources of optical turbulence.

National Weather Service charts summarized the synoptic scale activity over and around the Arizona sites between 17-28 September 1989. The six standard pressure levels referenced included:

Pressure (mb)	Equivalent Height Above Sea Level (km)
Surface	0.1
850	1.4
700	3.0
500	5.5
300	9.2
200	12.0

It should be noted that the equivalent heights indicated above represent averaged values. Actual height will vary, for any given pressure level, as Low and High pressure systems traverse the site.

Appendices B (Anderson Mesa) and C (USNO) furnish a more detailed review and summary of the National Weather Service synoptic charts for each session.

IV. DATA ANALYSIS

A. OPTICAL DATA ANALYSIS

1. Transverse Coherence Length Data

Transverse coherence length data acquired at both Anderson Mesa (20-25 September) and USNO (26-28 September) display dynamic atmospheric conditions. Table 2 synoptizes the individual transverse coherence length measurements into nightly averages, standard deviations, and standard deviations of the means. Assuming similar optical conditions at both sites, Figure 3 presents all the average values from Table 2, along with their one standard deviation envelopes (dashed lines). The increase of average r_o between 20-25 September indicates a transition from an optically turbulent atmosphere to a more optically stable environment. Though the last three sessions (USNO) have average r_o values less than the peak of 196 mm (25 September-Anderson Mesa), their magnitudes indicate that the atmospheric conditions were still less turbulent (greater magnitude) than the initial four sessions. The normalized percent frequency distribution plots (Figure 4) confirm the 20 to 28 September trends just described. The bin interval selected was 10 mm. This is the same bin-size used as in the un-normalized percent frequency distributions - Appendix E.

TABLE 2. TRANSVERSE COHERENCE LENGTH STATISTICS

Date (UTC)	Number of Data Points	Average r_o (mm)	Standard Deviation (mm)	Standard Deviation of Mean (mm)
20 Sept	150	41.8	7.0	0.6
21 Sept	366	68.9	19.1	1.0
22 Sept	373	76.4	30.2	1.6
23 Sept	452	91.2	24.4	1.1
25 Sept	328	196.4	75.9	4.2
26 Sept	276	157.0	63.4	3.8
27 Sept	542	99.9	27.2	1.2
28 Sept	286	140.0	40.5	2.4

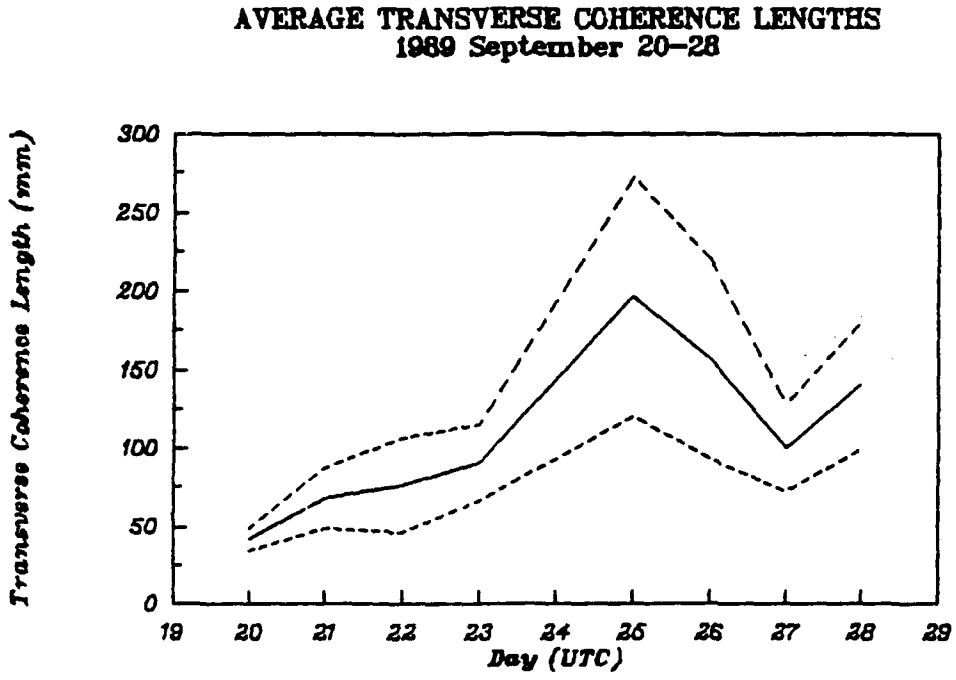

Fig 3. **Average Transverse Coherence Lengths (89 Sept 20-28)** Solid line is data average; Dashed line is standard deviation of the data.

NORMALIZED FREQUENCY DISTRIBUTION
Anderson Mesa, Az – 1989 September 20–25

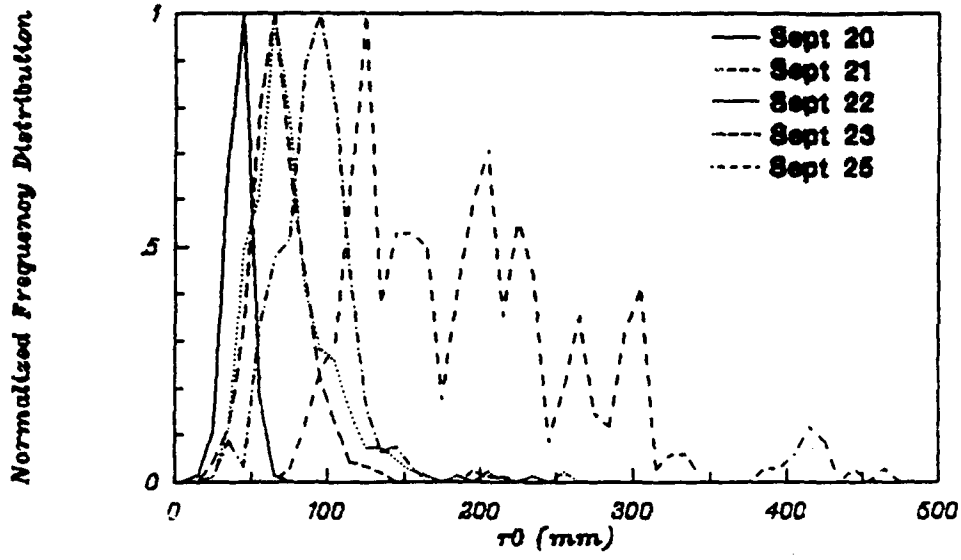

USNO, Flagstaff, Az – 1989 September 26–28

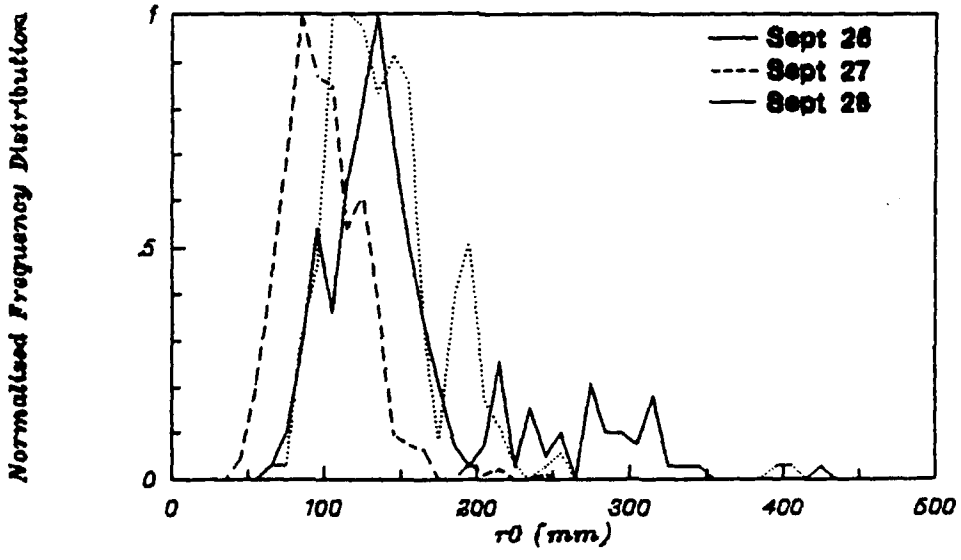

Fig 4. Normalized Transverse Coherence Length Frequency Distribution for: (a)Anderson Mesa, Az (89 Sept 20-25); (b) Naval Observatory, Az (89 Sept 26-28).

An inspection of the un-normalized frequency distribution (Appendix E) shows that fifty percent of the 20 September sampling session is around 50 mm. The corresponding empirical seeing quality histogram for this session (Appendix E) rates 90% of the samples taken as Poor. All subsequent nights display un-normalized peak frequencies which contain less than 28% of the sampling set. The lack of a dominant peak frequency implies a broad range of optical conditions in each sampling night.

The USNO normalized frequency distribution (Figure 4) displays a drop in the peak frequency from approximately 130 mm (26 September) to about 80 mm before increasing to 100-110 mm. Qualitatively, the Good to Excellent conditions of 26 September decay into Mediocre/Good on 27 September. The 28 September session, however, displays predominantly Good conditions (84% Frequency: See Appendix E).

Figure 5 presents a normalized frequency distribution based on the accumulation of all the Anderson Mesa and USNO transverse coherence length samples. As before, the bin-size is 10 mm. Despite the various dynamic atmospheric conditions, the experiment's mode is approximately 100 mm. A minor (second order) peak is present at 200 mm.

2. Isoplanatic Angle Data

Isoplanatic angle measurements are especially sensitive to turbulence aloft, particularly at the tropopause level (12-20 km). From 20 to 28 September 1989, the percent frequency modes are typically less than 25% of the dataset (Appendix F). Since the lack of a dominant frequency is also a characteristic of the r_o datasets (see above), this implies that broad turbulent contributions occurred throughout the entire atmosphere.

Table 3 condenses the individual isoplanatic angle measurements into nightly averages, standard deviations, and standard deviations of the means. Assuming similar optical conditions at both sites, Figure 6 displays all the average values from Table 3, along with their one standard deviation envelopes (dashed lines). The increasing trend between 17 and 22 September is consistent with the gradually increasing transverse coherence length trend over the same time period. This implies that turbulence in the upper atmosphere dominates the data. Between 17 and 23 September, the majority of the average isoplanatic angle values sampled

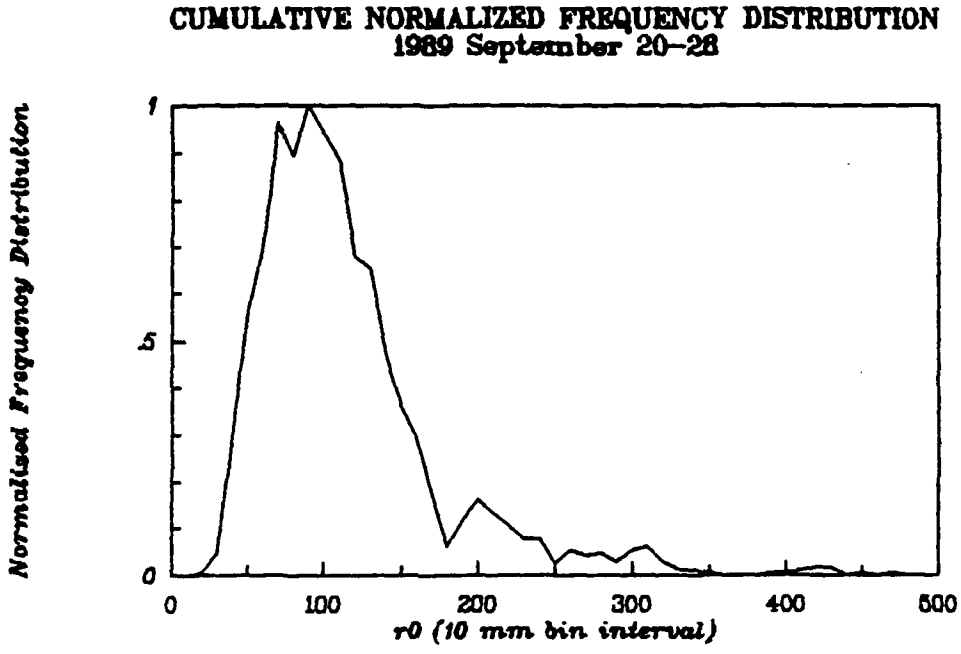

Fig 5. Cumulative Normalized r_o Frequency Distribution for the Anderson Mesa/USNO 1989 Sept 20-28 session.

TABLE 3. ISOPLANATIC ANGLE STATISTICS

Date (UTC)	Number of Data Points	Average θ_o (urad)	Standard Deviation (urad)	Standard Deviation of Mean (urad)
17 Sept	22	5.97	1.31	0.28
20 Sept	1637	6.84	2.80	0.07
21 Sept	3175	9.28	2.14	0.04
22 Sept	3017	11.17	1.91	0.04
23 Sept	3058	7.17	1.60	0.03
25 Sept	1339	15.72	3.12	0.08
26 Sept	728	15.56	3.64	0.14
27 Sept	2213	12.06	2.72	0.06
28 Sept	1166	11.25	2.34	0.07

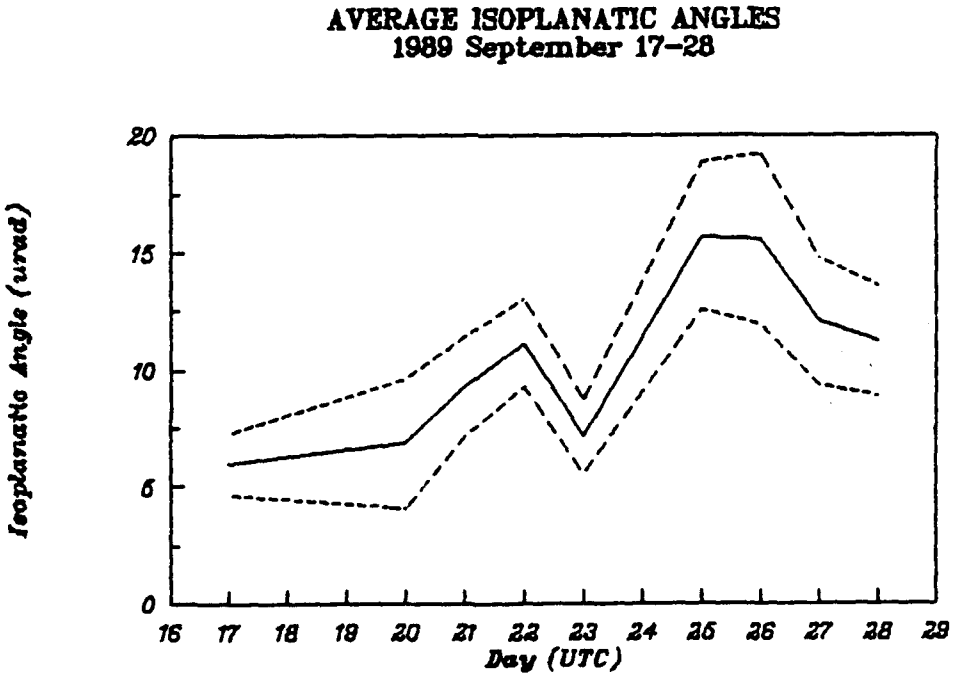

Fig 6. Average Isoplanatic Angle (89 Sept 17-28) - Solid line is data average; Dashed line is standard deviation of the data.

range 6-12 urad (Poor to Mediocre conditions). The implied abundance of turbulence aloft is consistent with the attributes of cold fronts traversing a site (Appendix B). The least turbulent conditions sampled during this experiment occur 25-26 September. The dominant quality of seeing is Good, 12-20 urad (Appendix F). Average isoplanatic angles for these two sessions is 15.7 and 15.6, respectively.

The decreasing average isoplanatic angles of 26 through 28 September (Figure 6) indicates a transition to more turbulent conditions. Though the average isoplanatic angle decreased by 22% between 26 and 27 September, the normalized frequency distribution (Figure 7) for these nights displays equivalent peak frequencies. On 27 September, the Good conditions (52%) are equivalent to the Mediocre/Poor quality of seeing (49%) statistically (Appendix F). The last night of measurements (28 September) extends the evolution to more turbulent conditions aloft with 38% of the dataset between 12-20 urad (Good) and 62% between 4-12 urad (Poor/Mediocre).

Figure 8 presents a normalized frequency distribution based on the accumulation of all the Anderson Mesa and USNO isoplanatic angle samples. The bin-size is 1 urad. The broad range of isoplanatic angles (centered at 9 urad) highlights the extensive atmospheric variations aloft during the experiment period.

Note: The 17 September data had a 22 sample count before cloud cover terminated the session. The limited measurements deceptively increase the percent frequency statistics and therefore, these statistics should be ignored.

B. RAWINSONDE DATA ANALYSIS

Upper-air balloon measurements made at Anderson Mesa and USNO sampled both the thermodynamic (pressure, temperature, humidity) and horizontal wind information (wind direction and speed). Since the reprocessed Loran-C balloon wind information was unavailable for inclusion at the time of publication, this report includes only the thermodynamic variables.

NORMALIZED FREQUENCY DISTRIBUTION
Anderson Mesa, AZ – 1989 September 17–25

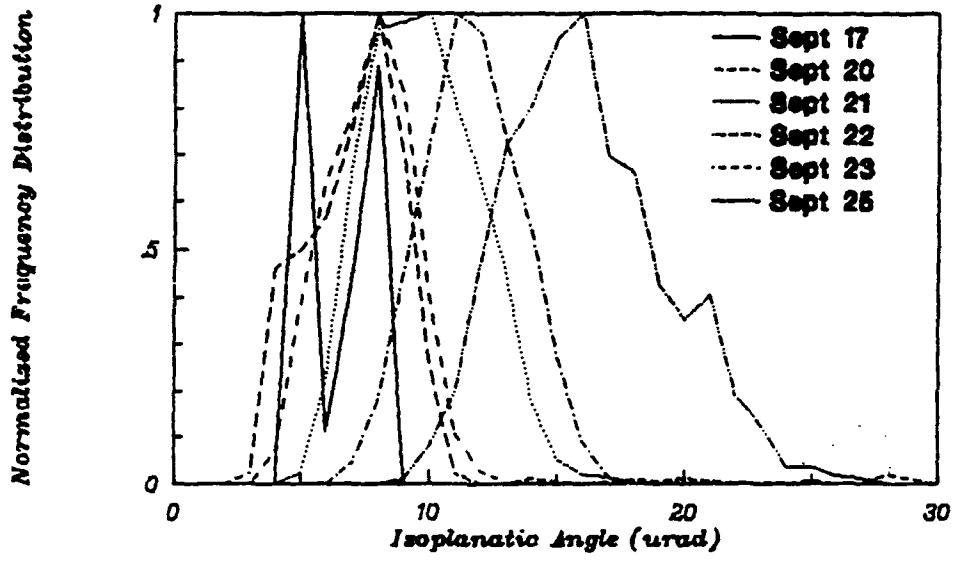

USNO, Flagstaff, Az – 1989 September 26–28

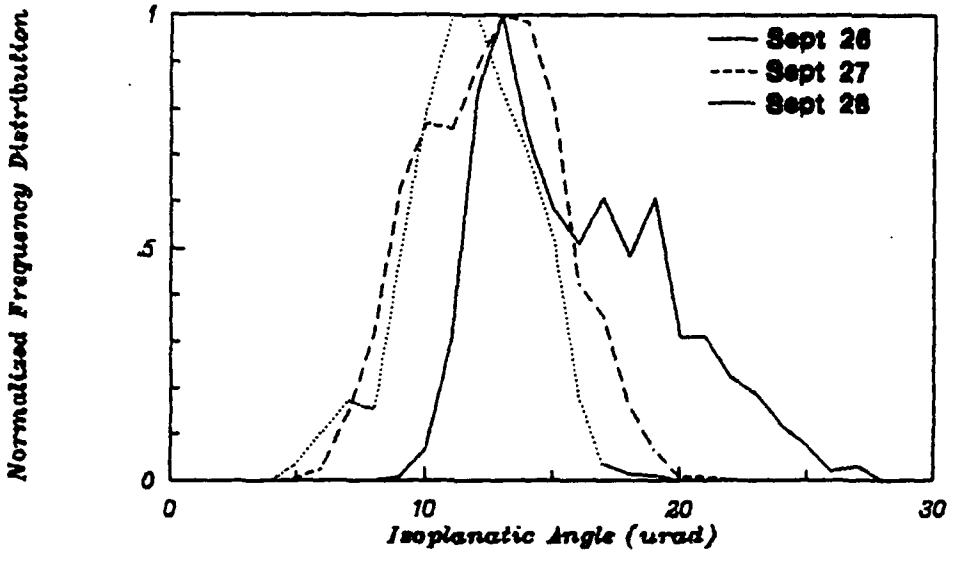

Fig 7. Normalized Isoplanatic Angle Frequency Distribution for: (a) Anderson Mesa, Az (89 Sept 17-25); (b) Naval Observatory, Az (89 Sept 26-28).

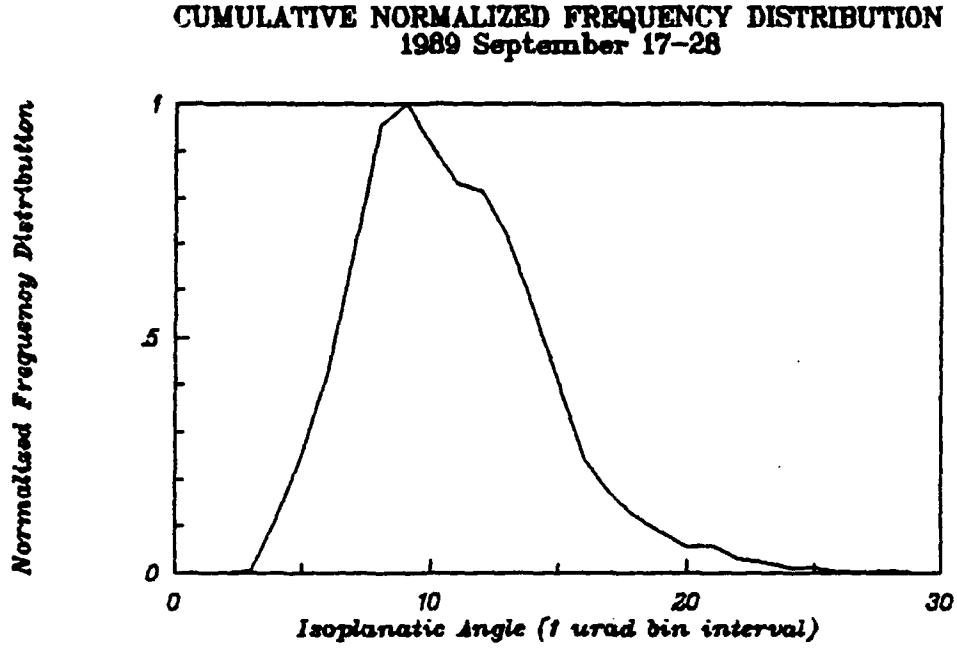

Fig 8. Cumulative Normalized θ_o Frequency Distribution for the Anderson Mesa/USNO 1989 Sept 17-28 session.

Thermodynamic soundings, presented in the form of vertical atmospheric profiles (Appendices G and H), and summarized in Table 4, serve as a guide to detect the probable locations of optically turbulent layers. Of particular importance is the height of the atmospheric boundary layer (ABL) and the number of temperature inversion levels in each sounding, and the variation with time in the height of the atmospheric freezing level.

Low-level wind jet maxima and relatively large wind shears often occur near the top of the atmospheric boundary layer, as well as other (higher) levels which display a similar temperature inversion. Since wind shear and mechanical mixing are correlated, all temperature inversion layers within a given sounding are suspect as regions of possible optical turbulence. Hence, the more inversion levels an atmospheric profile possesses, the greater the potential for there to be turbulence which limits the effective optical "seeing". This is especially true when the sounding inversions are strong (dT > 5 Celsius) and coincide with a correspondingly large drop in the relative humidity (dH > 40%), as is often the case at the top of the ABL.

Table 4 presents information to help evaluate the seeing quality of a night, as based upon the above assumptions. From it, we surmise that the night of 26-27 September (soundings USN92620 and USN92703) had possibly good seeing at USNO while the night of 20-21 September (soundings ANM92020 and ANM92104) had potentially mediocre seeing at Anderson Mesa.

A rigorous rawinsonde analysis is possible only with the inclusion of detailed wind information, particularly the levels of high wind shear. Without such data, only a crude assessment of the potential seeing quality based on strengths, locations, and the number of temperature inversion levels can be made.

C. GENERAL SYNOPTIC WEATHER REVIEW

1. Anderson Mesa, Arizona

The synoptic weather data acquired during the 17-25 September 1989 Anderson Mesa measurement session fit into two categories: frontal and non-frontal conditions. For this application, frontal weather is defined by either the presence of an upper level trough or the passage of a

TABLE 4. THERMODYNAMIC INFORMATION - ANDERSON MESA/USNO

Sounding Name	Site Code (AM/USNO)	Number of Temperature Inversion Layers*	Height MSL of Atmospheric Boundary Layer+# (m)	Height MSL Freezing Level+ (m)
ANM91921	AM	6	3364	3636
ANM92020	AM	6	3614	5064
ANM92104	AM	7	3038	5092
ANM92120	AM	4	2945	4993
ANM92204	AM	6	3042	5114
ANM92220	AM	5	2816,4843	4621
ANM92304	AM	5	3048,4778	4512
ANM92504	AM	6	5082	4662
USN92522	USNO	7	5045	4493
USN92620	USNO	3	5588	4595
USN92703	USNO	3	3587,4687	4558
USN92720	USNO	4	3784 (?)	5220

* A temperature inversion layer, in this case, is defined as any layer displaying either increasing or constant ambient temperature with increasing height.

When multiple levels are selected, the higher layer is the residual atmospheric boundary layer (ABL) developed during the daylight hours, while the lower level is the newly developing nighttime ABL.

+ Height MSL = height above mean sea level (meters).

surface cold/warm front. Both categories of unsettled weather will affect the atmospheric optical quality adversely . Characteristically, non-frontal weather has very stable upper level atmospheric conditions, with generally stagnant air and a high pressure center or ridge overhead. While the cold fronts traversed Anderson Mesa, average transverse coherence lengths for this site ranged from 42 to 112 mm (17-22 September). Non-frontal conditions generated an average transverse coherence length of 196 mm (25 September). Weather conditions for 23 September provided elements of both frontal and non-frontal characteristics. For more detailed information, see Appendix B.

2. USNO, Arizona

Transverse coherence lengths measured at the USNO (26-28 September 1989) were principally Good (100-200 mm). The synoptic weather pattern during the 26-28 September 1989 sampling session included a High pressure system between 700 and 200 mb. The surface conditions were variable/unsettled. Surface winds averaged 5-10 knots (kt) from the southern quadrants. During the entire measurement session, winds aloft were from the western quadrants at 50 kt and less. Appendix C provides additional synoptic weather information.

V. DATA SUMMARY

Table 5 consolidates key optical/meteorological parameters acquired between 17 and 28 September 1989. While several elements within it appear earlier, the "Empirical % >= 'Good' " columns (Parts A and B) are seen for the first time. Here, the Optical Empirical Seeing Quality scale defined in Appendicies E and F quantifies the percentage of the individual datum points within an observing session that fall in the Good or better classifications. Another column in the meteorological parameters section (Part C), the "Frontal/Non-Frontal/Transistional", aids in interpreting the potential optical quality over the night. Here, transitional implies a changeover period from either frontal or non-frontal weather conditions, while frontal and non-frontal are as defined in Section IV.

The following discussion assimilates the various important elements presented previously but separately in the data analysis section, and codified below (with the help of Table 5) into one succinct summary.

Optical conditions gradually improved during the initial four nights of data acquisition. The meteorological forcing may be inferred from the rawinsonde time sections in Figure 9. Here, a significant change from a cold to warm air mass appears as a sharp increase in freezing level heights (over 1400 m) from the 20 September minimum. Likewise, the 750 and 700 mb pressure surfaces also confirm this trend by displaying a gradual, but definite, increase in their heights (Figure 9).

A transition from frontal to non-frontal conditions occurs on 23 September 1989. Despite the overall improvement in optical conditions, residual turbulence aloft appears as a temporary decrease in isoplanatic angles (23 September).

The most favorable optical conditions occur between 25 and 26 September. Mean values for both isoplanatic angles and transverse coherence lengths are "Good". The percent of optical data registering greater than or equal to these Good conditions is more than 82%. The large number of temperature inversions displayed in the 25-26 September rawinsonde profiles, implying possibly poor optical conditions, can be explained. The main cause of optical

TABLE 5. SUMMARY OF OPTICAL/METEOROLOGICAL DATA - ANDERSON MESA (1989 Sept 17-25)/ USNO (1989 Sept 26-28)

A. Transverse Coherence Length:				B. Isoplanatic Angle:		
Sept Date (UTC)	Mean Value (mm)	Empirical: Dominant Conditions	% >= "Good"	Mean Value (urad)	Empirical: Dominant Conditions	% >= "Good"
17				5.97	Poor(100%)	0
20	41.8	Poor(90%)	0	6.84	Poor(65%)	2
21	68.3	Mediocre(81%)	6	9.28	Mediocre(57%)	12
22	76.4	Mediocre(70%)	16	11.17	Mediocre(63%)	33
23	91.2	Mediocre(65%)	32	7.17	Poor(66%)	0
25	196.4	Good(52%)	96	15.72	Good(78%)	89
26	157.0	Good(66%)	86	15.56	Good(69%)	83
27	99.9	Mediocre(54%)	46	12.06	Good(52%)	52
28	139.7	Good(84%)	90	11.25	Mediocre(54%)	38

C. Atmospheric Structure/Synoptic Weather Conditions:

Sept Date (UTC)	Frontal/ Non-frontal/ Transitional (F/NF/T)	Height MSL of Freezing Level*# (m)	Number of Temperature Inversion Layers+
17	F		
20	F	3636	6
21	F	5064,5092	6,7
22	F	4993,5114	4,6
23	T	4621,4512	5,5
25	NF	4662	6
26	NF	4493	7
27	T	4595,4558	3,3
28	F	5220	4

* Height MSL = height above mean sea level (meters).

Multiple heights represent more than one sounding.

+ Temperature inversion, in this case, is defined as any layer displaying either increasing or constant ambient temperature with increasing height.

turbulence is density variations. These variations are a function of both the temperature gradient and wind shear (Richardson Number). During 25-26 September, the authors suspect that the wind sheer was not sufficient to induce turbulence in these layers.

With the return of frontal activity (27-28 September), atmospheric optical conditions begin to deteriorate. The effect was initially recorded in the transverse coherence lengths (27 September), then the isoplanatic angles (28 September). A sudden height increase (over 650 m) in the Figure 9 rawinsonde freezing levels marks the onset of frontal activity. During the last session, transverse coherence lengths maintain large values despite the potentially turbulent optical conditions. Ninety percent of the transverse coherence lengths collected are greater than or equal to the Good classification of empirical seeing quality.

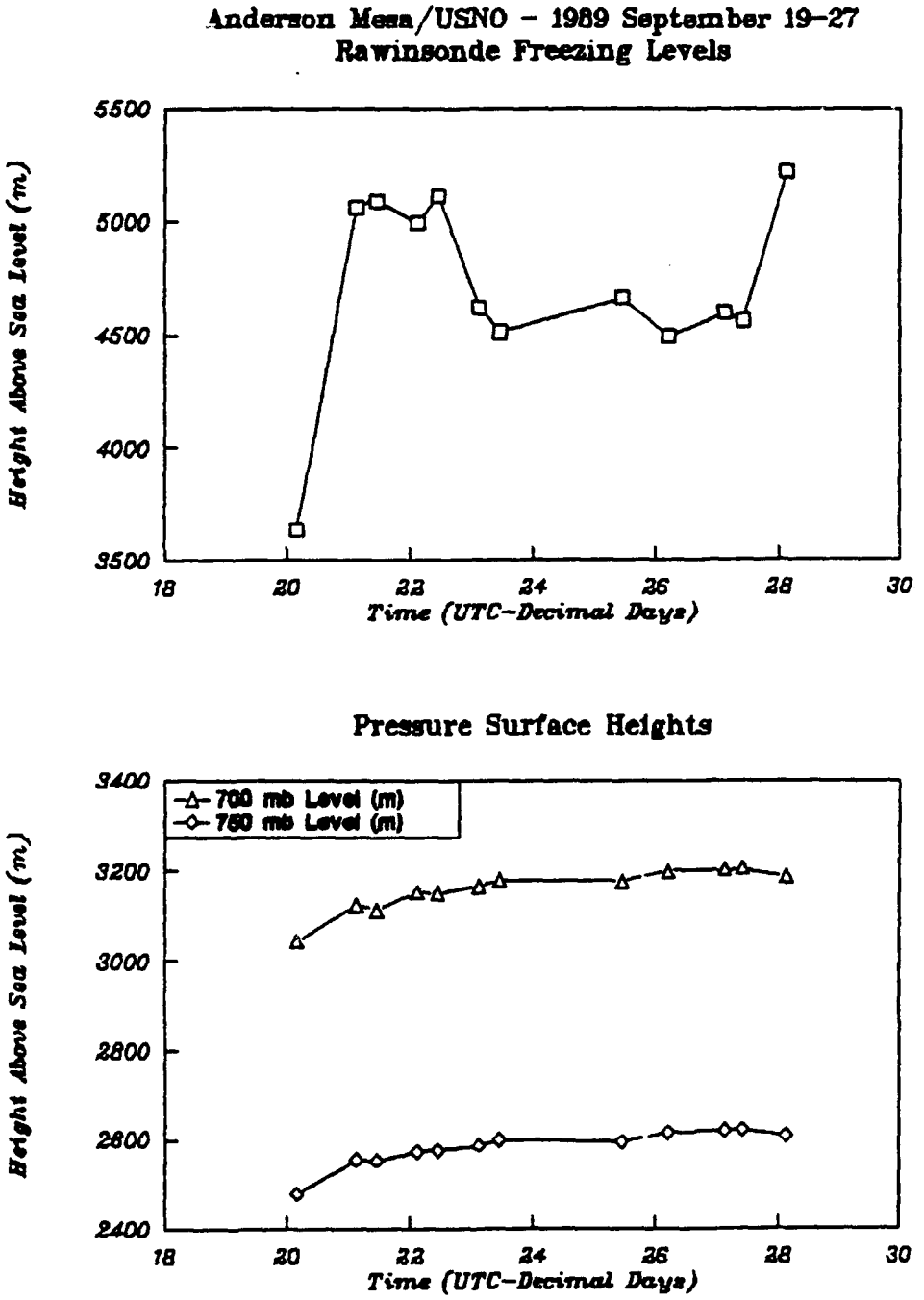

Fig 9. Rawinsonde Freezing Levels and Pressure Surface Heights recorded between 1989 Sept 20-28 UTC.

VI. RECOMMENDATIONS

The original intent of this study was to evaluate the Flagstaff, Arizona region as a potential site for a large baseline stellar interferometer. The snapshot of optical conditions sampled over Anderson Mesa (17-25 September) and the United States Naval Observatory - Flagstaff (26-28 September) displays a broad range of atmospheric events. Consistent with other areas, the optical turbulence over Flagstaff increases with the onset of frontal activity. Despite the constant colliding of cold and warm air masses typical for this area in September, significant Good to Excellent seeing conditions occurred. Knowing that Excellent seeing exists under less than ideal weather patterns, one must ask how often these Excellent seeing conditions prevail. Sampling every night for years would be the ideal recommendation. A more realistic recommendation, however, is to improve the statistical sampling by making seasonal 7-10 night long snapshots of optical data while pursuing a climatological study of the thermodynamic and shear producing events. In summary, it is the authors' opinions that the Flagstaff region warrants further consideration and measurements.

APPENDIX A. OPTICAL VARIABLES DEFINED

Two parameters that characterize atmospheric optical turbulence are the transverse coherence length, r_o, and the isoplanatic angle, θ_o. The following description of these optical parameters is borrowed from Vaucher (1989) Correlation of Atmospheric Optical Turbulence and Meteorological Measurements:

A. Transverse Coherence Length

"The transverse coherence length, r_o, is a measure of the lateral autocorrelation length of the electric field propagating through the turbulent atmosphere. Because of the Fourier transform properties of an imaging system, r_o is also a measure of the spatial frequency response of the atmosphere, the atmospheric modulation transfer function. Viewed as a component of a linear system, the atmosphere acts like a low pass filter suppressing the high spatial frequencies, or details of an image."

The coherence length for a plane wave, r_o is

$$r_o = 2.1 \left[1.46\, k^2 \int_o^L C_n^2\,(z)\, dz\right]^{-3/5} .$$

"The parameter r_o represents the distance transverse to the direction of propagation where, on average, the correlation of the electric field is $e^{-3.44}$ (Fried, 1966).

To interpret r_o consider the following:

1. For an optical aperture d smaller than the coherence length, the electric field across the aperture is coherent. The angular resolution will be proportional to λ/d.

2. For an optical aperture larger than the coherence length, the correlation across the aperture is limited to regions of r_o. The electromagnetic intensities across the aperture will add (energy is conserved). The optical system's average angular resolution will be proportional to λ/r_o. (Walters, Favier and Hines, 1979).

3. Visually, for apertures smaller than r_o, atmospheric turbulence results in image centroid motion, a process called 'tilt'. In telescopes larger than r_o, the image is broken up into multiple speckles, each associated with a r_o sized region. The angle λ/r_o determines the overall envelope of the complex image.

4. With respect to measuring the atmospheric optical turbulence, large r_o values, such as 200-400 mm, indicate a small amount of optical turbulence is present along the integrated path. Conversely, small r_o magnitudes, such as 20-40 mm, imply a large amount of optical turbulence exists along the integrated path."

B. Isoplanatic Angle

The isoplanatic angle, θ_o, is an angular measurement of spatial coherence between two intersecting rays (Walters, 1985). Given two light sources a small angle θ apart, the random atmospheric phase fluctuations along the two paths are different. At the atmosphere top the two paths undergo unique path distortions. At the surface, the turbulent interaction is common to both rays. θ_o is the angle between rays such that the accumulated phase fluctuations are correlated to within e^{-1} of a perfect correlation.

Fried (1982) develops a mathematical representation for θ_o for aperture $d >> r_o$:

$$\theta_o = [\ 2.91\ k^2 \int_o^\infty C_n^2(z)\ z^{5/3}\ dz\ ]^{-3/5}\ ,$$

where k is $2\pi/\lambda$, wavenumber of light; C_n^2 is the refractive index structure parameter; and, z is the altitude from the ground."

"When θ_o magnitudes are small (1-4 urad), the optical turbulence along the integrated path, and especially around the tropopause level, is large. Conversely, when θ_o values are large (12-20 urad), optical turbulence is small."

APPENDIX B. DAILY SYNOPTIC WEATHER SUMMARY-ANDERSON MESA,AZ

Site: Anderson Mesa, Flagstaff, Arizona
Time Period: 17-25 September 1989
Equipment Used: Transverse Coherence Length Sensor
Isoplanatic Angle Sensor
Rawinsondes
National Weather Service Synoptic Summaries

Data acquired during the 17-25 September 1989 Anderson Mesa measurement session can be generalized into two categories: frontal and non-frontal conditions. While the cold fronts traversed Anderson Mesa, transverse coherence lengths for this site ranged from 50 to 150 mm (17-22 September 1989). "Non-frontal" conditions generated transverse coherence lengths between 100 and 450 mm (25 September 1989). September 23, 1989 provided elements of both frontal and non-frontal characteristics.

ANDERSON MESA, ARIZONA (1989)

Observations: 17 Sept,0030 hr - 25 Sept,0600 hr (local time)
17 Sept,0730 hr - 25 Sept,1300 hr (UTC)

GENERAL SYNOPTIC METEOROLOGICAL SUMMARY:

17 September 1989: An approaching front coupled with 7/10 to 9/10 cloud cover severely limits the 17 September 1989 sampling session. Though the polar jet is still west of the site, the isoplanatic angles acquired average only 7 and 4 urad.

20 September 1989: The 20 September 1989 observing begins soon after sunset (approximately 0230 UTC). Dense cloud cover terminates the session around 1000 UTC. The transverse coherence lengths are acquired between the partly cloudy skies.

Between 1200 UTC, 19 September and 1200 UTC, 20 September, a cold front crosses over the site generating quite a bit of unsettled (turbulent) conditions. A 70-90 knot (kt) polar jet (300 and 200 mb levels) over the site completes the very turbulent profile (atmospheric structure).

21 September 1989: Post-frontal weather conditions persist over the observation site. The front is about 4 degrees latitude (440 km) east of Anderson Mesa, Arizona (0000 UTC). The north-northeasterly flow over northern Arizona compliments the development of a surface High pressure system centered over Wyoming. From 850-300 mb, the site is situated between a Low centered over Wyoming/Utah and a High over Texas/Mexico. At 200 mb (only), the site experiences a southwesterly 70-90 kt jet. During the 0000-1200 UTC time period the jet moves from directly overhead northward. By 1200 UTC, the site is on the trailing edge of the accelerated 70 kt westerly winds.

22 September 1989: Borderline Good seeing conditions (Appendices E and F) coincide with the gradual return to a non-frontal (non-turbulent) environment. The surface High

over Wyoming is more organized. From 850 to 500 mb a High pressure system dominates the non-coastal western states (including Arizona). Aloft, however, the site continues to straddle a Low centered over the Dakotas and a High over Mexico. Winds are northwesterly and generally weak at 30-50 kt.

23 September 1989: A thermal Low over Baha/Mexico proper is accompanied by scattered clouds and south/southeasterly surface winds over much of Arizona. A cold front over northeastern New Mexico moves southwest over New Mexico towards Arizona. These southeasterly winds persist from the surface to 700 mb (500 mb chart was unavailable for analyses). Throughout the 700-200 mb layer, a High pressure system/ridge exists over the site. No jet stream is evident over the immediate site.

24 September 1989: Extensive cloud cover prohibits optical measurements.

25 September 1989: Both optical sensors indicate Good to Very Good conditions (Appendices E and F). The "trof" generating September 24th's abundant cloud cover is over New Mexico. Skies are initially 1/10 to 4/10 covered. Over the site, the sky transitions from cloudy to clear. Between 850-200 mb levels, a high develops over the site. Winds are generally from the northern quadrants at moderate wind speeds (<50 kt).

APPENDIX C. DAILY SYNOPTIC WEATHER SUMMARY-USNO, AZ

Site: United States Naval Observatory (USNO), Flagstaff, Arizona
Time Period: 26-28 September 1989
Equipment Used: Transverse Coherence Length Sensor
Isoplanatic Angle Sensor
Rawinsondes
National Weather Service Synoptic Charts

Optical data acquired during the 26-28 (UTC) September 1989 USNO measurement session were taken in hopes of deriving a correlation between the USNO arc-second and the NPS transverse coherence length measurements. Because the Naval Observatory is located near Anderson Mesa, Arizona the optical values/meteorological analysis serves a dual purpose.

In general, the transverse coherence lengths were Good (100-200 mm). Consistently high values (average value approximately 200 mm) were observed between 0845-1045 UTC on 26 September. Somewhat low values (100-70 mm) were sampled between 0830-1230 UTC, 27 September.

The synoptic weather pattern during the 26-28 September 1989 sampling session included a High pressure system between 700 and 200 mb. The surface conditions were variable/unsettled. Surface winds were generally from the southern quadrants at 5-10 knots (kt). During the entire measurement session, winds aloft were from the western quadrants at 50 kt and less.

UNITED STATES NAVAL OBSERVATORY, ARIZONA (1989)

Observations: 25 Sept,2145 hr - 27 Sept,2315 hr (local time)
26 Sept,0445 hr - 28 Sept,0615 hr (UTC)

GENERAL SYNOPTIC METEOROLOGICAL SUMMARY:

26 September 1989: The sampling session begins around 0445 UTC and is terminated around 1045 UTC due to cloud cover. The optical values measured are generally Good to Very Good. The synoptic weather pattern over the site consists of a High pressure/Ridge structure from 700 to 200 mb. Below this layer is an unorganized Low with just enough energy to support local cloud development.

27 September 1989: The synoptic weather pattern over the site still displays a High pressure/Ridge structure from 700 to 200 mb. The surface to 850 mb remains unsettled. However, the site appears to be indirectly influenced by a surface High centered over northeastern New Mexico/Oklahoma panhandle (850 mb). Surface to 850 mb winds are southerly, southeasterly at 5-10 knots (kt).

28 September 1989: A High pressure system persists in the upper layers (700-200 mb). The surface to 850 mb layer appears to be on the boarder of a High centered over Colorado. Surface to 850 mb winds are southeasterly (southwesterly) at 5-10 kt.

During the entire sampling session, no upper level polar jet is observed directly over the Naval Observatory site. Winds aloft are generally from the western quadrants at 50 kt and less.

APPENDIX D. RAW OPTICAL DATA (1989 September 17-28)

Appendix D displays all the processed Transverse Coherence Lengths and Isoplanatic Angles sampled between 17-28 September 1989. Each figure displays the individual points per night.

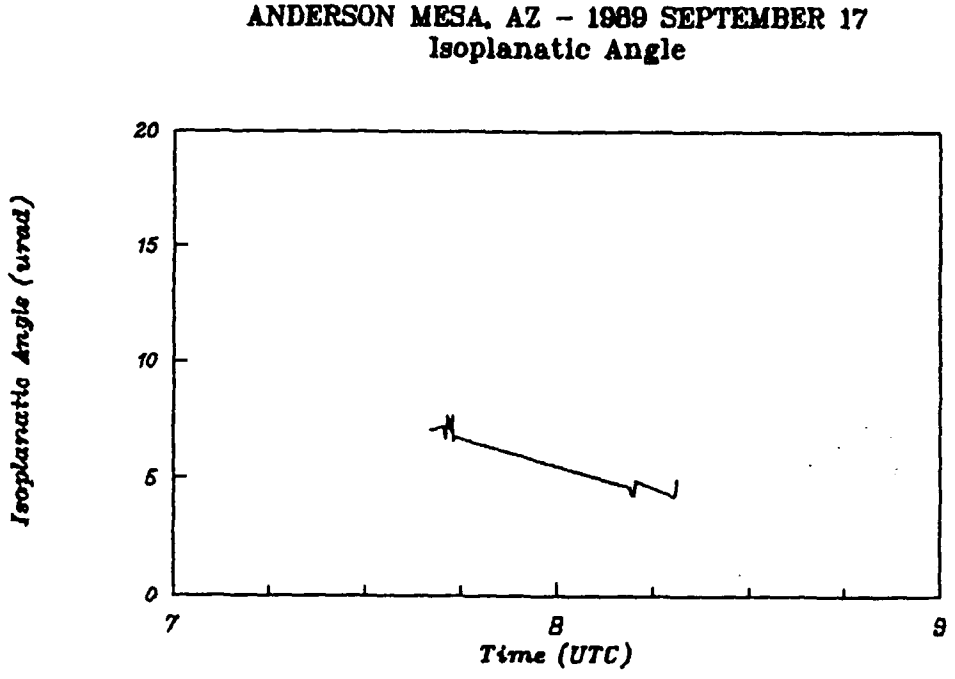

Fig 10. Anderson Mesa, Az Optical Data: 1989 September 17

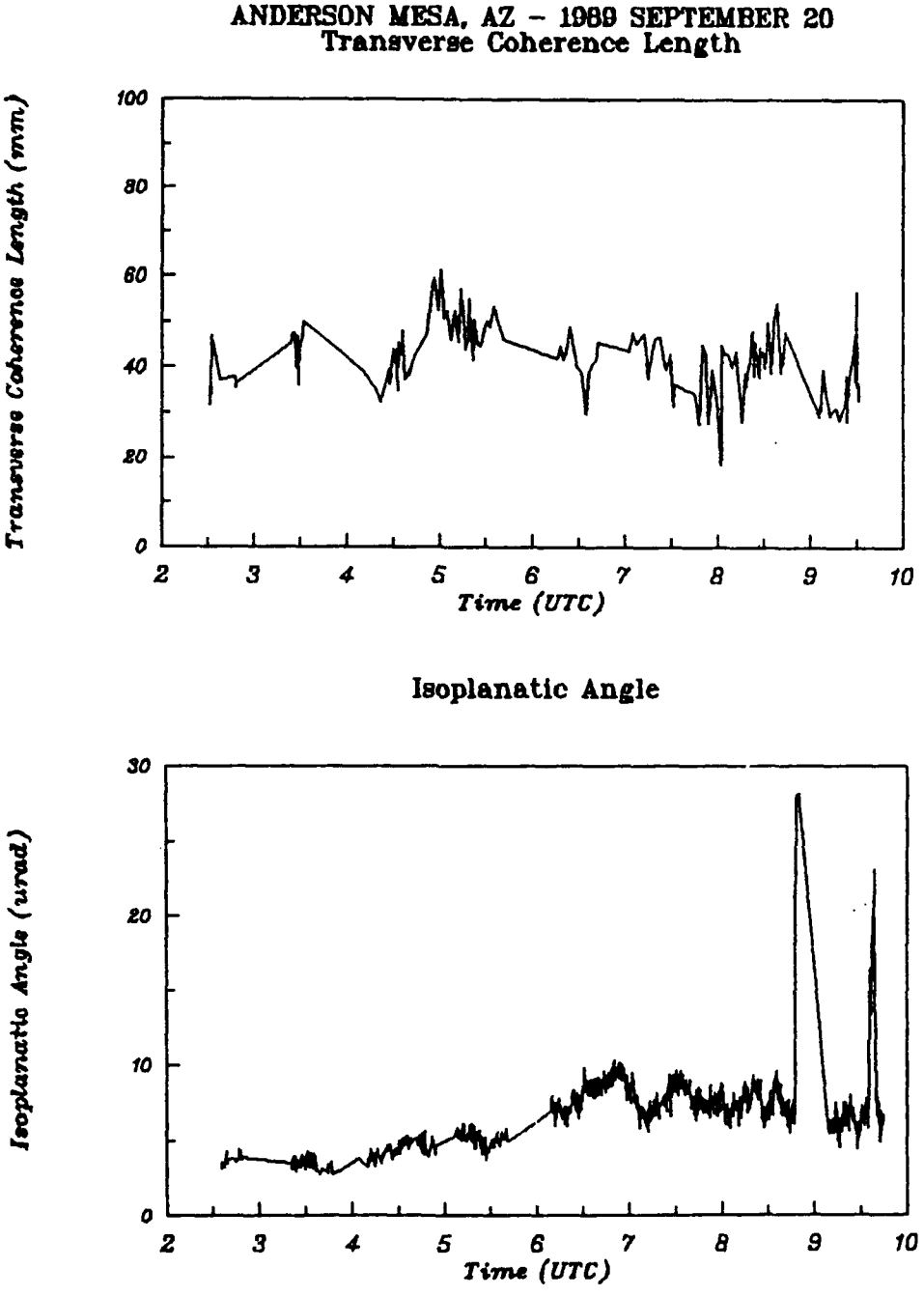

Fig 11. Anderson Mesa, Az Optical Data: 1989 September 20

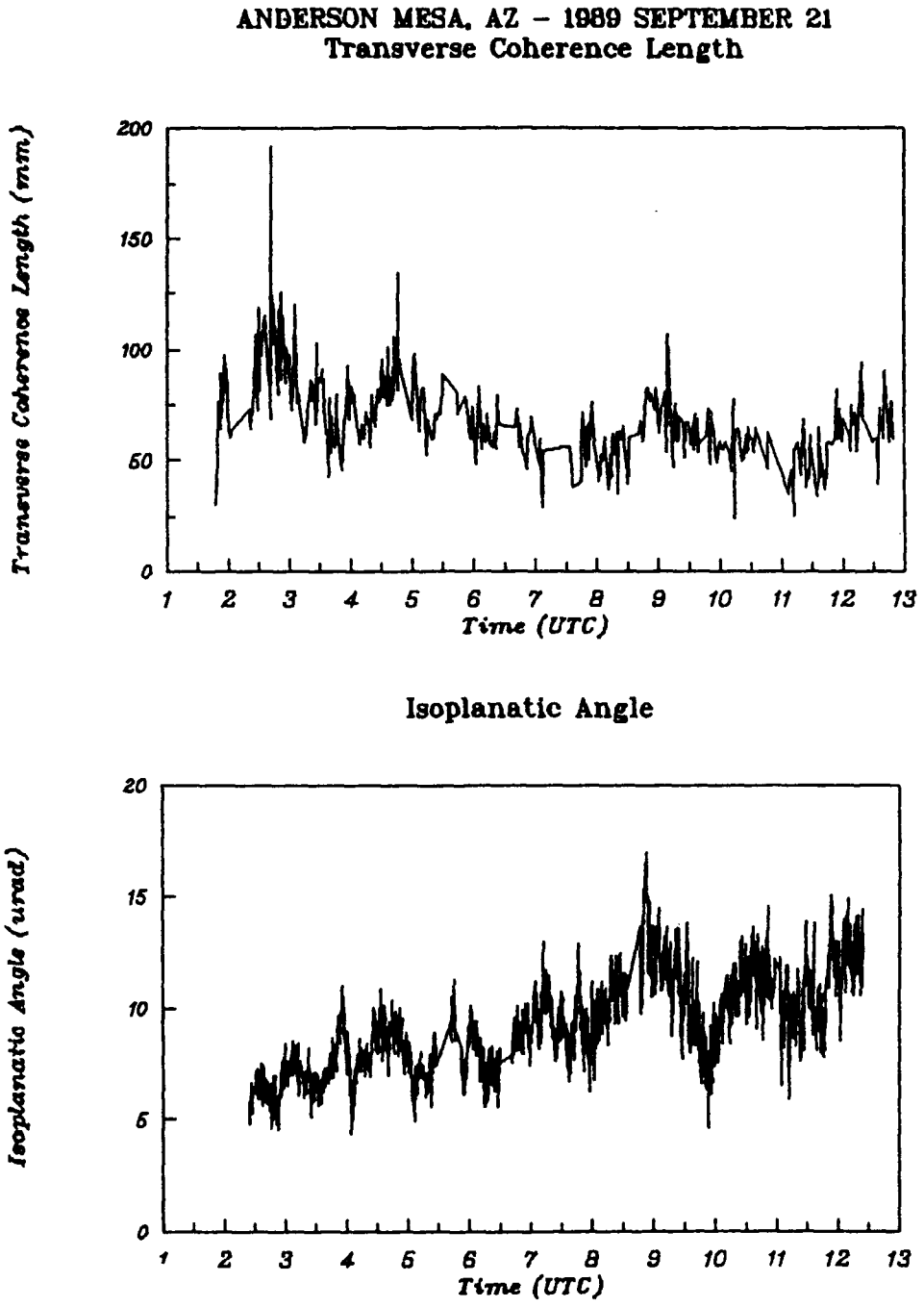

Fig 12. Anderson Mesa, Az Optical Data: 1989 September 21

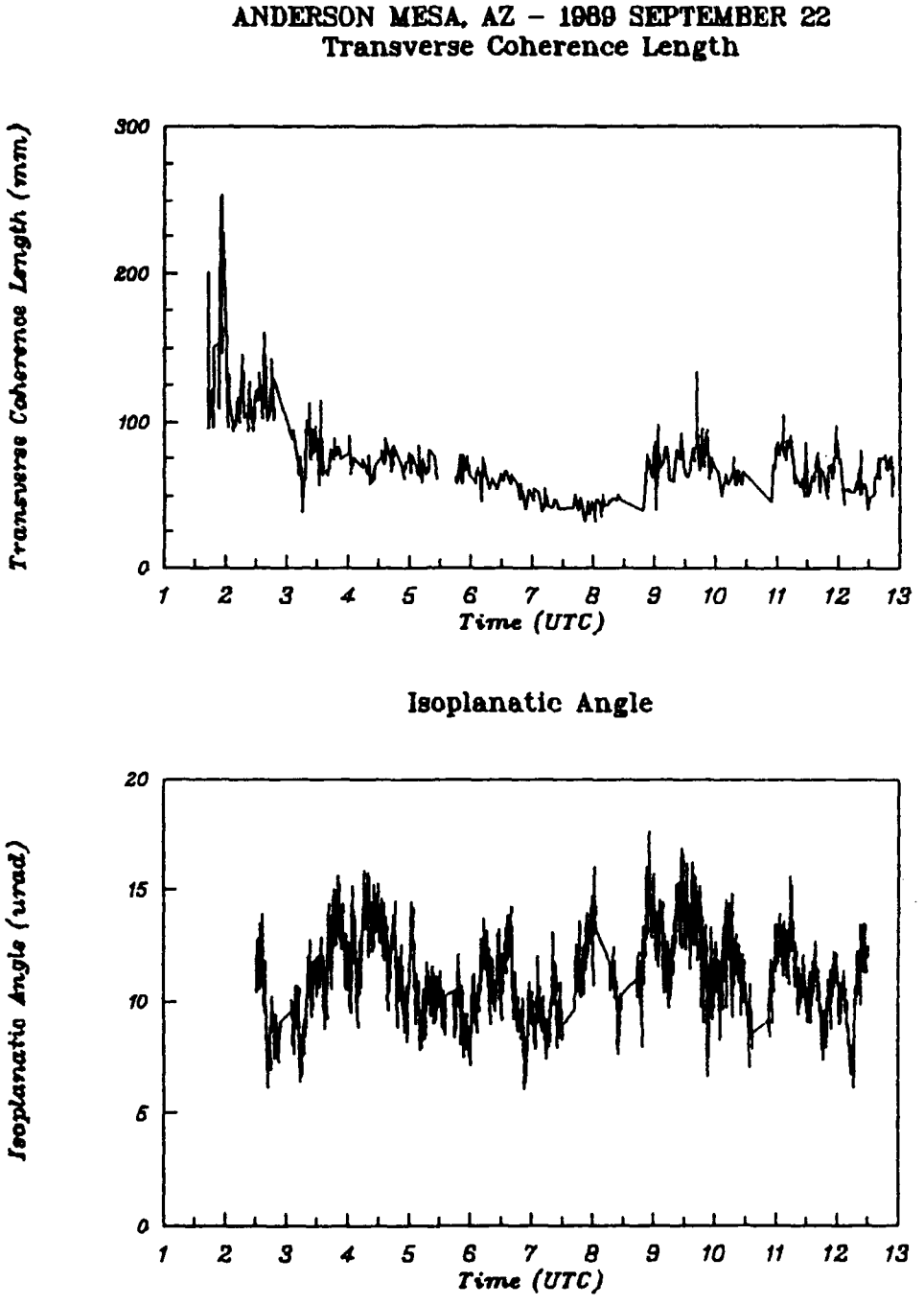

Fig 13. Anderson Mesa, Az Optical Data: 1989 September 22

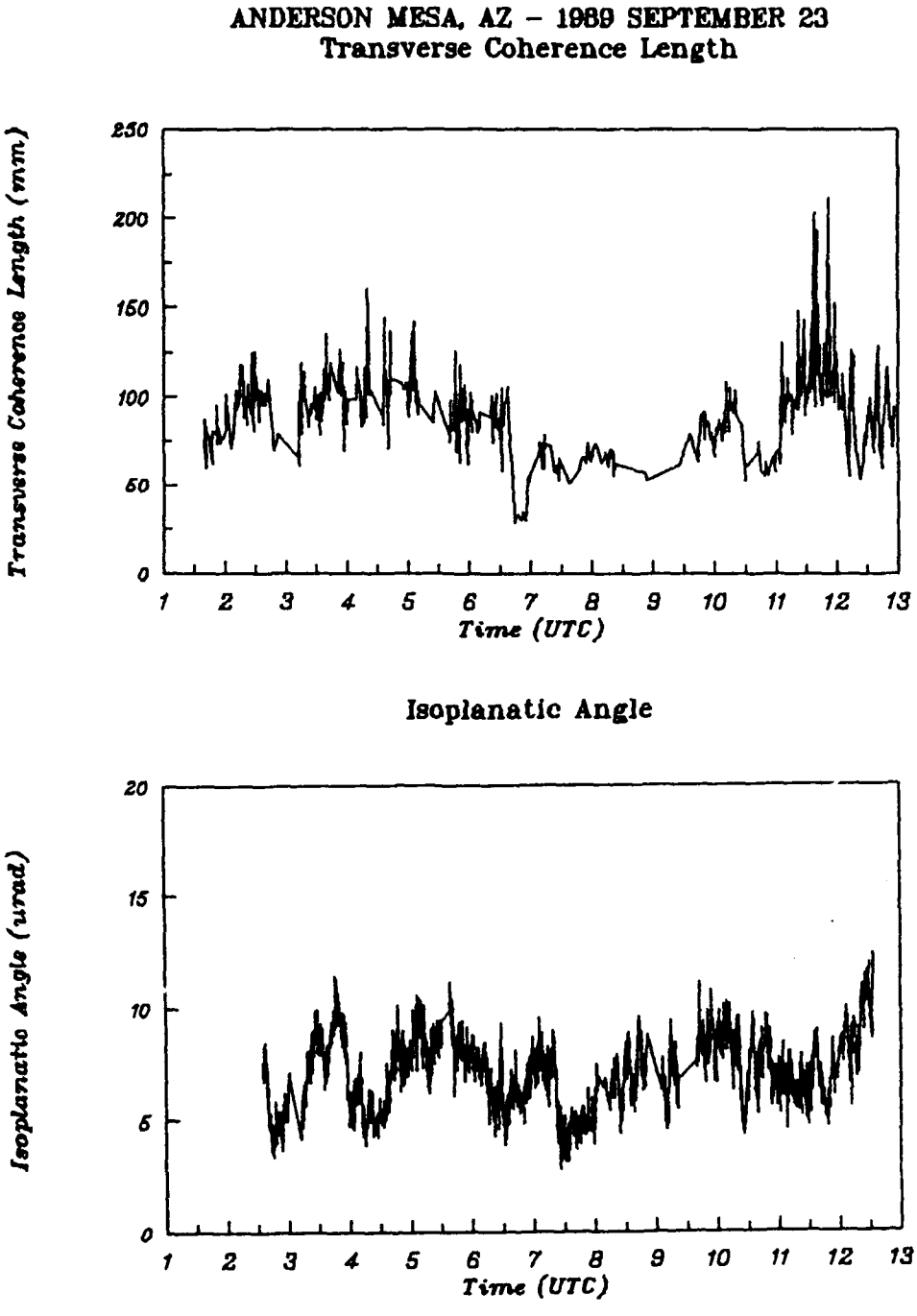

Fig 14. Anderson Mesa, Az Optical Data: 1989 September 23

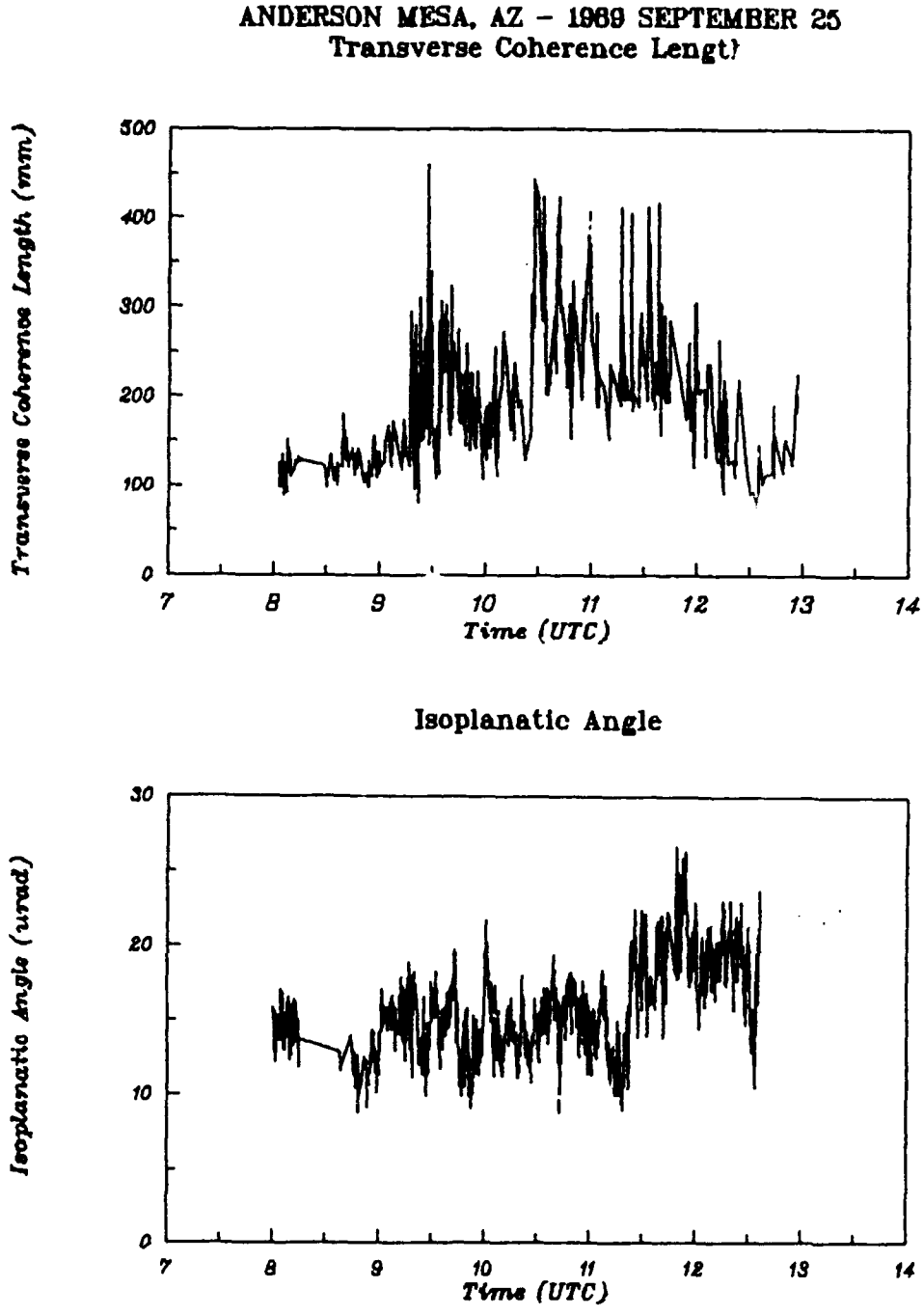

Fig 15. Anderson Mesa, Az Optical Data: 1989 September 25

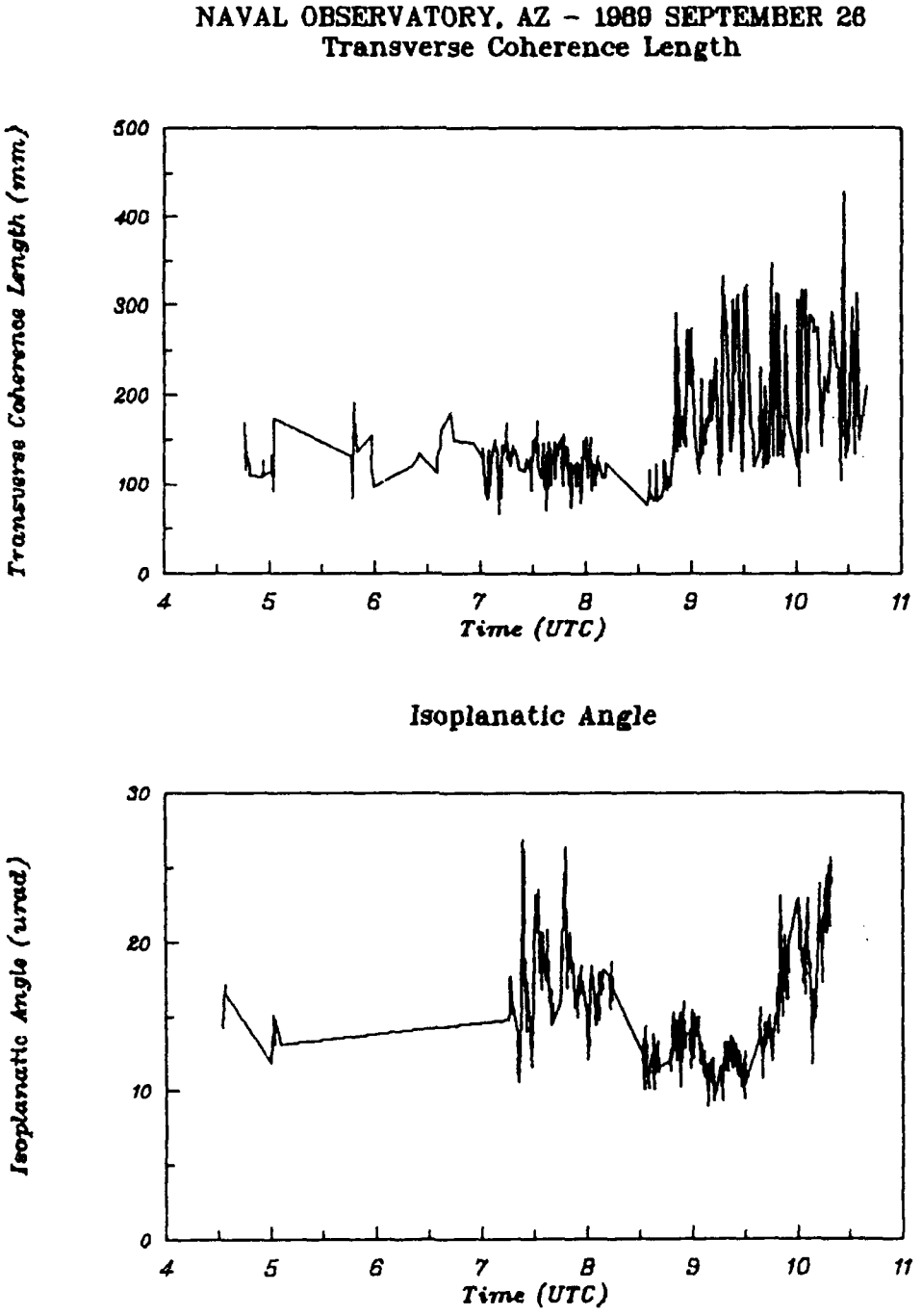

Fig 16. USNO, Az Optical Data: 1989 Sept 26

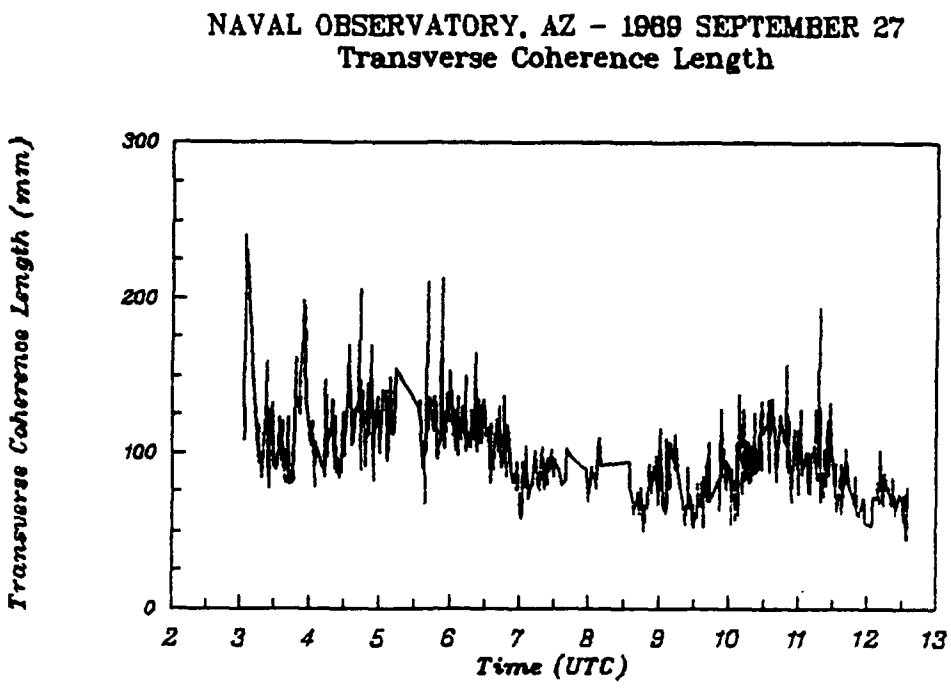

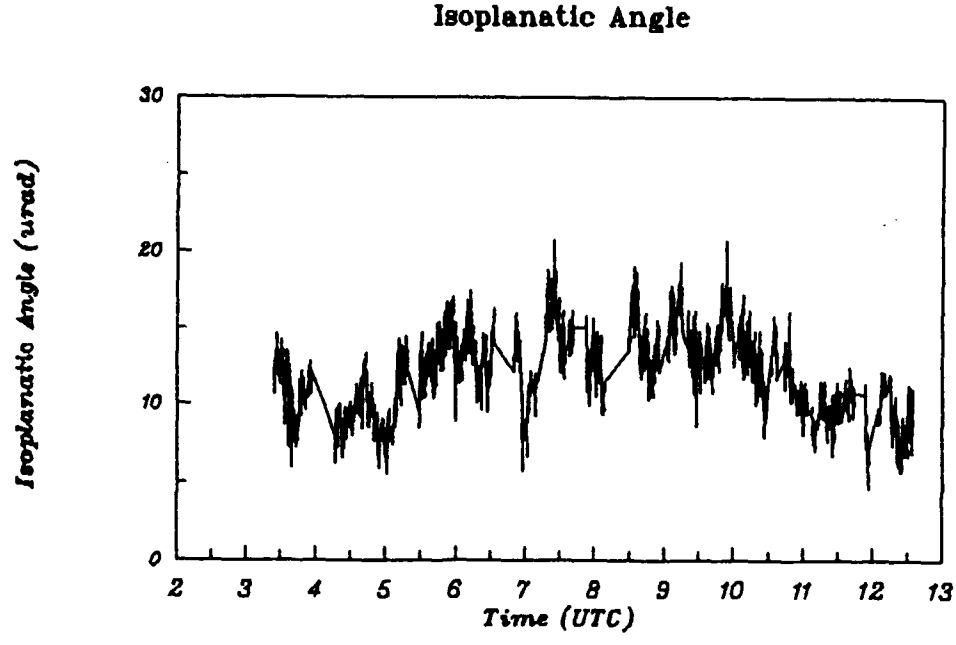

Fig 17. USNO, Az Optical Data: 1989 Sept 27

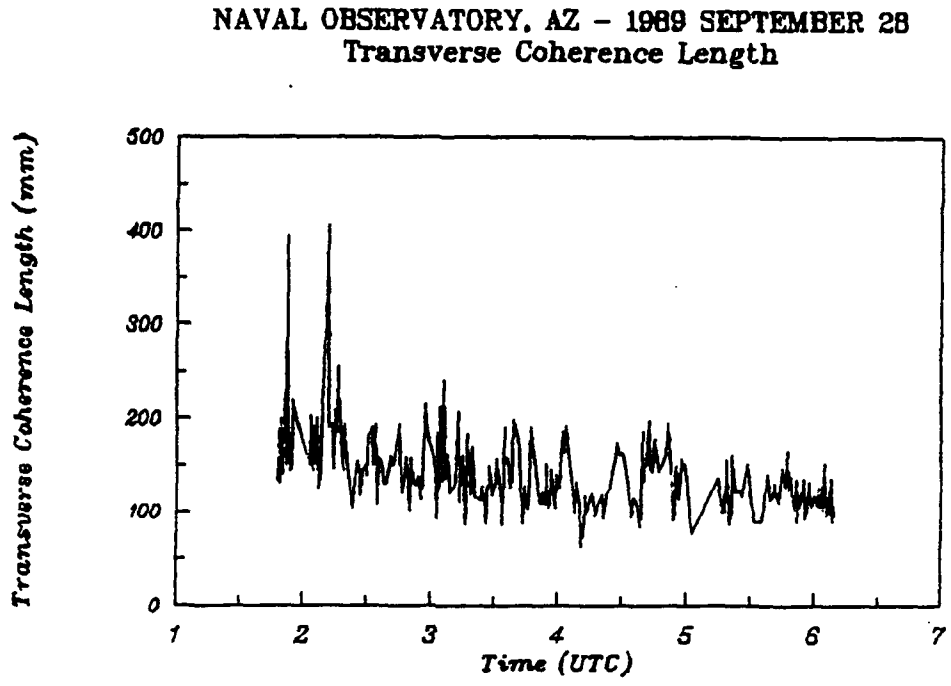

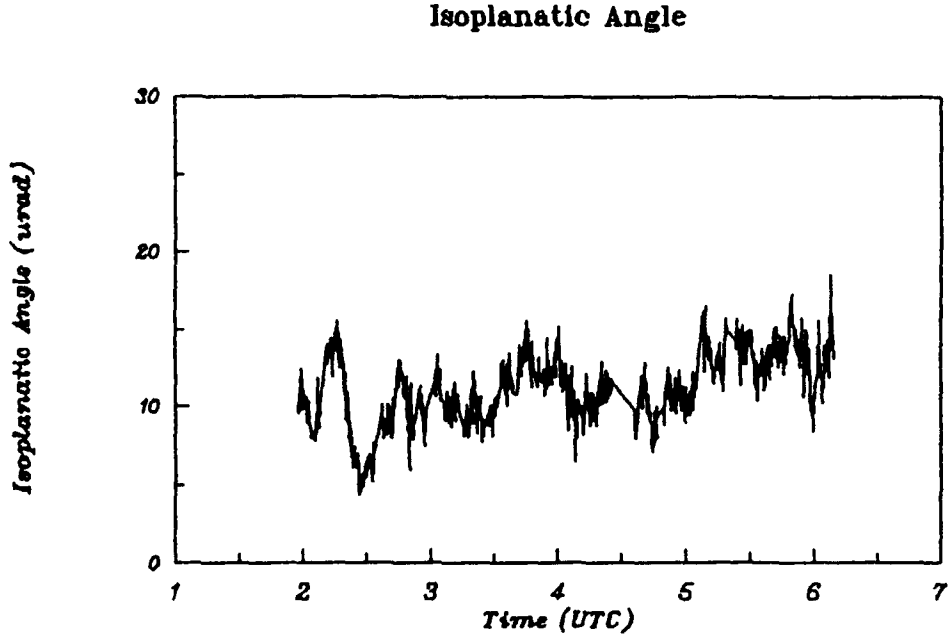

Fig 18. USNO, Az Optical Data: 1989 Sept 28

APPENDIX E. TRANSVERSE COHERENCE LENGTH STATISTICS

Appendix E presents the transverse coherence length un-normalized percent frequency distribution for each observing night (bin interval is 10 mm). Empirical seeing quality histograms are also included. The bin intervals selected for this qualitative interpretation are a product of approximately 50 site surveys spanning 18-40 degrees latitude and 65-156 degrees longitude. The specific empirical seeing quality intervals are:

Empirical Seeing Quality	r_o measurement (mm)
Poor	00 - 50
Mediocre	51 - 100
Good	101 - 200
Very Good	201 - 300
Excellent	301 - 500

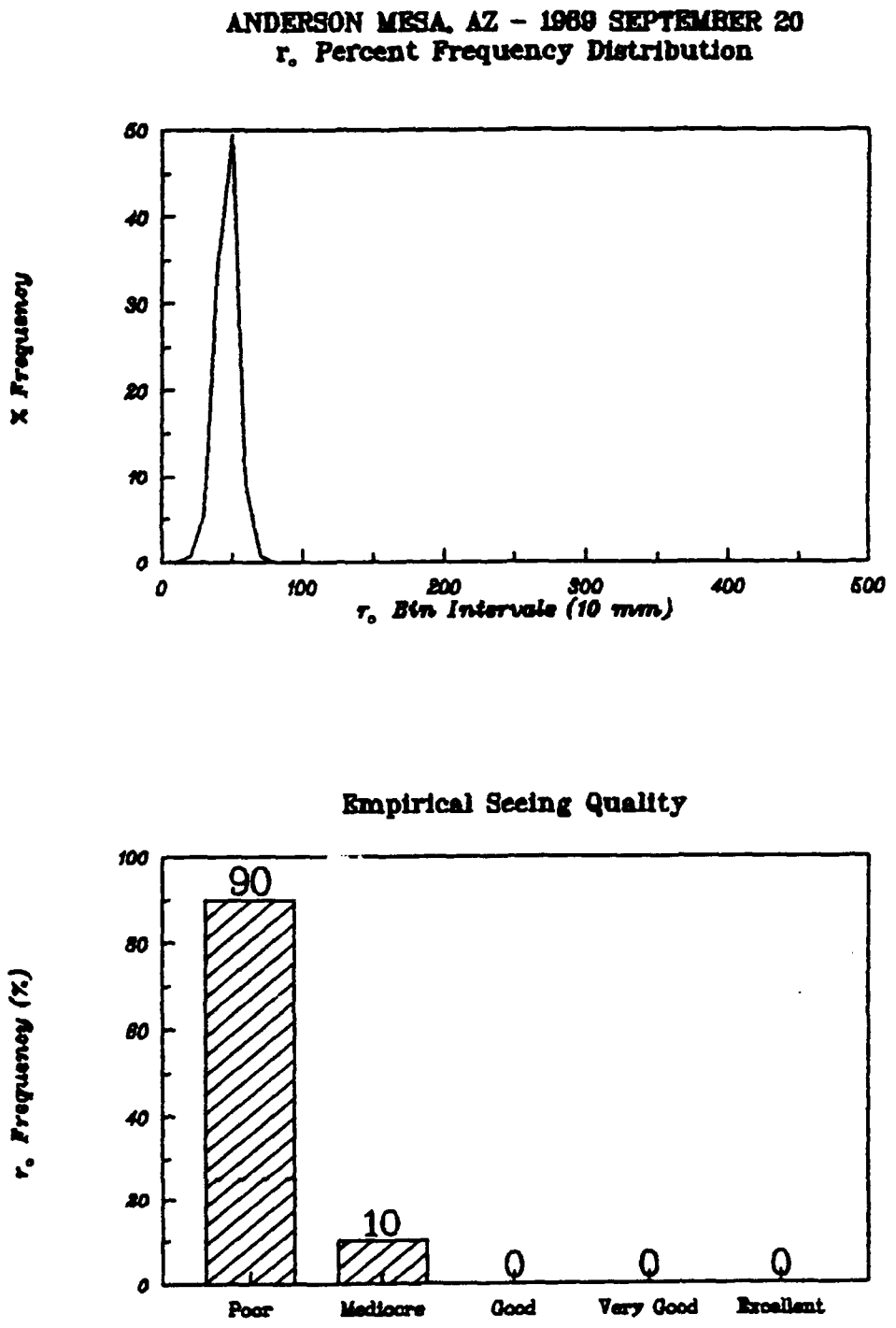

Fig 19. Anderson Mesa, Az r_o Statistics: 1989 Sept 20

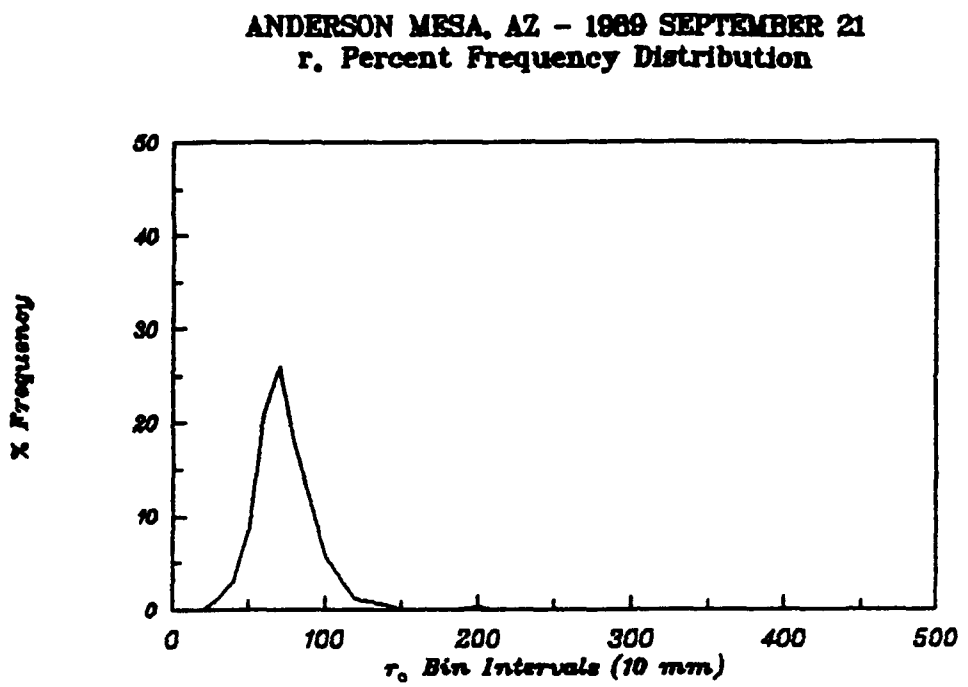

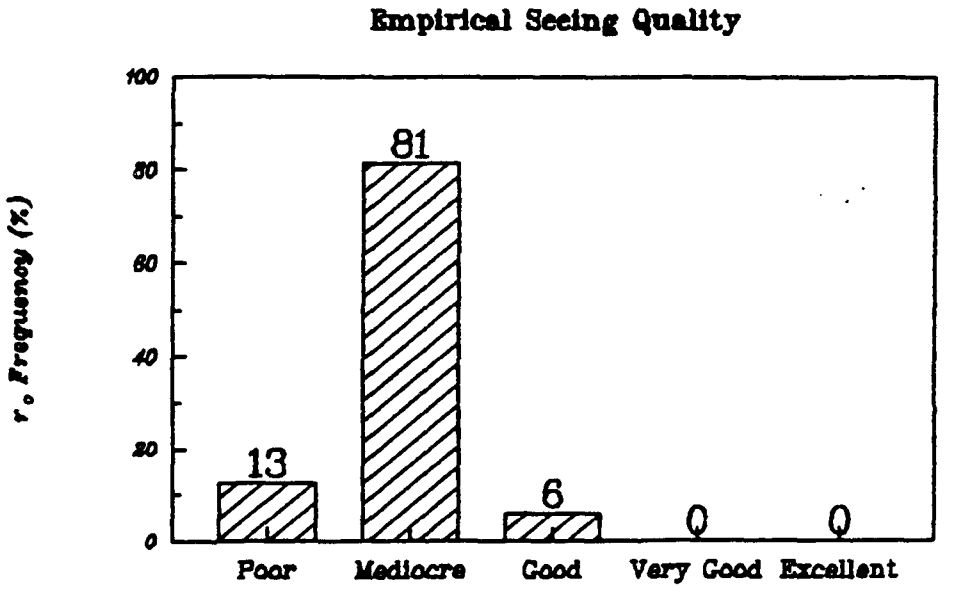

Fig 20. Anderson Mesa, Az r_o Statistics: 1989 Sept 21

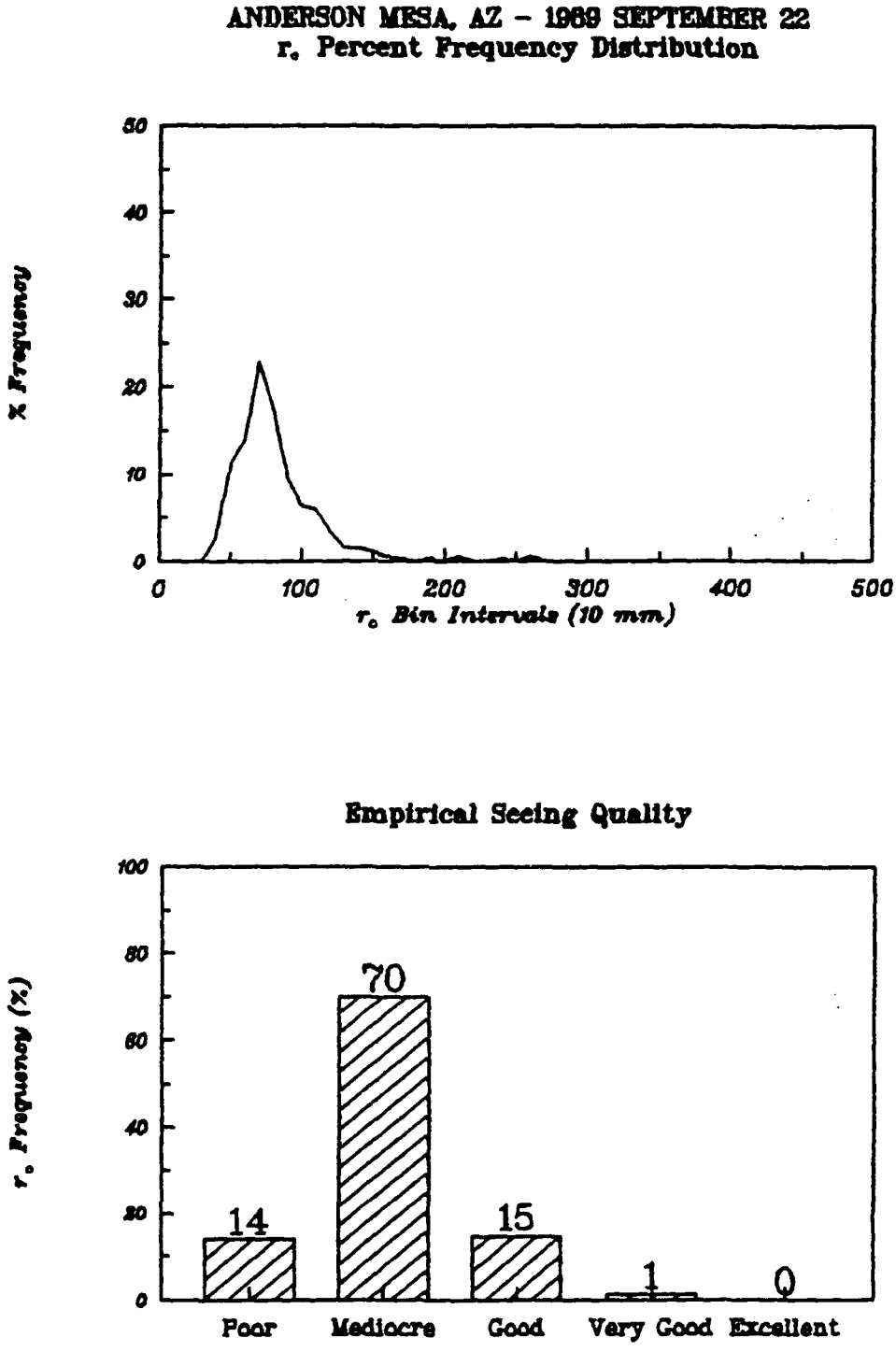

Fig 21. Anderson Mesa, Az r_o Statistics: 1989 Sept 22

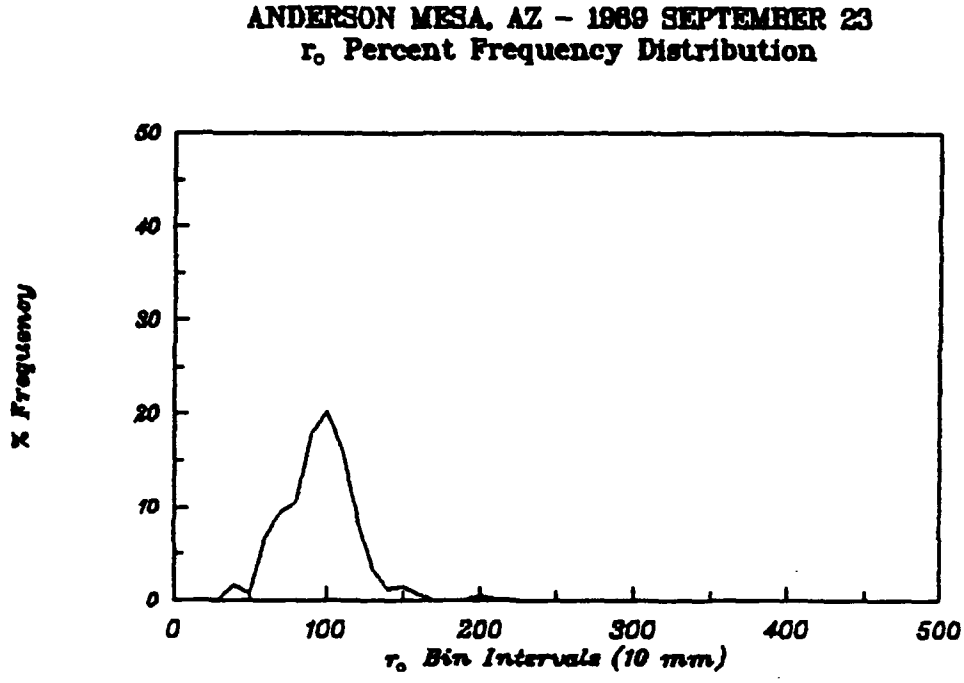

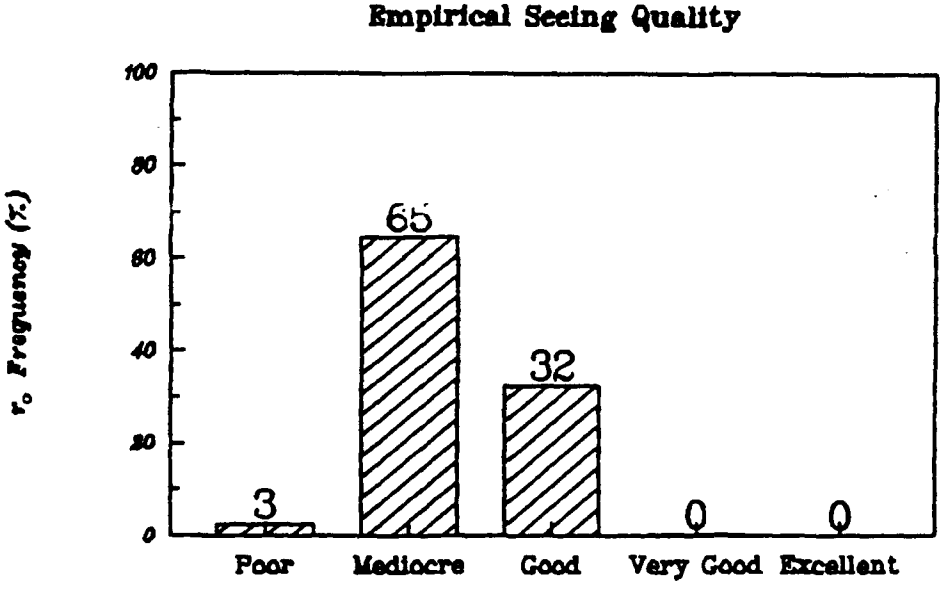

Fig 22. Anderson Mesa, Az r_o Statistics: 1989 Sept 23

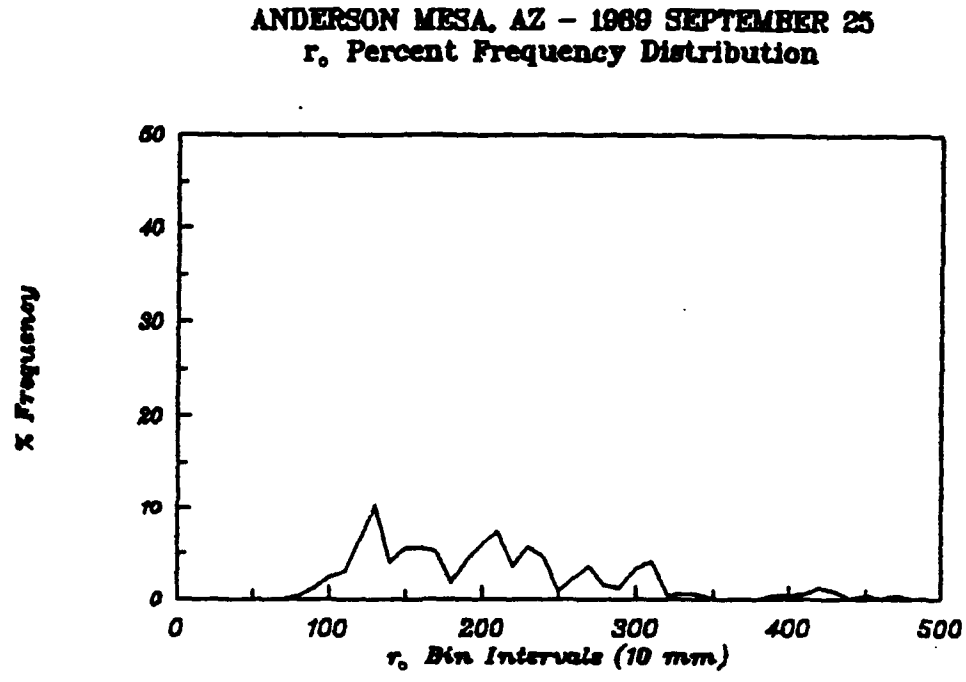

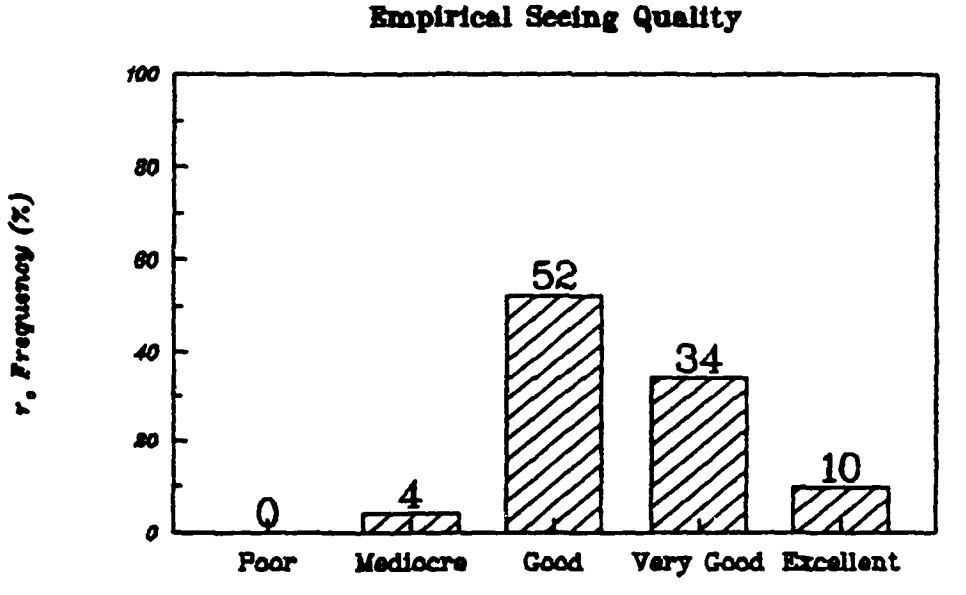

Fig 23. Anderson Mesa, Az r_o Statistics: 1989 Sept 25

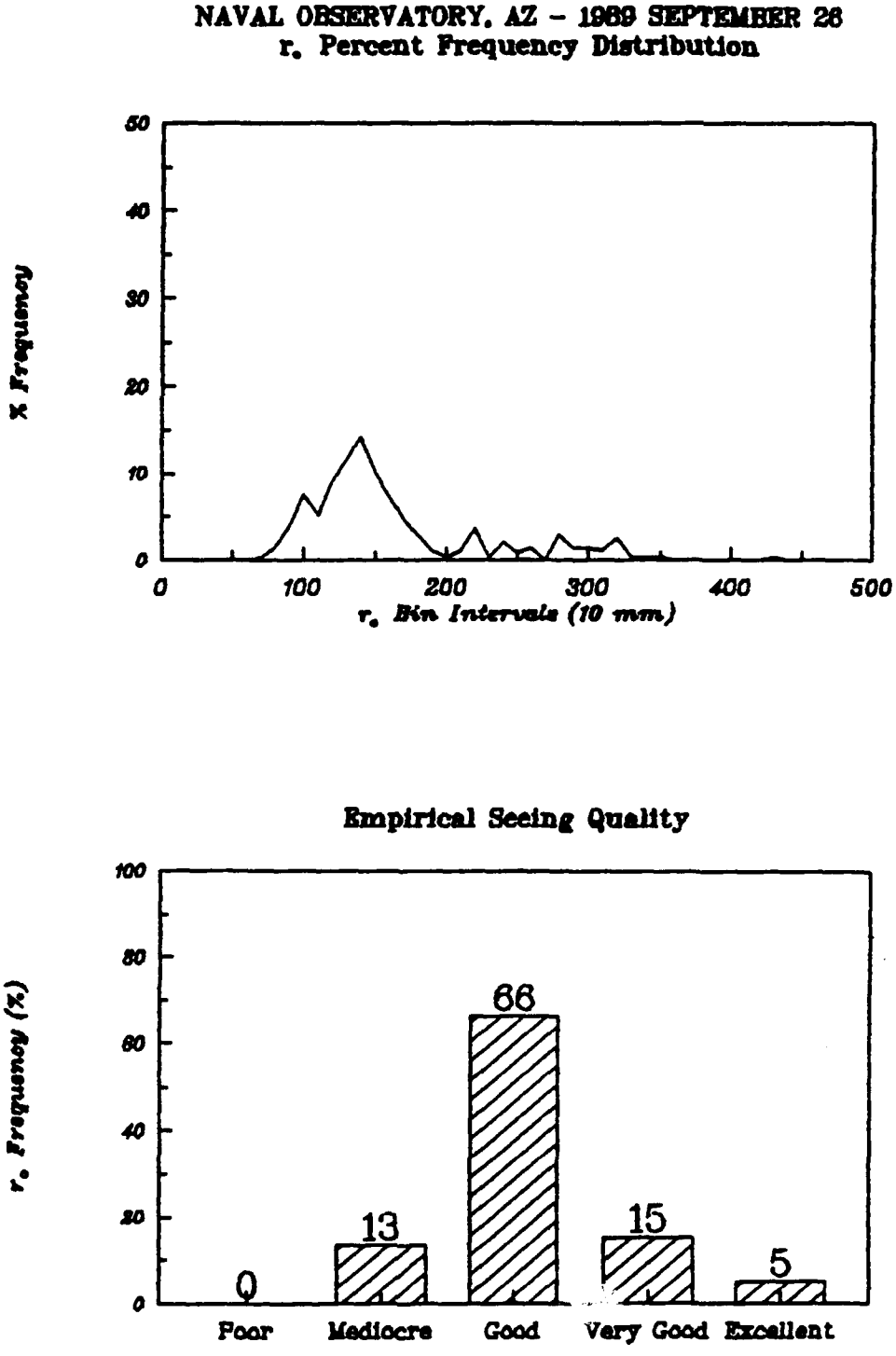

Fig 24. USNO, Az r_o Statistics: 1989 Sept 26

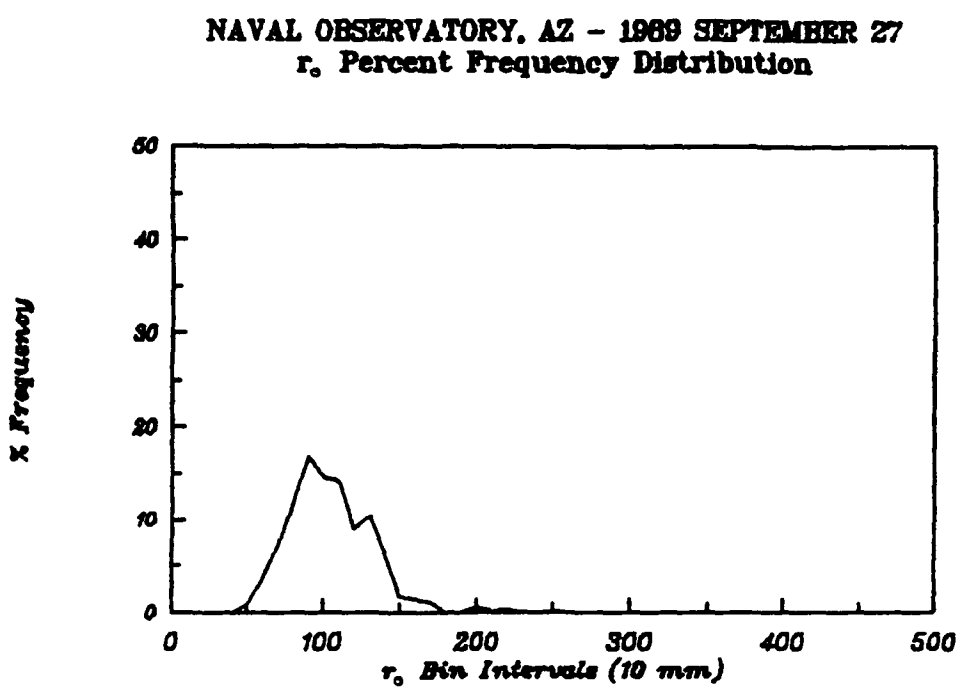

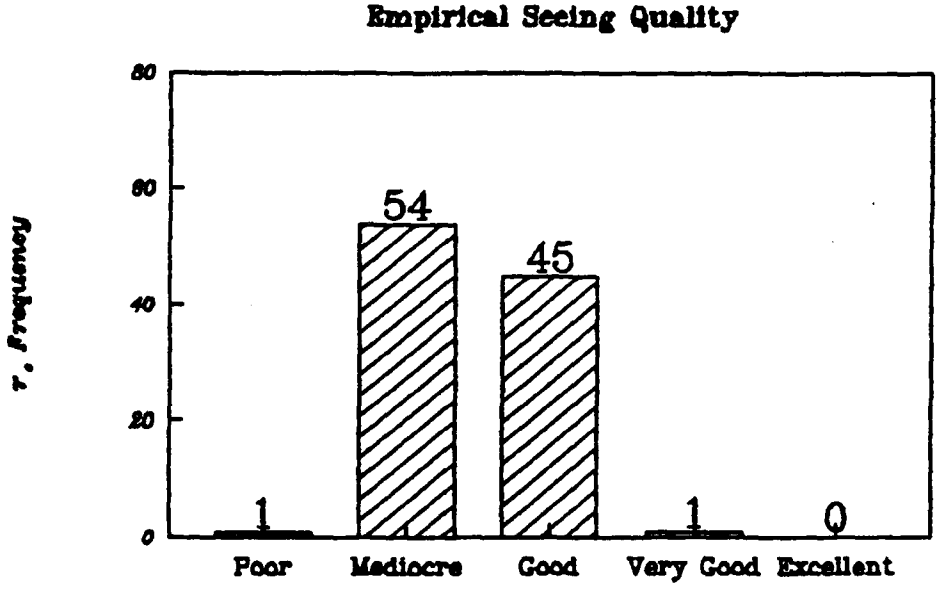

Fig 25. USNO, Az r_o Statistics: 1989 Sept 27

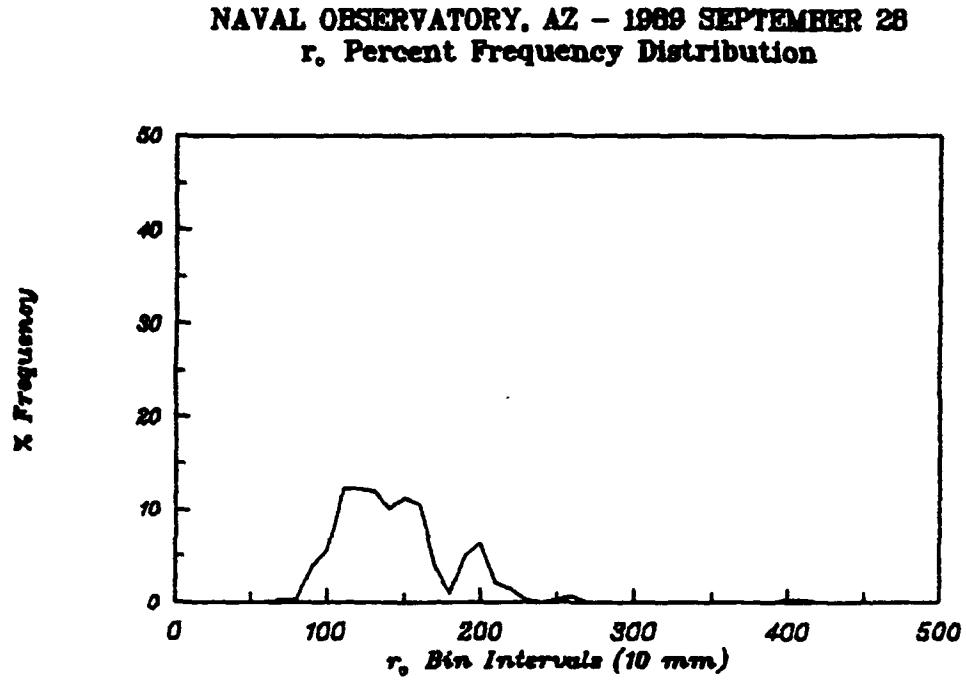

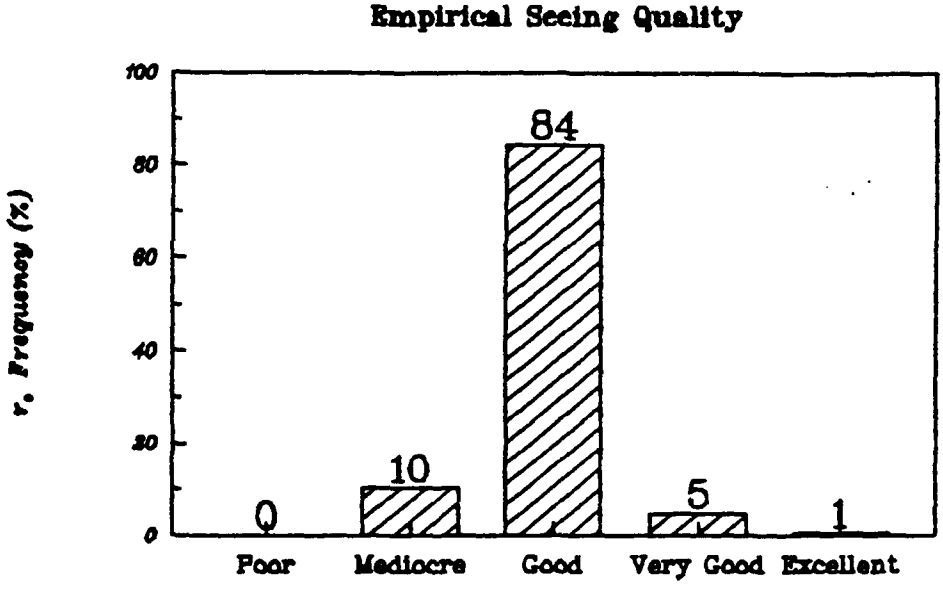

Fig 26. USNO, Az r_o Statistics: 1989 Sept 28

APPENDIX F. ISOPLANATIC ANGLE STATISTICS

To assist with the interpretation of the isoplanatic angle measurements, an un-normalized frequency distribution and an empirical seeing quality plot for each sampling session have been provided in Appendix F. The bin-size for this frequency distribution is 1 urad. The empirical seeing quality graphs use the following bin intervals:

Empirical Seeing Quality	θ_o measurement (urad)
Very Poor	0 - 4.0
Poor	4.1 - 8.0
Mediocre	8.1 - 12.0
Good	12.1 - 20.0
Very Good	20.1 - 30.0
Excellent	30.1 - 50.0

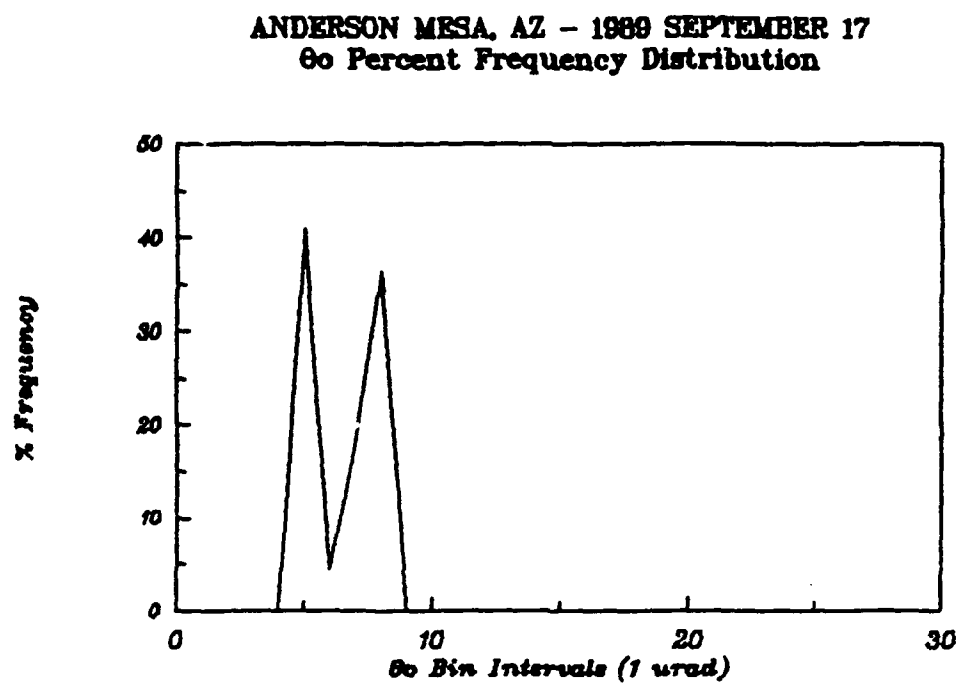

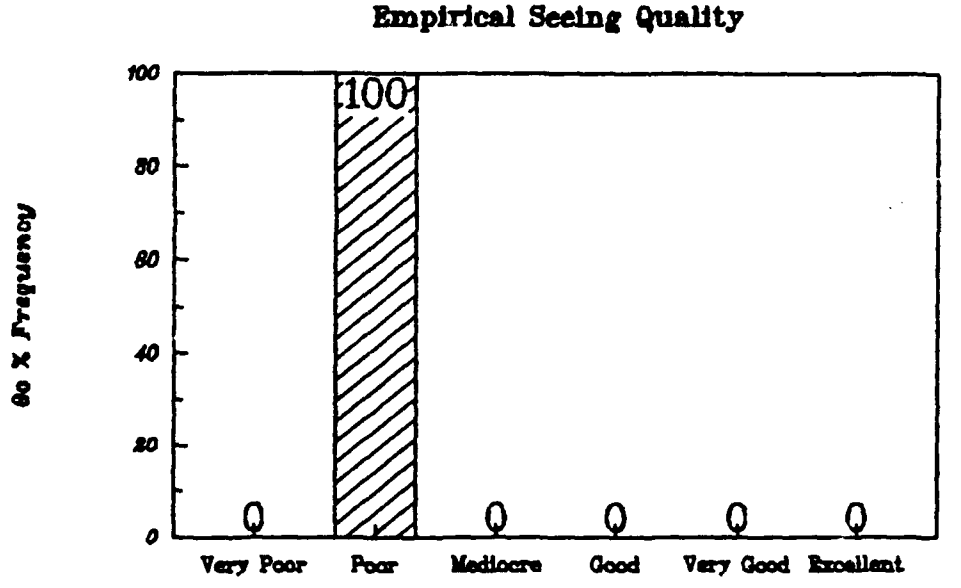

Fig 27. Anderson Mesa, Az θ_o Statistics: 1989 Sept 17

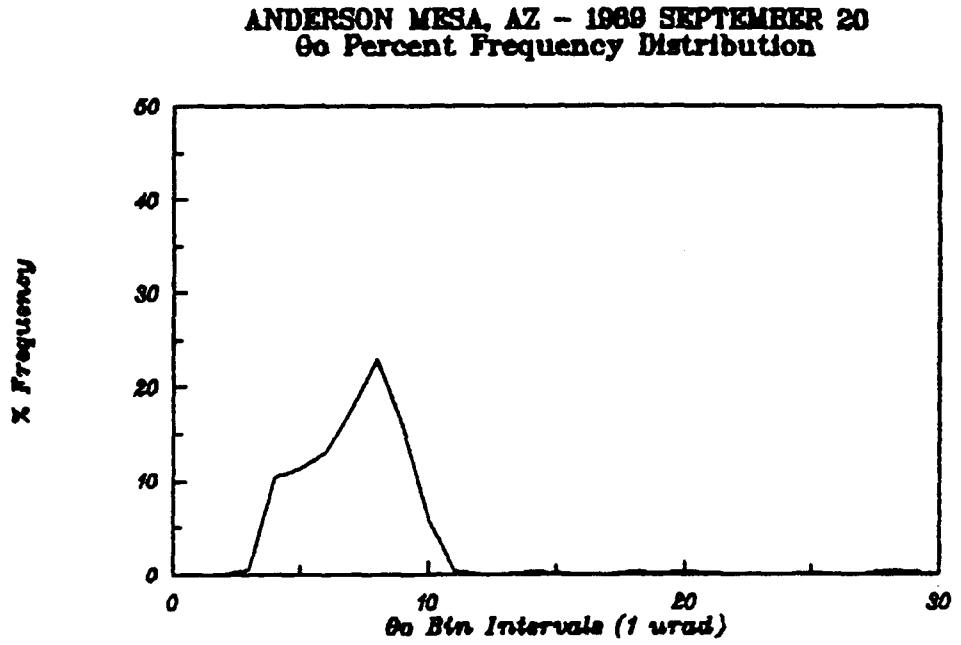

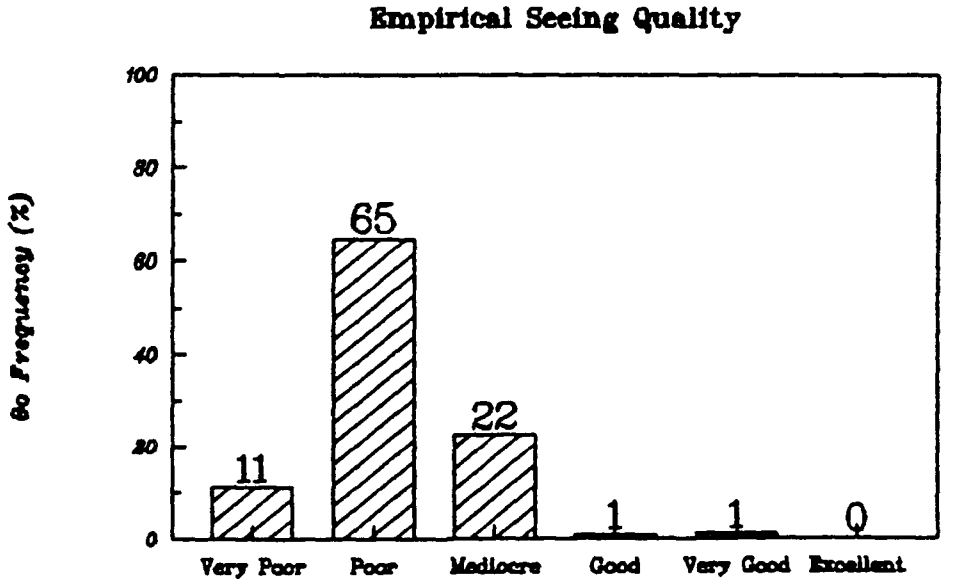

Fig 28. Anderson Mesa, Az θ_o Statistics: 1989 Sept 20

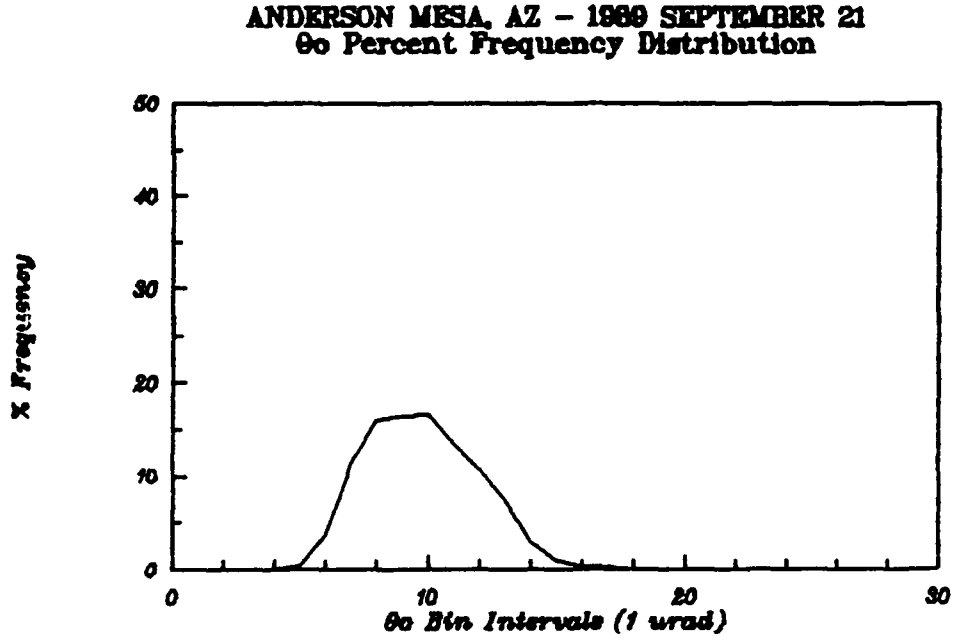

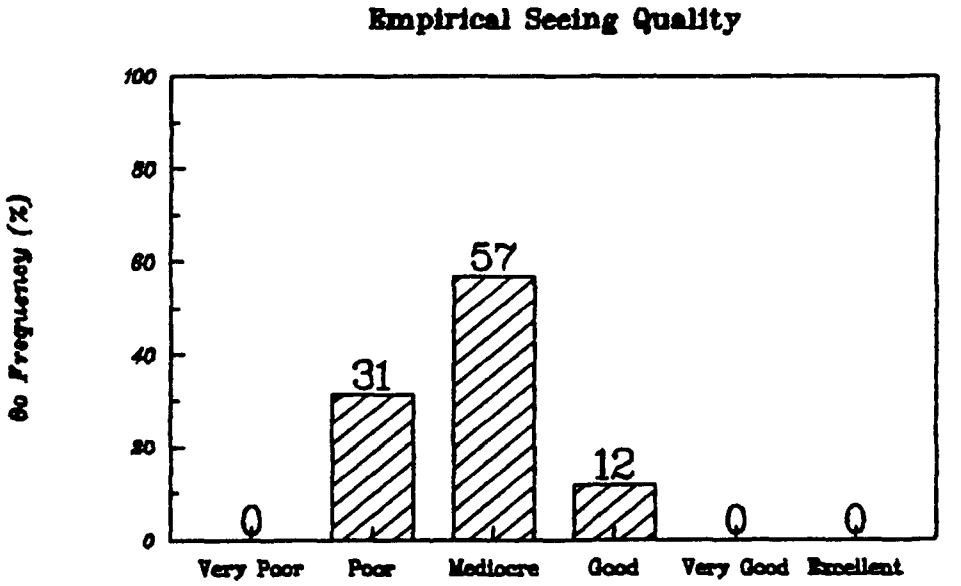

Fig 29. Anderson Mesa, Az θ_o Statistics: 1989 Sept 21

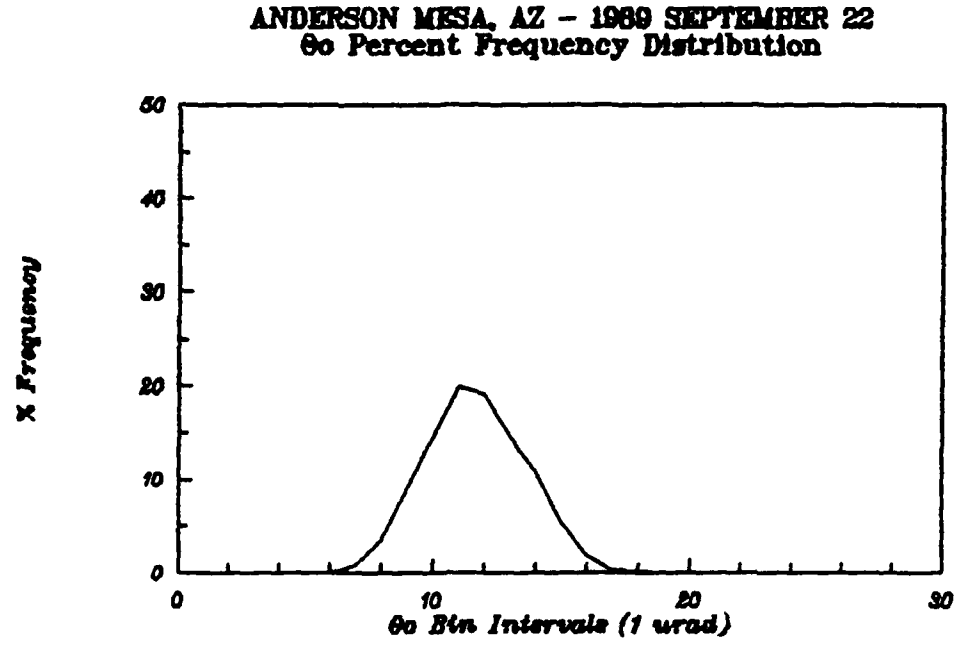

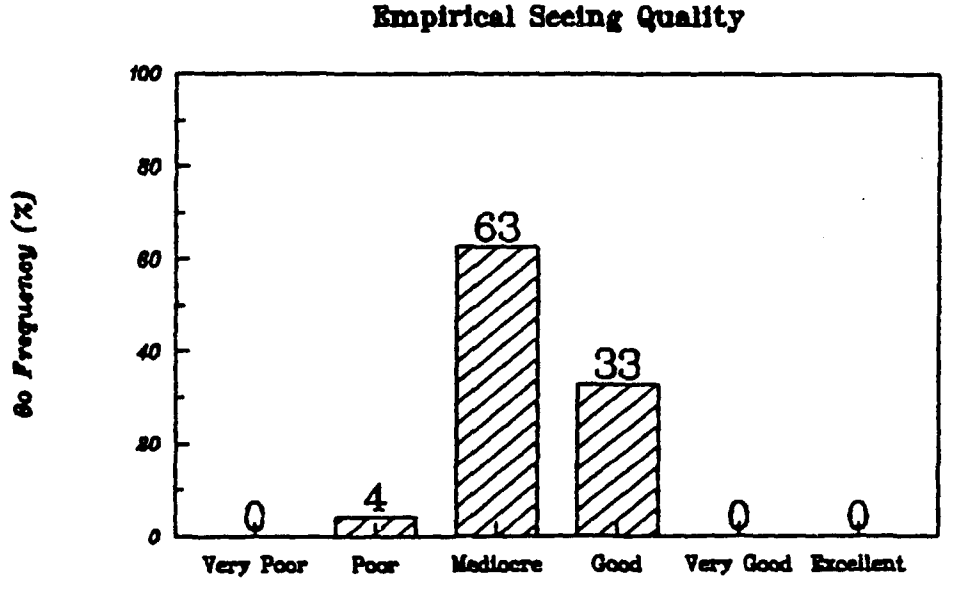

Fig 30. Anderson Mesa, Az θ_o Statistics: 1989 Sept 22

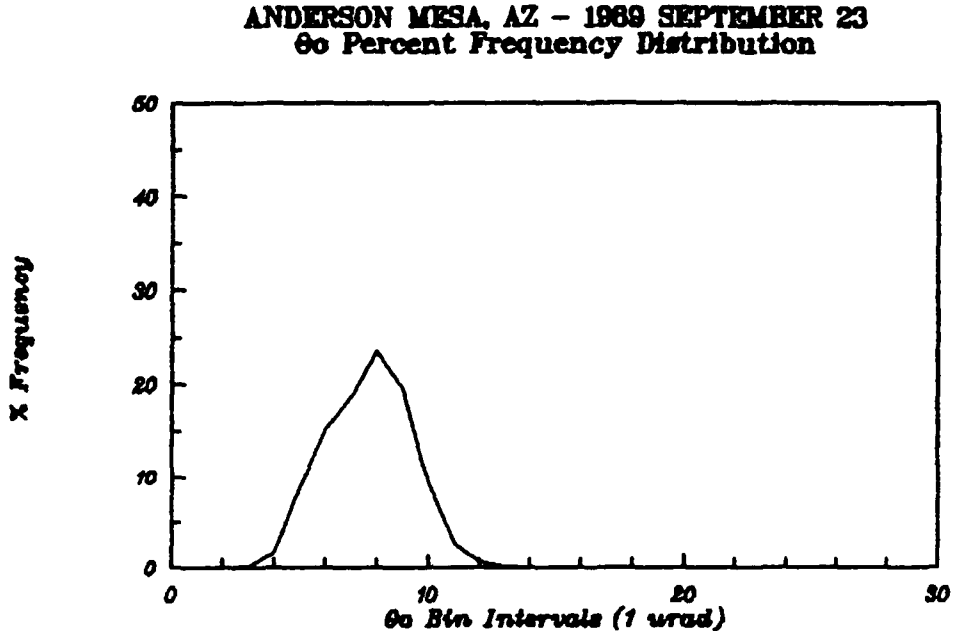

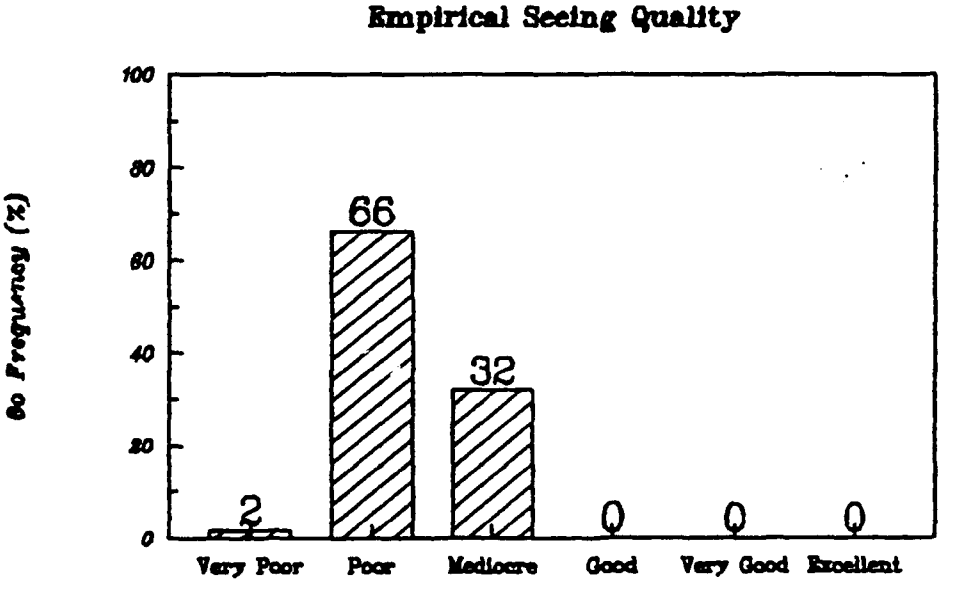

Fig 31. Anderson Mesa, Az θ_o Statistics: 1989 Sept 23

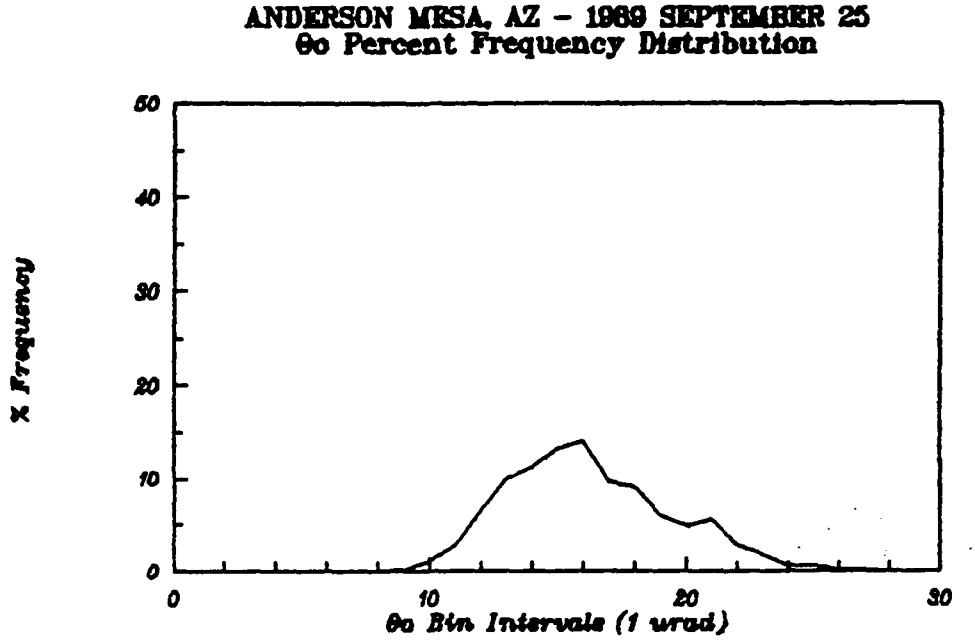

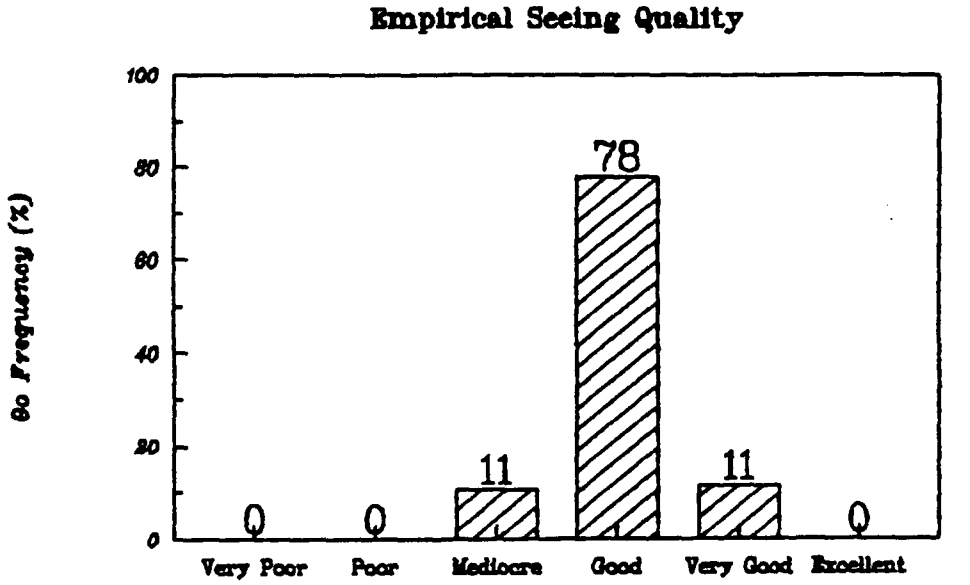

Fig 32. Anderson Mesa, Az θ_o Statistics: 1989 Sept 25

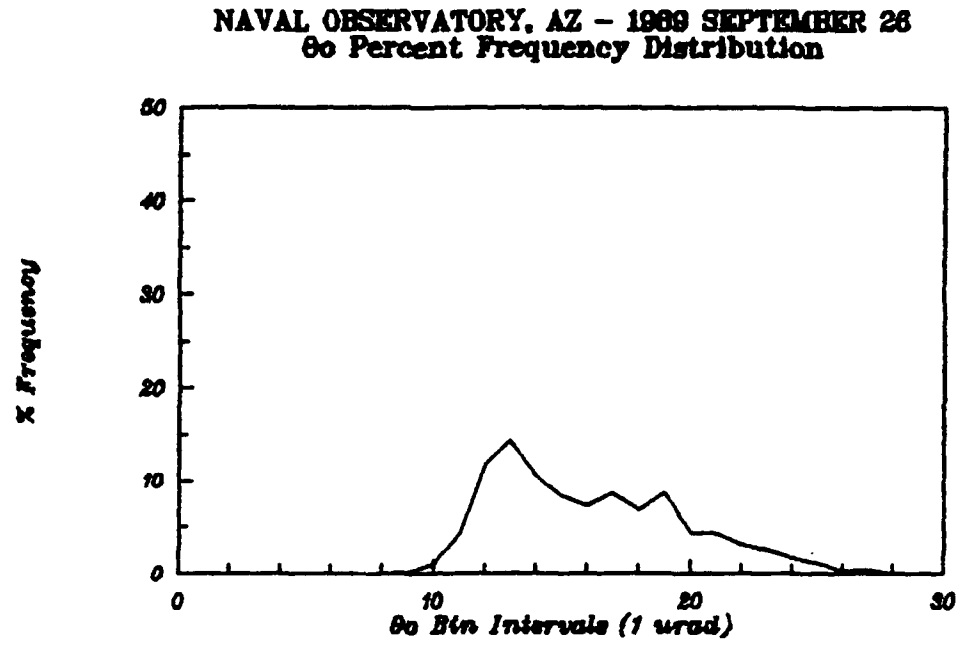

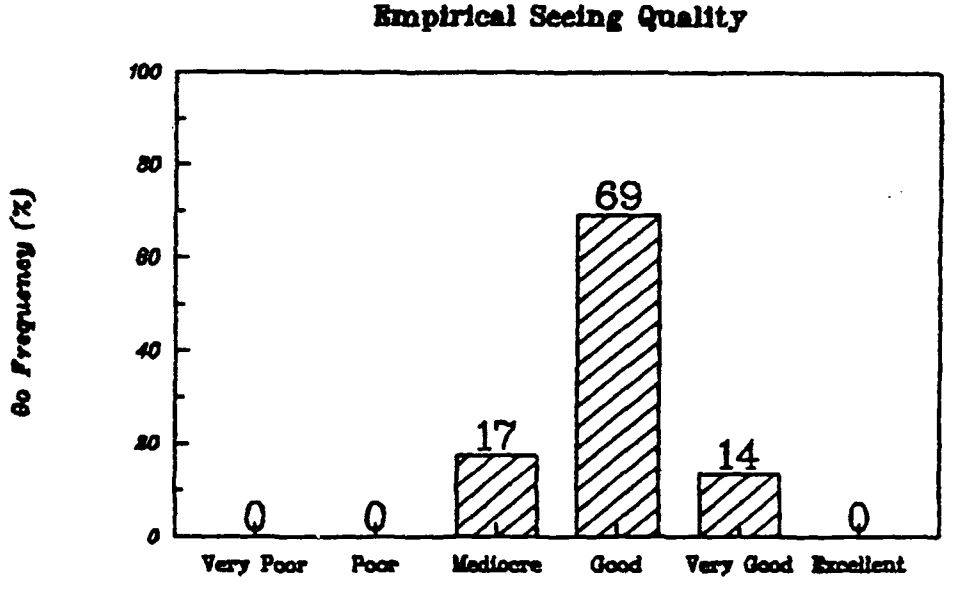

Fig 33. USNO, Az θ_o Statistics: 1989 Sept 26

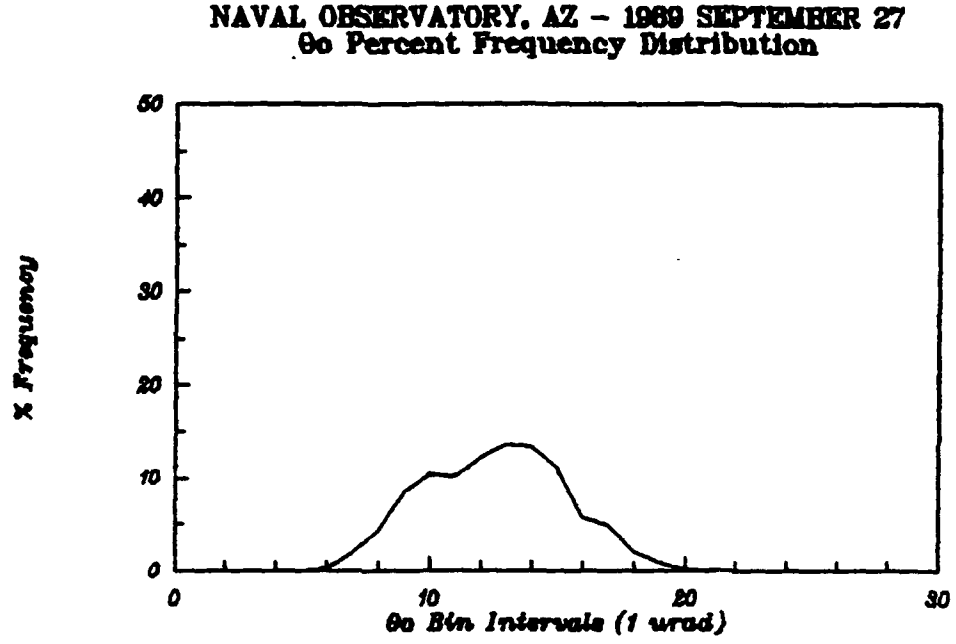

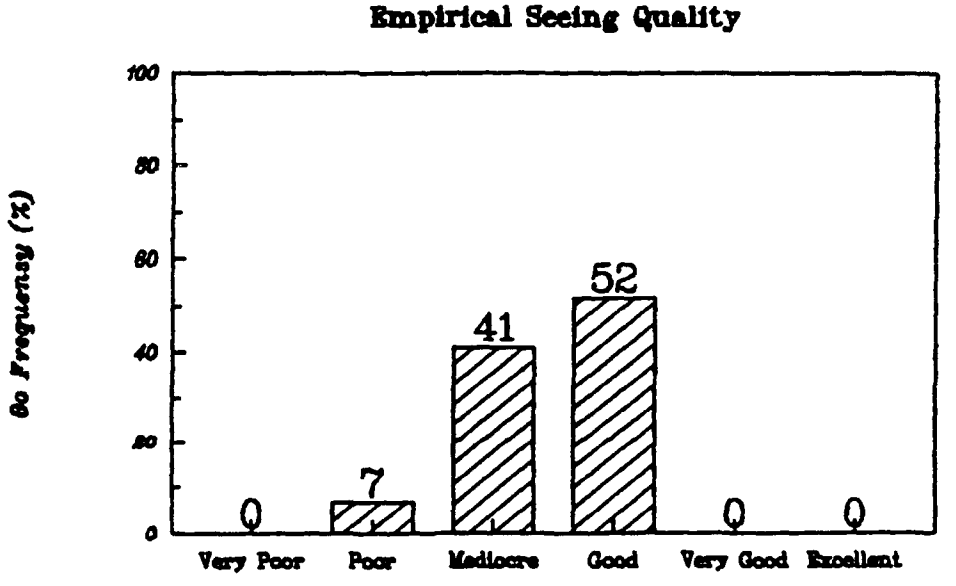

Fig 34. USNO, Az θ_o Statistics: 1989 Sept 27

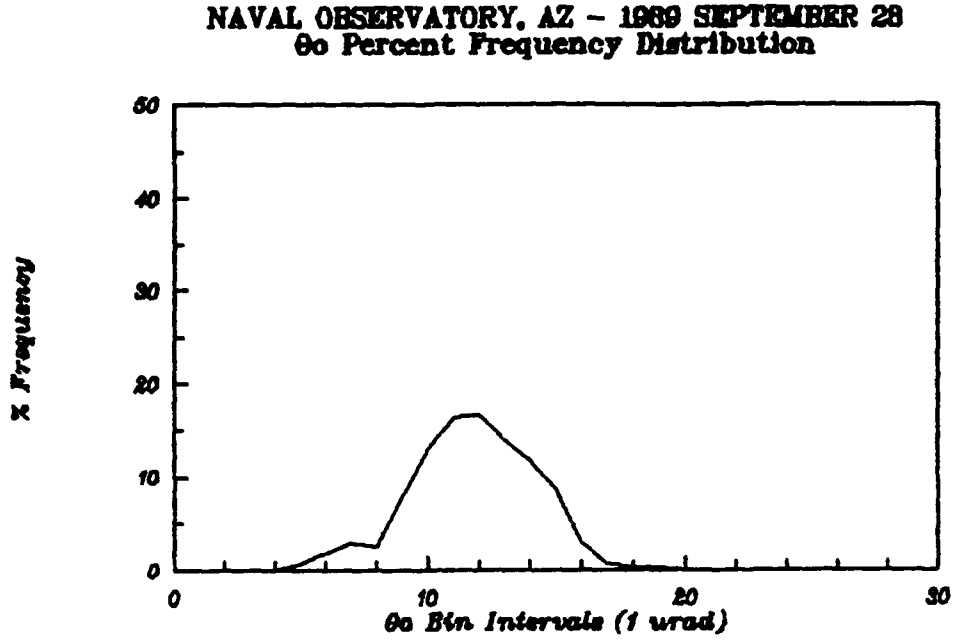

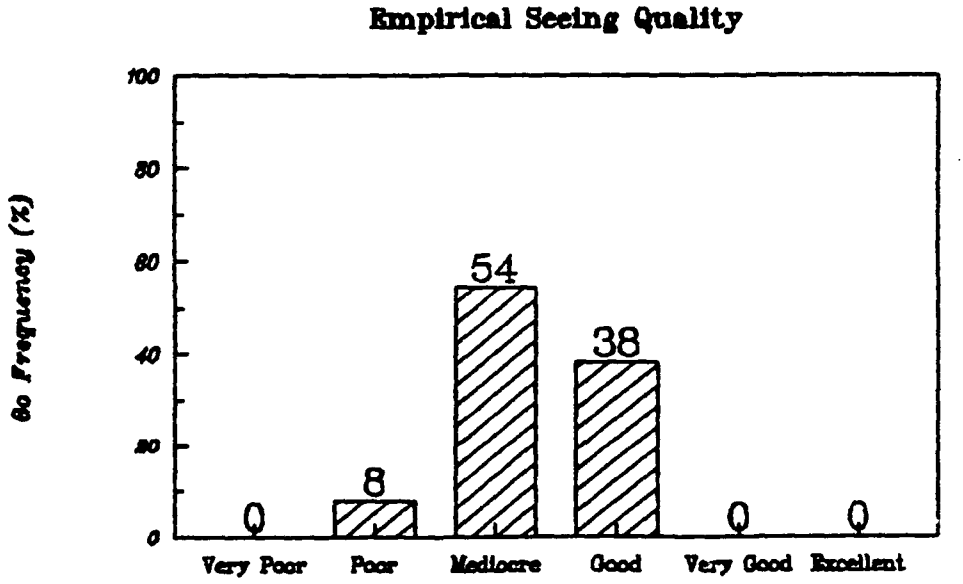

Fig 35. USNO, Az θ_o Statistics: 1989 Sept 28

APPENDIX G. RAWINSONDE THERMODYNAMIC PROFILES (Entire Sounding)

Appendix G includes two tables of balloon launch specifications, plus the entire rawinsonde thermodynamic profiles for both Anderson Mesa (1989 Sept 19-25 MST) and USNO (1989 Sept 26-28 MST), Flagstaff, Arizona. To facilitate quick inspection, all sounding heights are with respect to the local ground level. The following site elevations allow the conversion to height above mean sea level (MSL):

ANDERSON MESA(31" telescope dome): 7210 feet or 2198 meters,
USNO(61" telescope dome): 7560 feet or 2304 meters.

TABLE 6. BALLOON LAUNCH SCHEDULE - ANDERSON MESA/USNO

Sounding Name	Sounding Number	Night Number	Site* (AM/USNO)	Local Launch Date (yymmdd)	Local Launch Time (MST)
ANM91921	1	1	AM	890919	21:00
ANM92020	2	2	AM	890920	20:33
ANM92104	3	2	AM	890921	03:55
ANM92120	4	3	AM	890921	19:57
ANM92204	5	3	AM	890922	03:48
ANM92220	6	4	AM	890922	20:04
ANM92304	7	4	AM	890923	03:40
ANM92504	8	5	AM	890925	03:41
USN92522	1	1	USNO	890925	22:20
USN92620	2	2	USNO	890926	20:29
USN92703	3	2	USNO	890927	02:46
USN92720	4	3	USNO	890927	20:06

* AM = Anderson Mesa-Lowell Observatory, Flagstaff, Arizona;
USNO = United States Naval Observatory, Flagstaff, Arizona.

TABLE 7. LAUNCH SPECIFICATIONS - ANDERSON MESA/USNO

Sounding Name	Site Code (AM/USNO)	Sounding Duration (min)	Maximum Height MSL* (m)	Average+ Vertical Resolution (m)	Local Loran-Wind Information (Yes/No)
ANM91921	AM	50.9	10874.7	3.6	Yes
ANM92020	AM	69.1	16377.4	4.3	Yes
ANM92104	AM	96.3	20895.7	4	Yes
ANM92120	AM	81.9	20200.4	4.6	Yes(partial)
ANM92204	AM	119.5	17839.2	2.7	Yes
ANM92220	AM	99.2	22145.1	4.2	Yes
ANM92304	AM	76.6	19201.4	4.6	No
ANM92504	AM	119.6	9162.4	1.2	Yes(partial)
USN92522	USNO	77.7	20341.5	4.8	Yes
USN92620	USNO	74.6	19424.7	4.7	No
USN92703	USNO	101.8	23436.7	4.3	Yes
USN92720	USNO	75.3	20078.1	4.9	Yes(mostly)

* Height MSL = height above mean sea level.

+ The average height resolution between vertical sample points in a particular sounding.

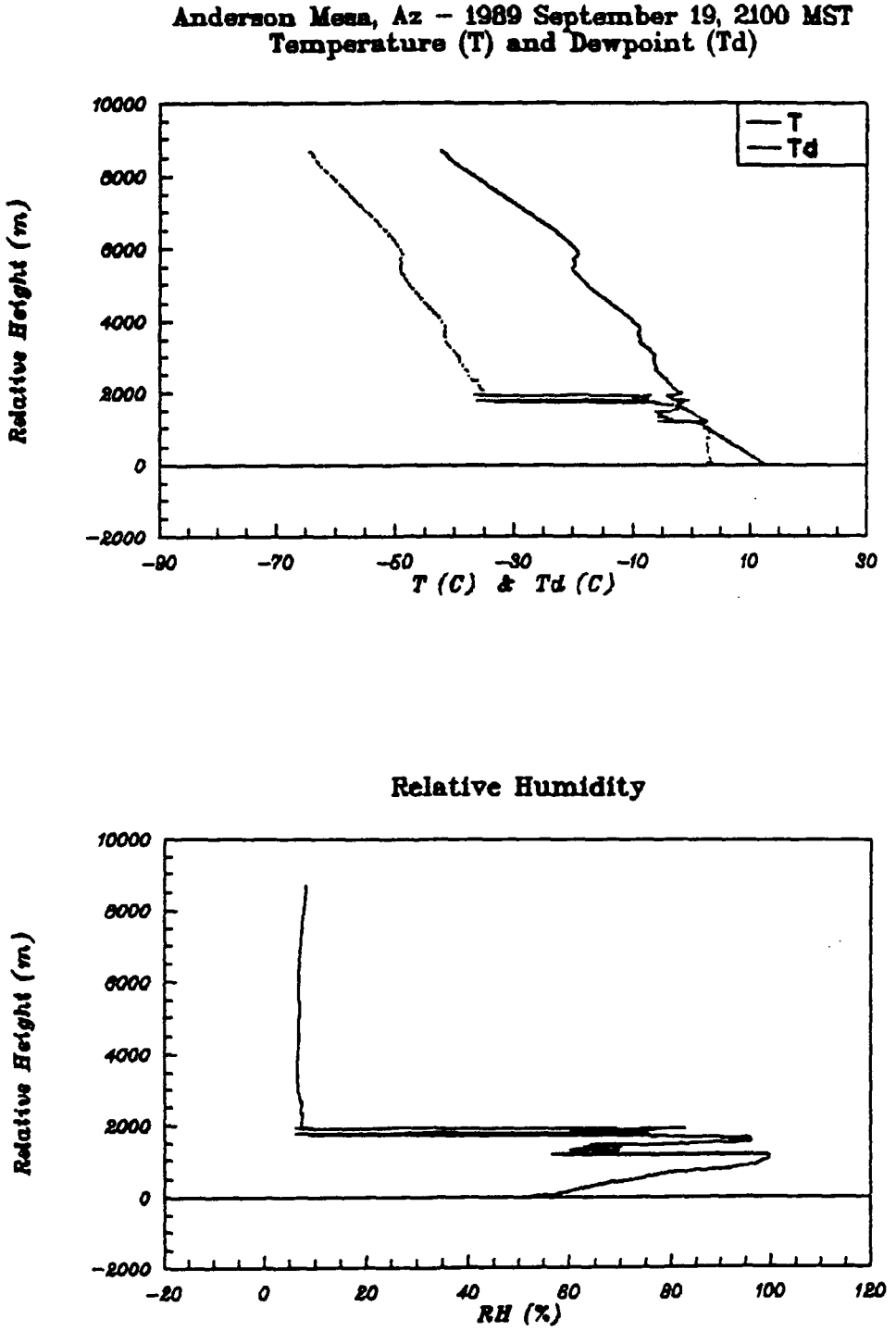

Fig 36. Entire Rawinsonde Profile: 1989 Sept 19, 2100 MST

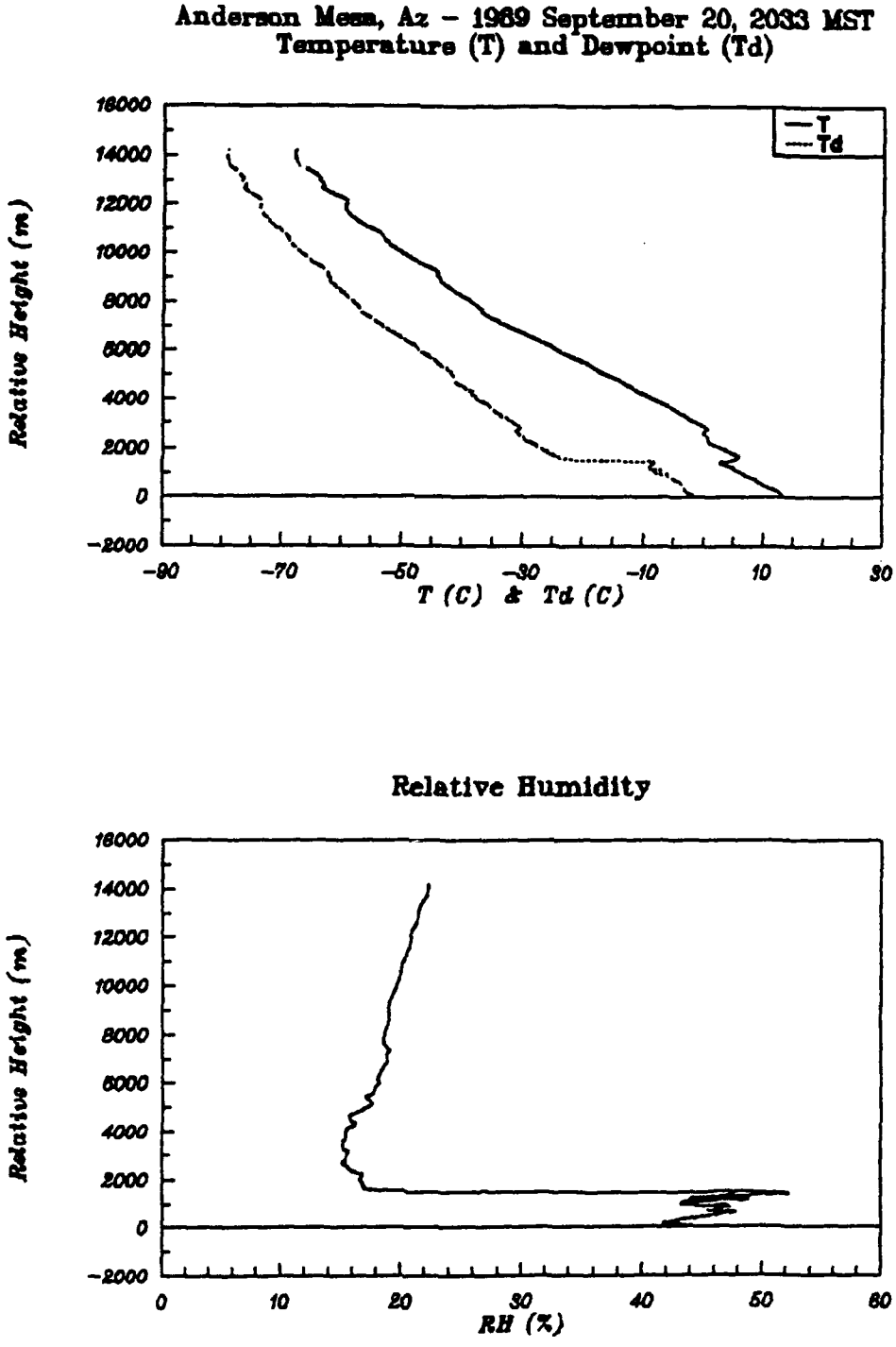

Fig 37. Entire Rawinsonde Profile: 1989 Sept 20, 2033 MST

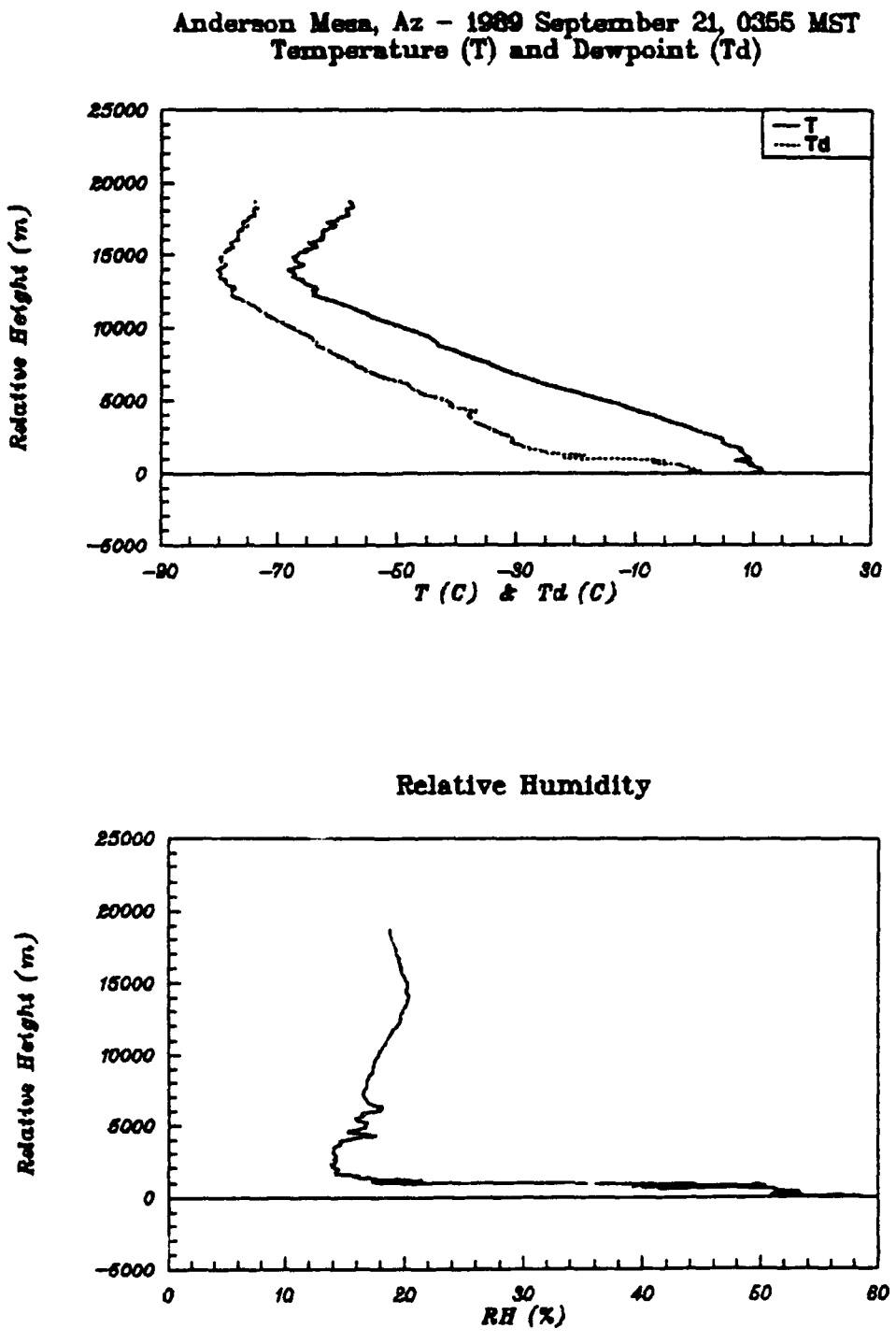

Fig 38. Entire Rawinsonde Profile: 1989 Sept 21, 0355 MST

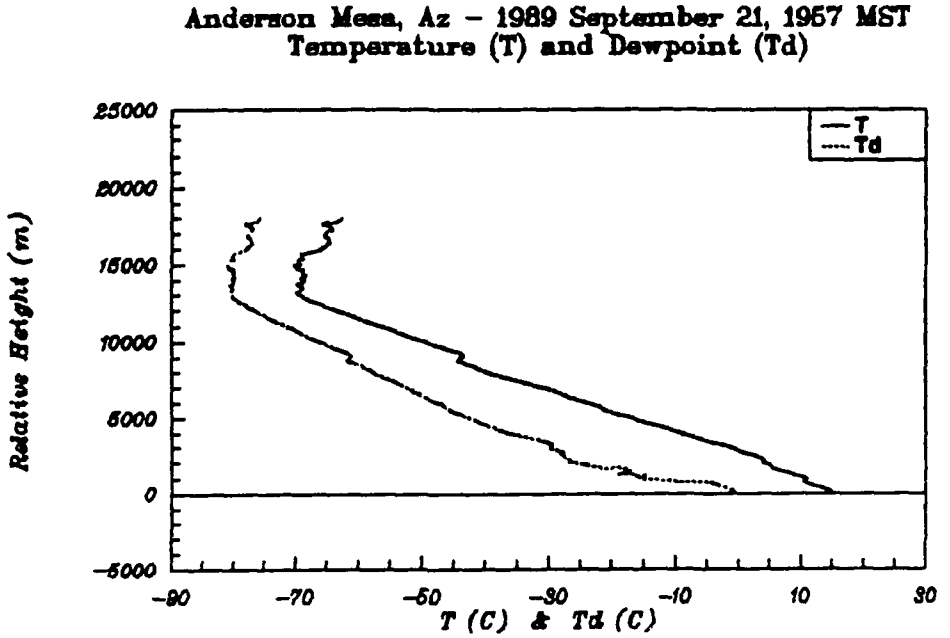

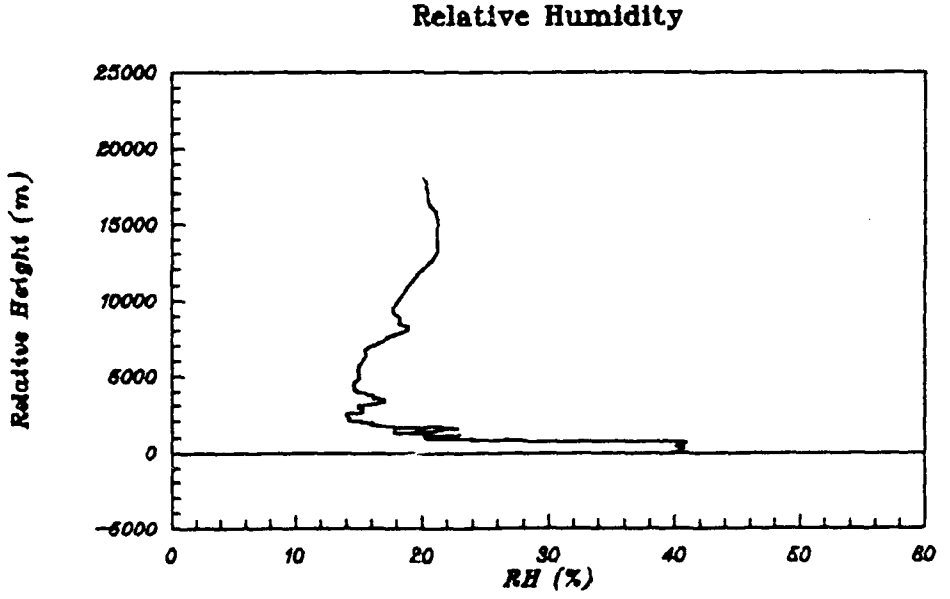

Fig 39. Entire Rawinsonde Profile: 1989 Sept 21, 1957 MST

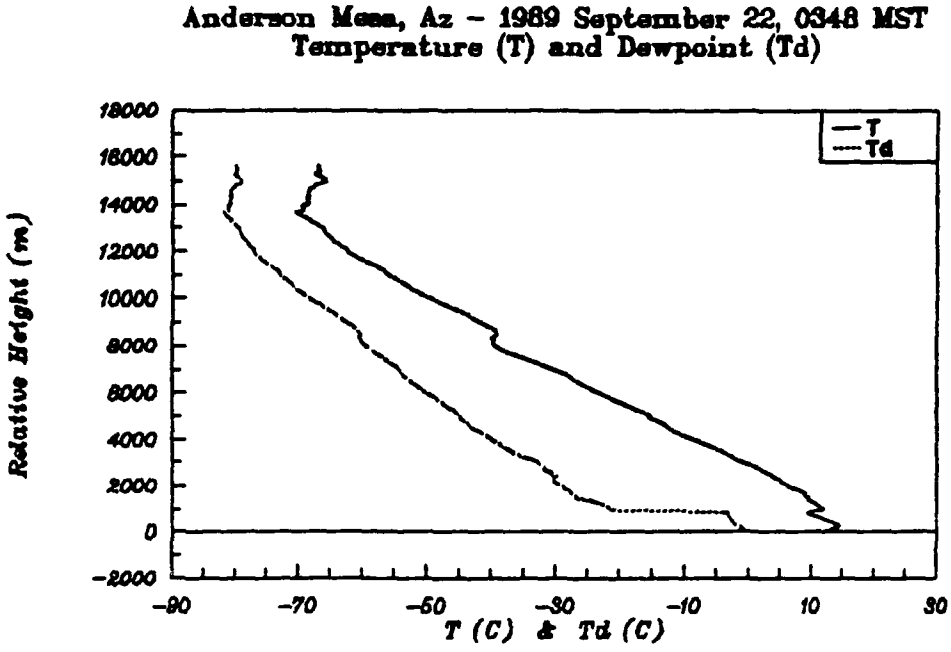

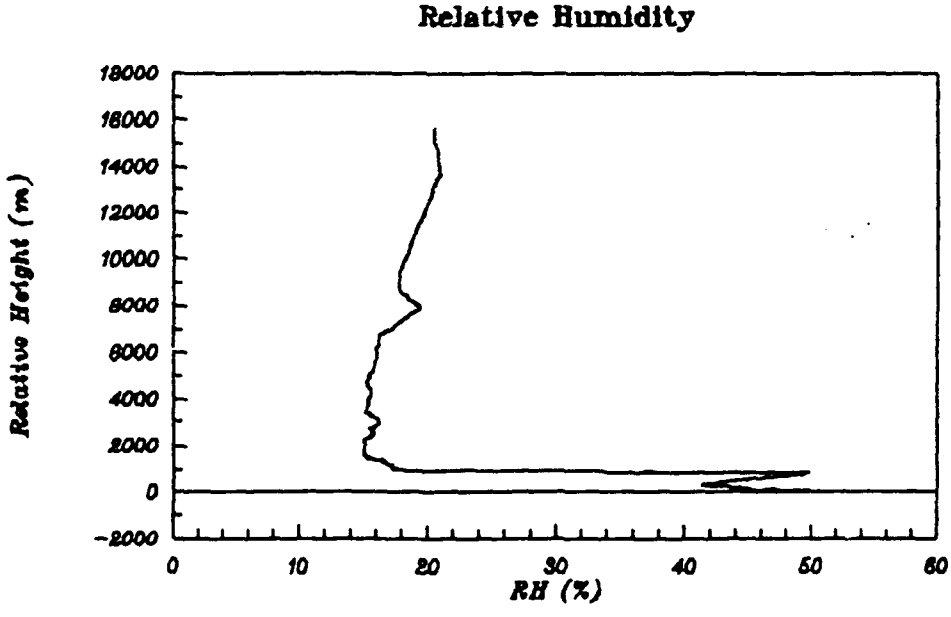

Fig 40. Entire Rawinsonde Profile: 1989 Sept 22, 0348 MST

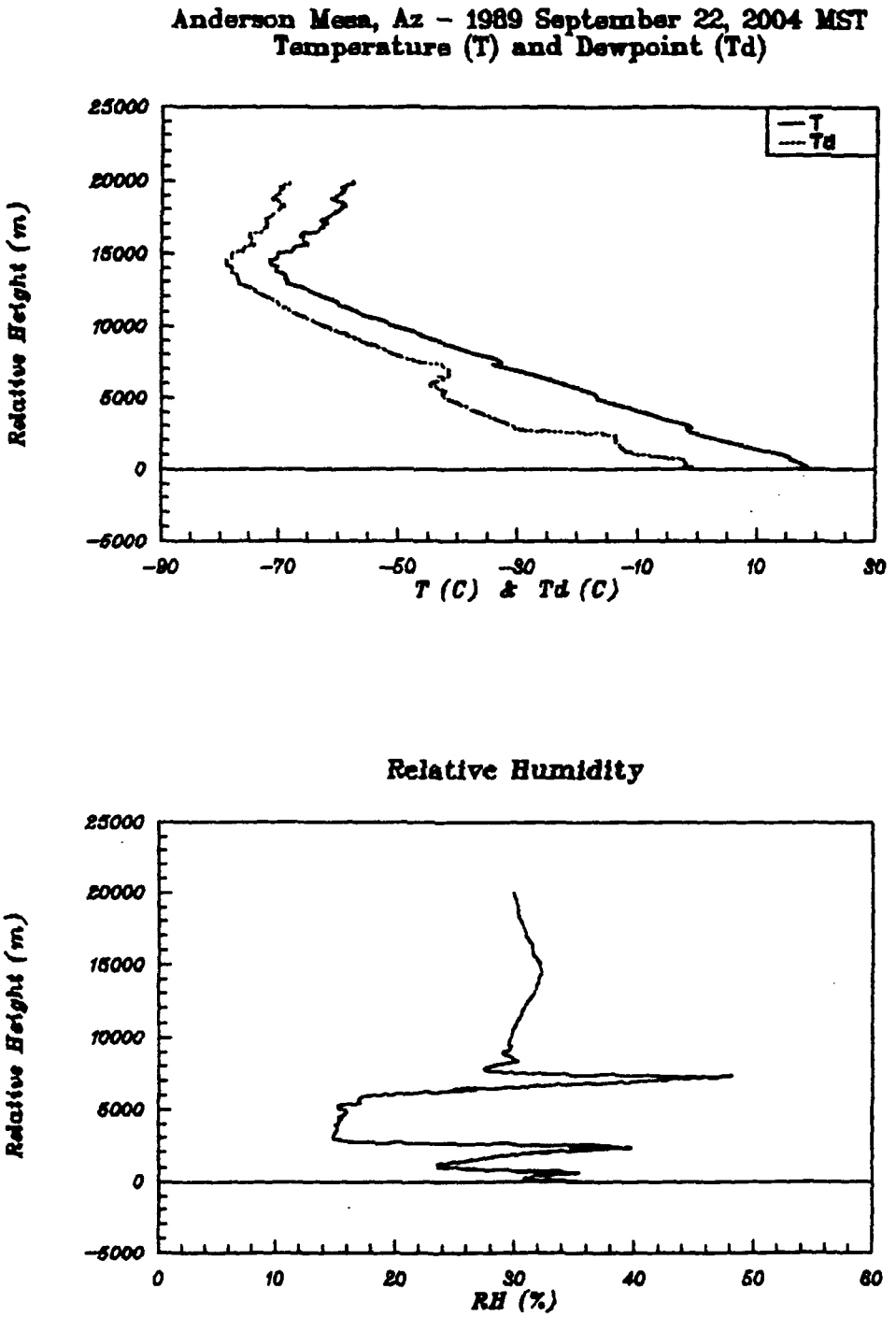

Fig 41. Entire Rawinsonde Profile: 1989 Sept 22, 2004 MST

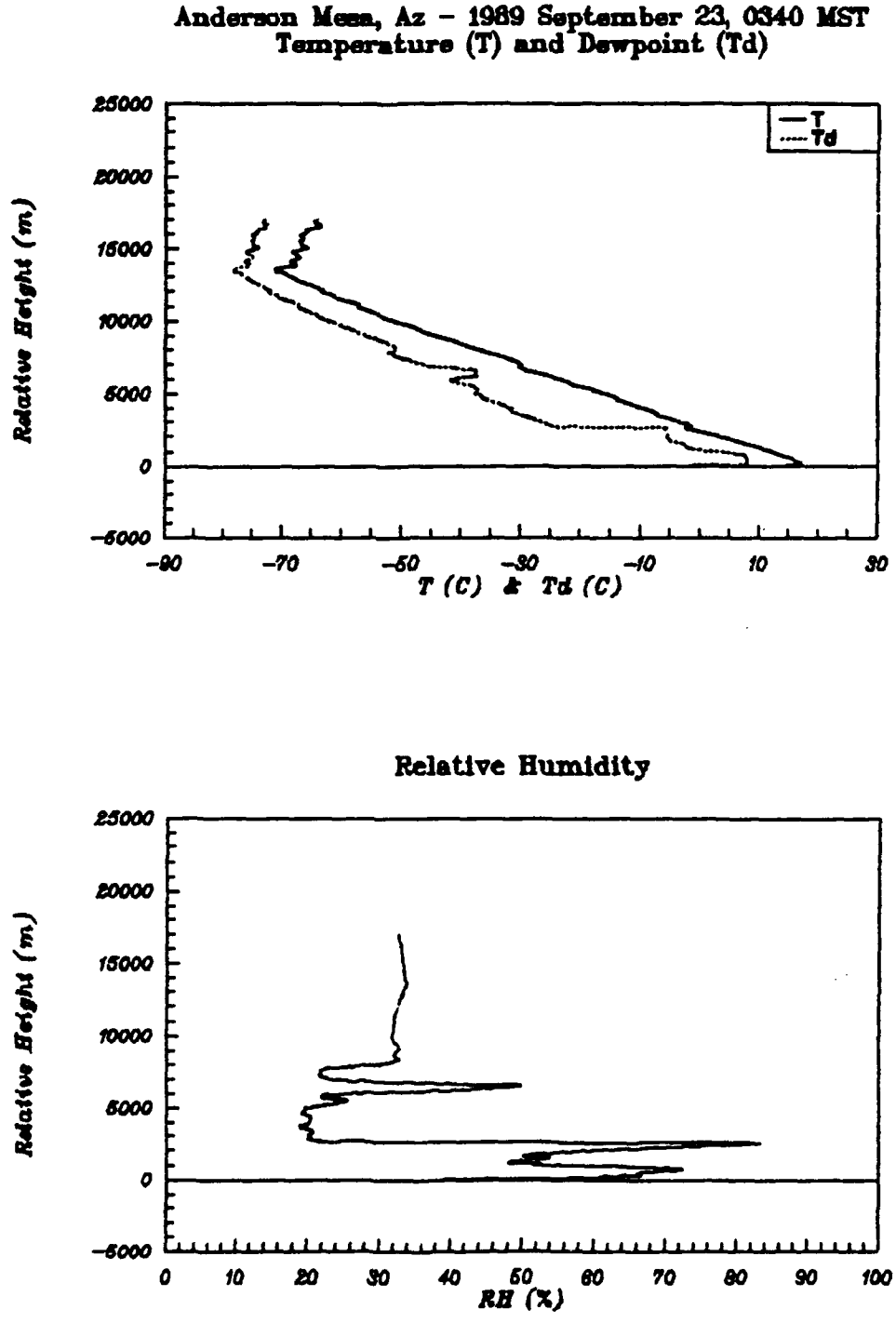

Fig 42. Entire Rawinsonde Profile: 1989 Sept 23, 0340 MST

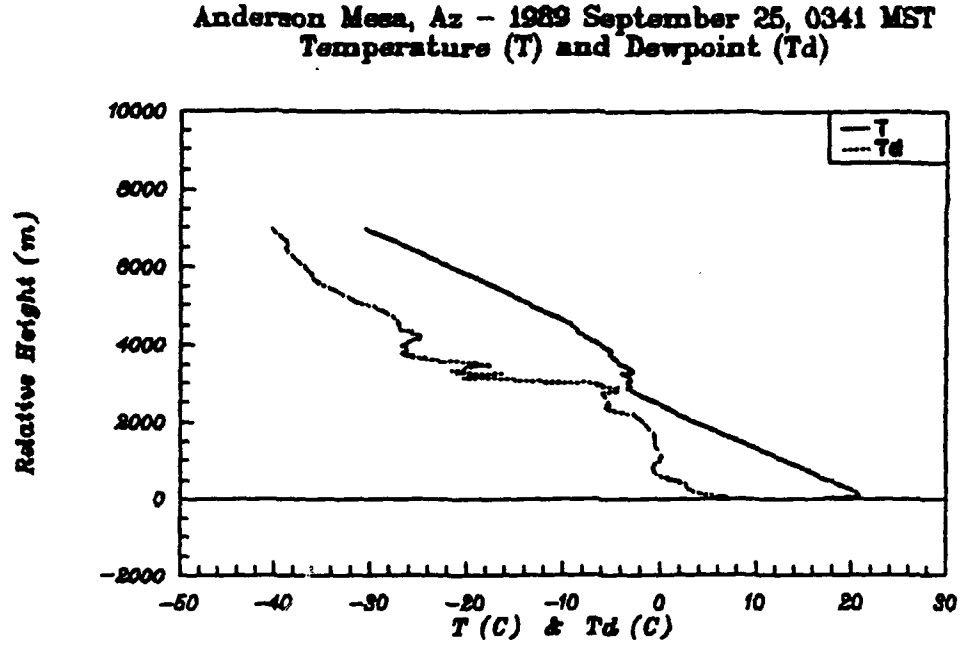

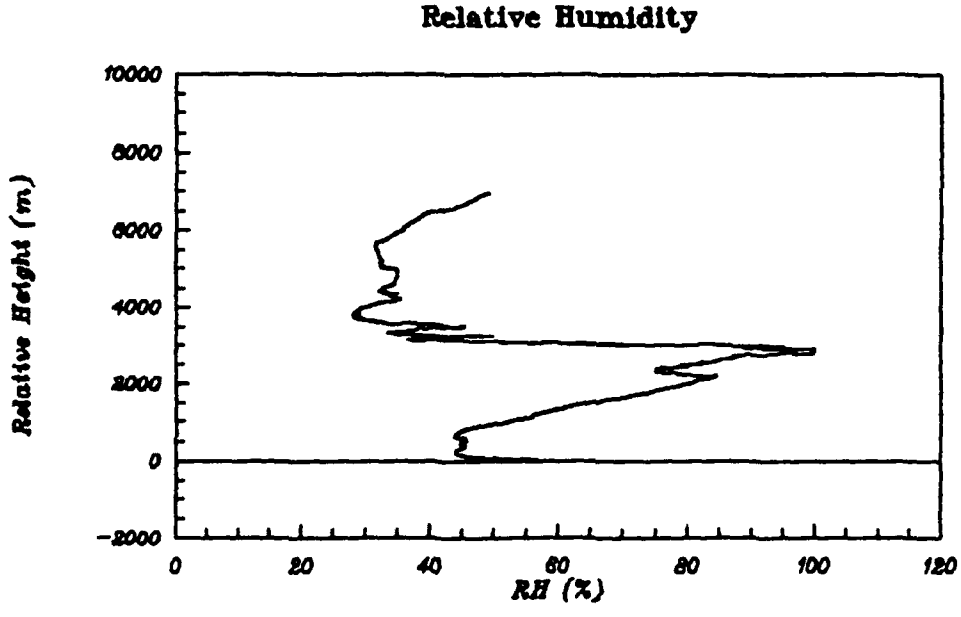

Fig 43. Entire Rawinsonde Profile: 1989 Sept 25, 0341 MST

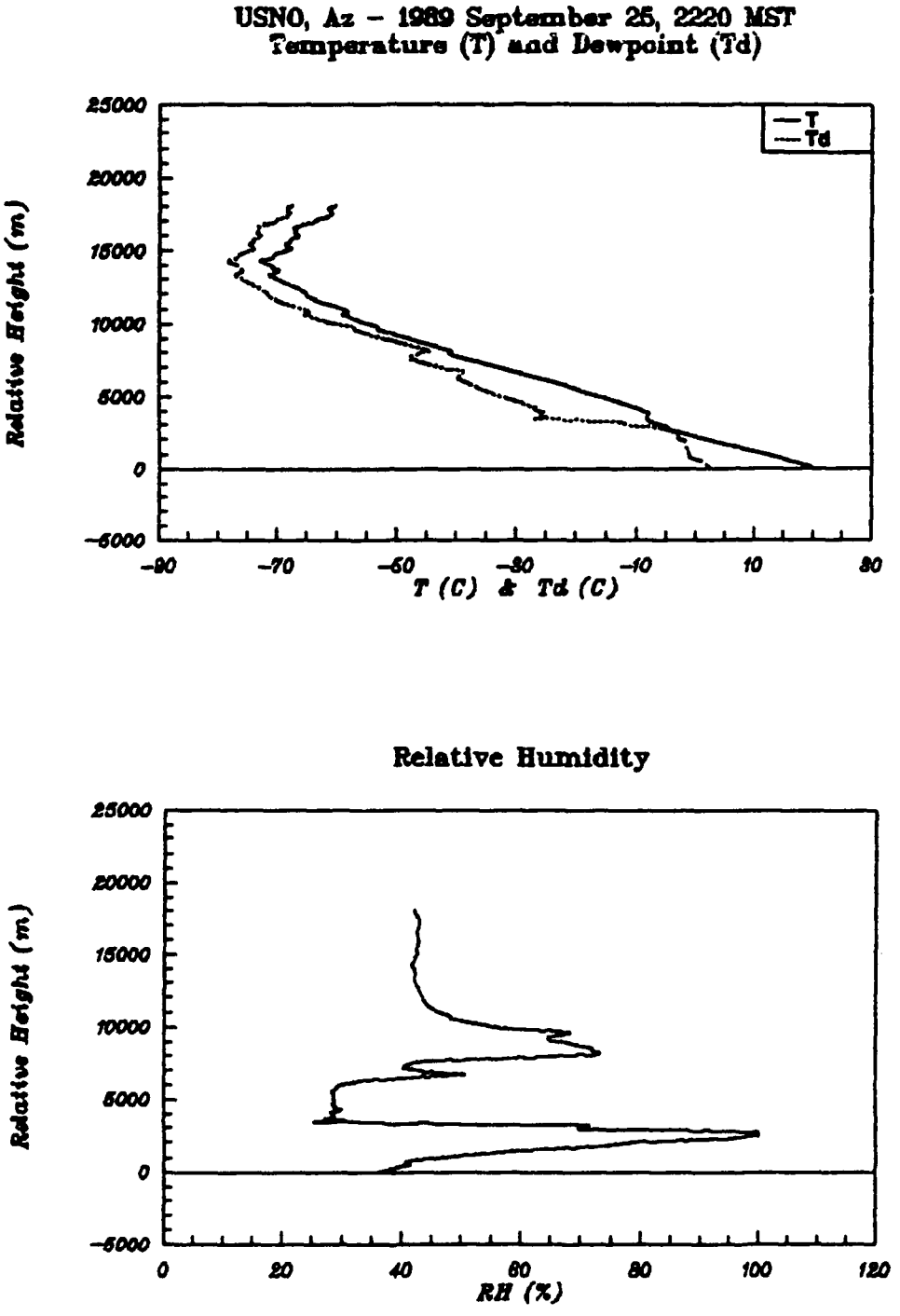

Fig 44. Entire Rawinsonde Profile: 1989 Sept 25, 2220 MST

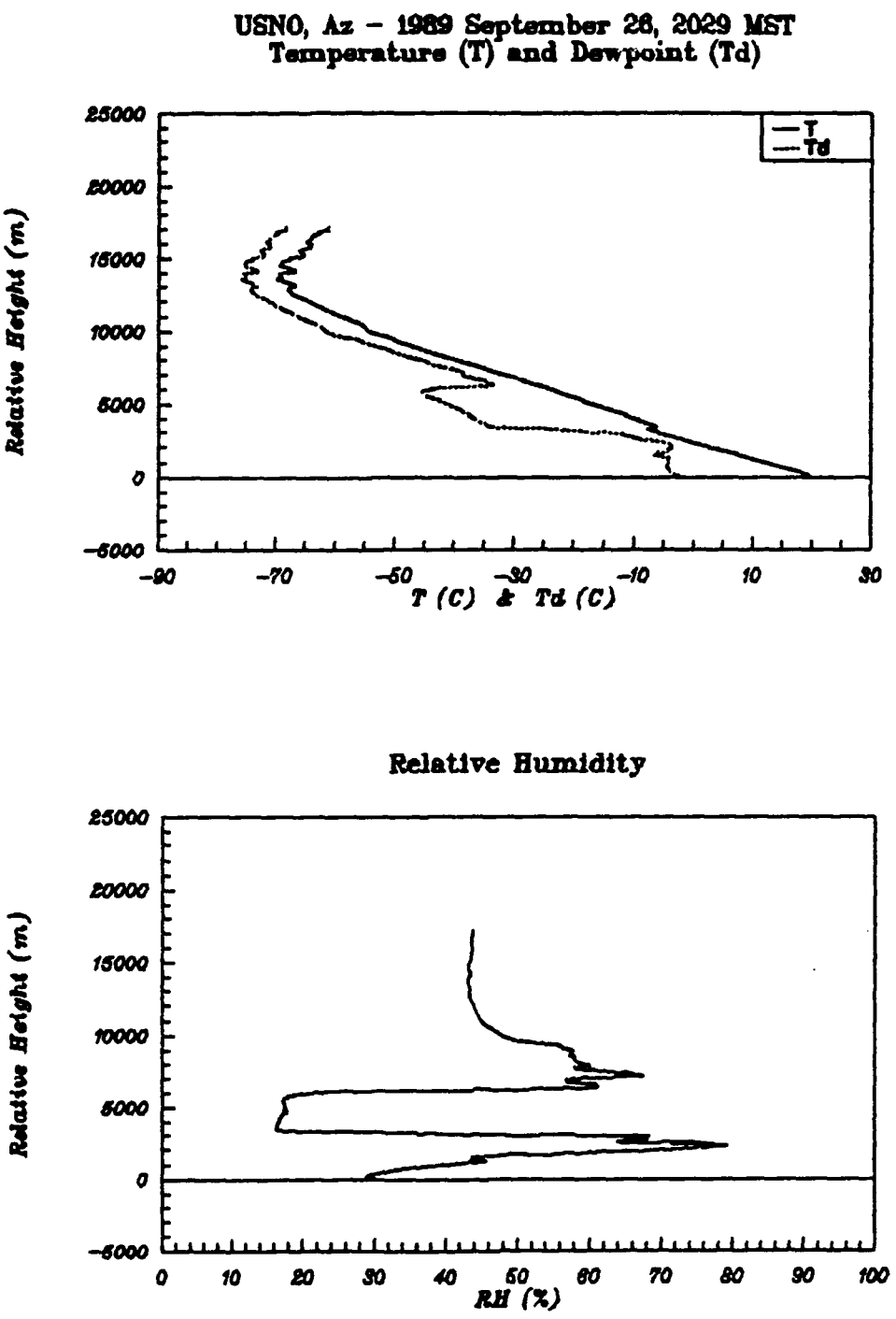

Fig 45. Entire Rawinsonde Profile: 1989 Sept 26, 2029 MST

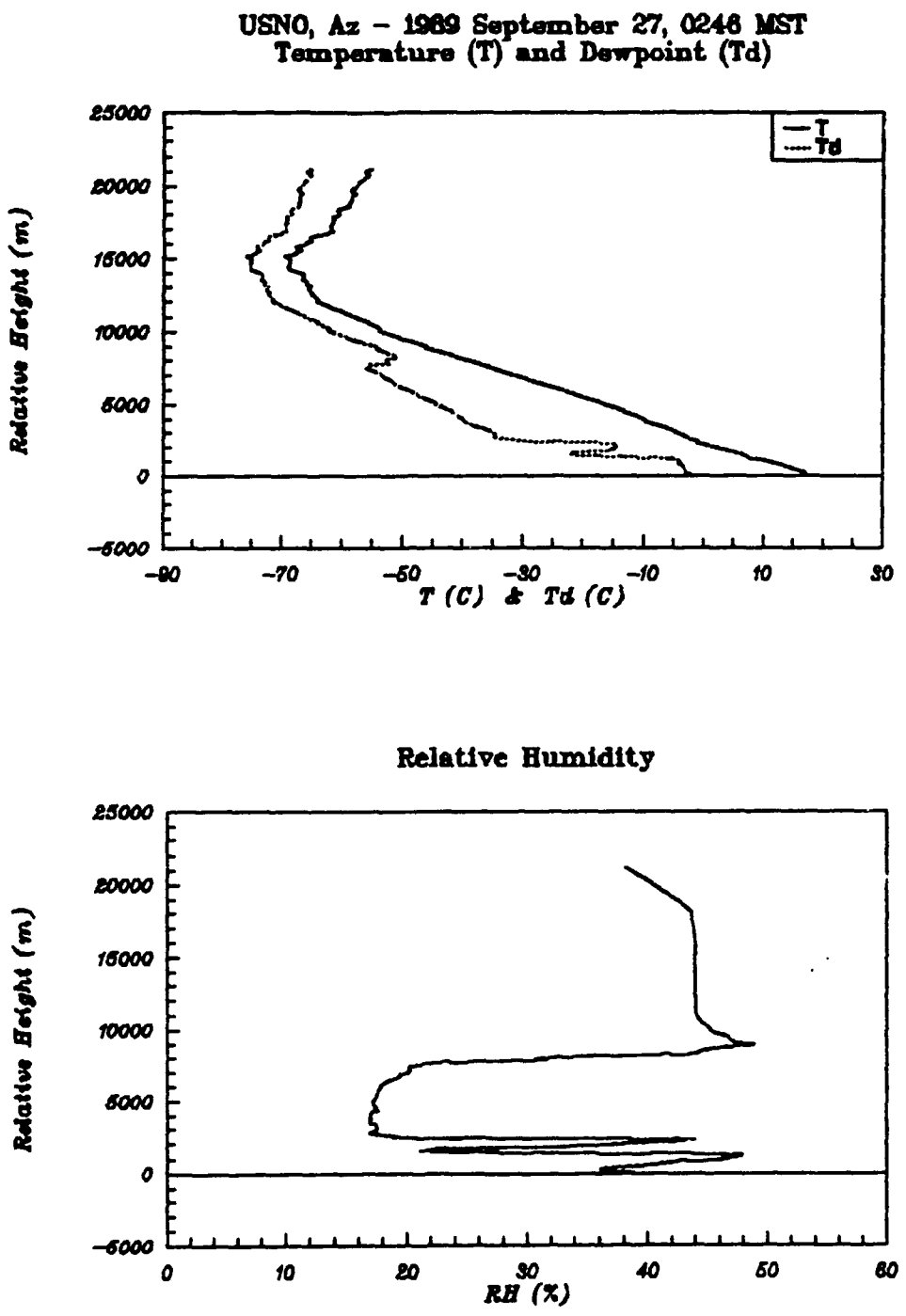

Fig 46. Entire Rawinsonde Profile: 1989 Sept 27, 0246 MST

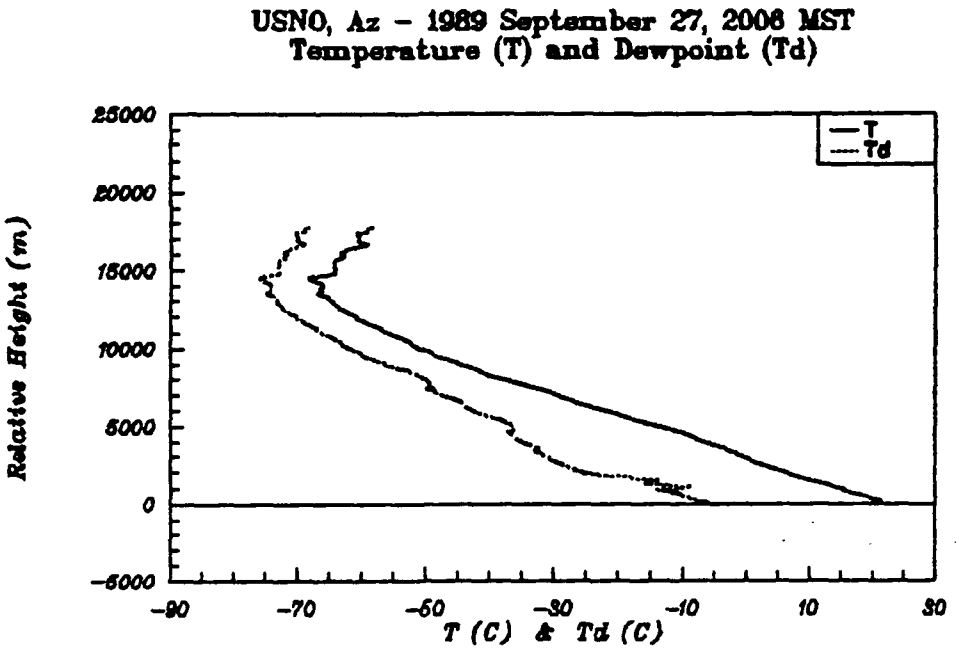

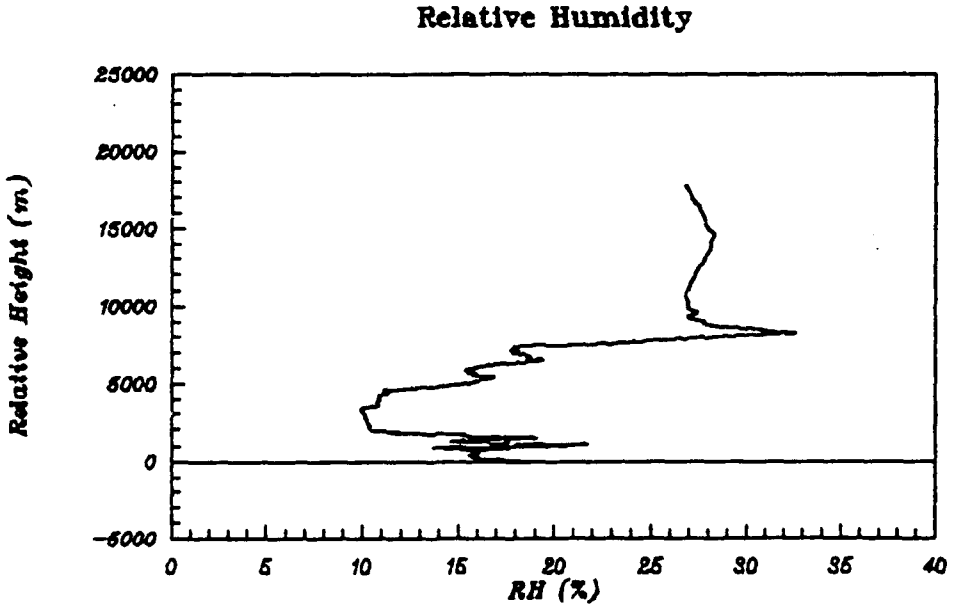

Fig 47. Entire Rawinsonde Profile: 1989 Sept 27, 2006 MST

APPENDIX H. RAWINSONDE THERMODYNAMIC PROFILES (First 3-KM Only)

Appendix H includes only the first three kilometers of each thermodynamic rawinsonde profile presented in Appendix G. Sites and dates are the same as in Appendix G. As before, all heights are with respect to local ground level.

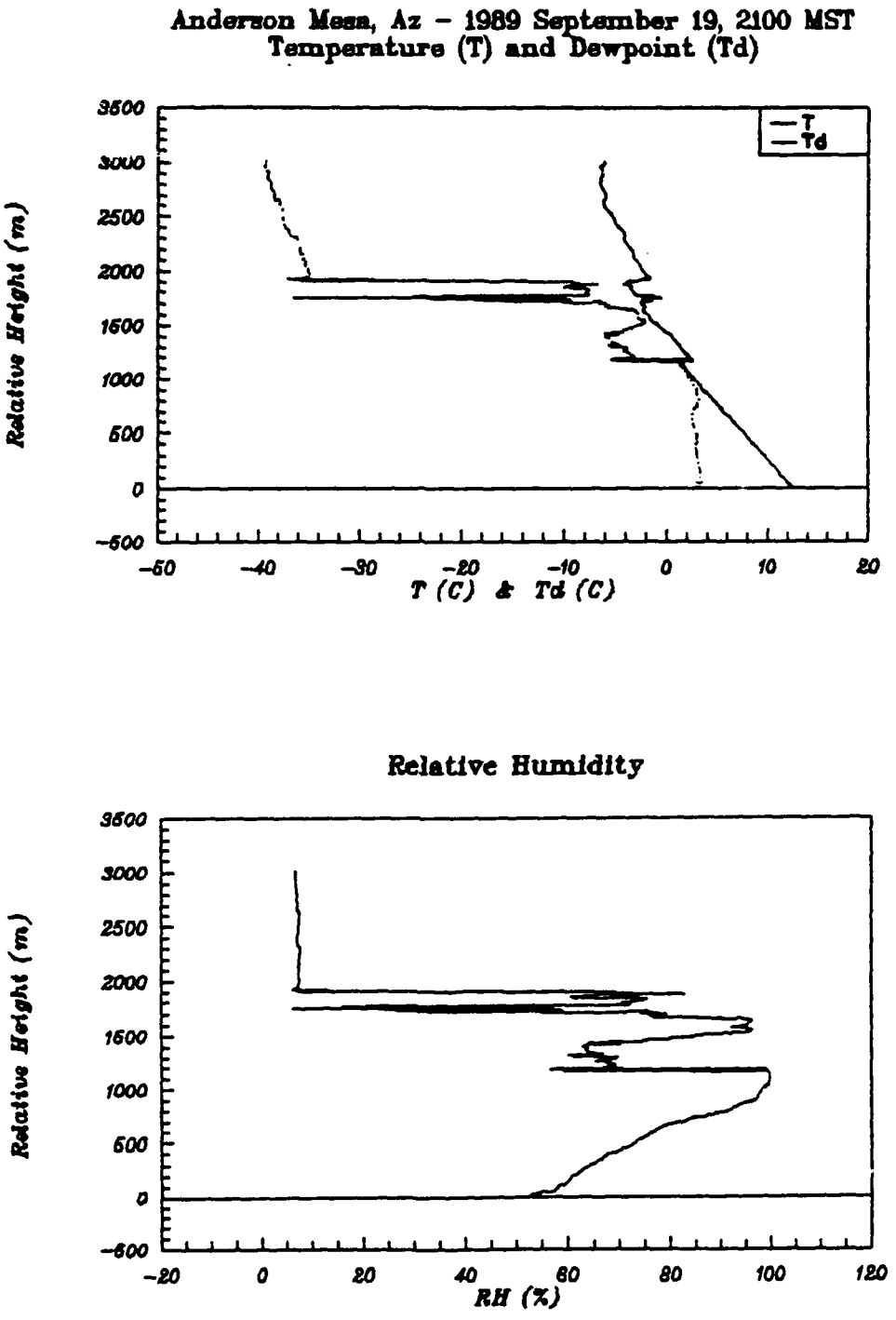

Fig 48. Rawinsonde Profile First 3-km: 89 Sept 19, 2100 MST

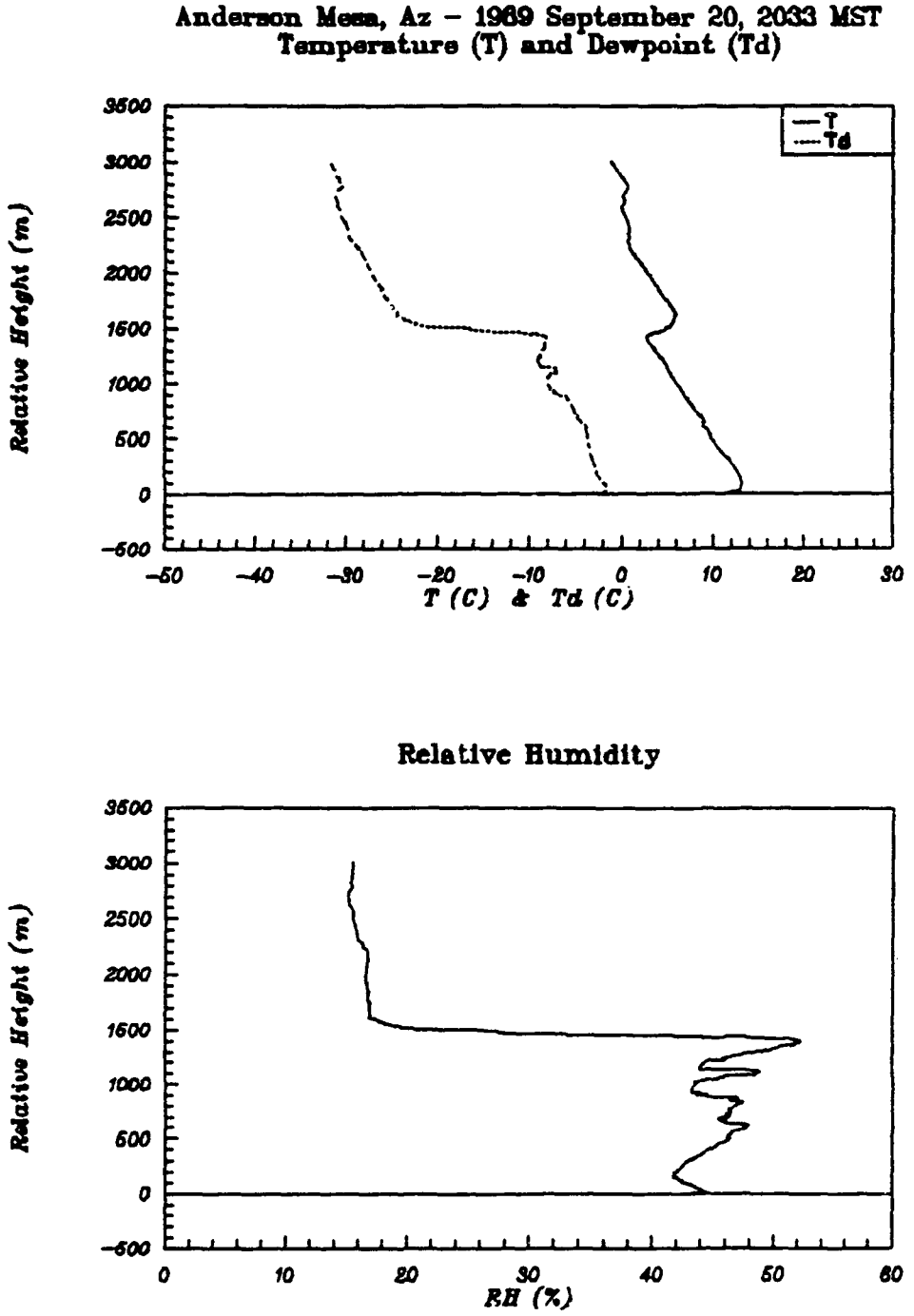

Fig 49. Rawinsonde Profile First 3-km: 89 Sept 20, 2033 MST

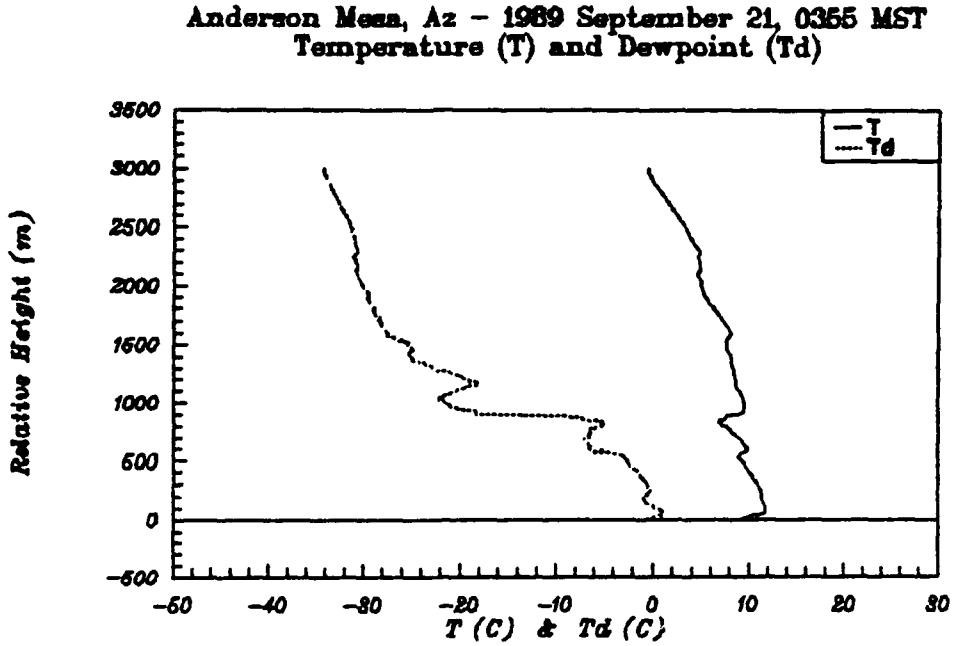

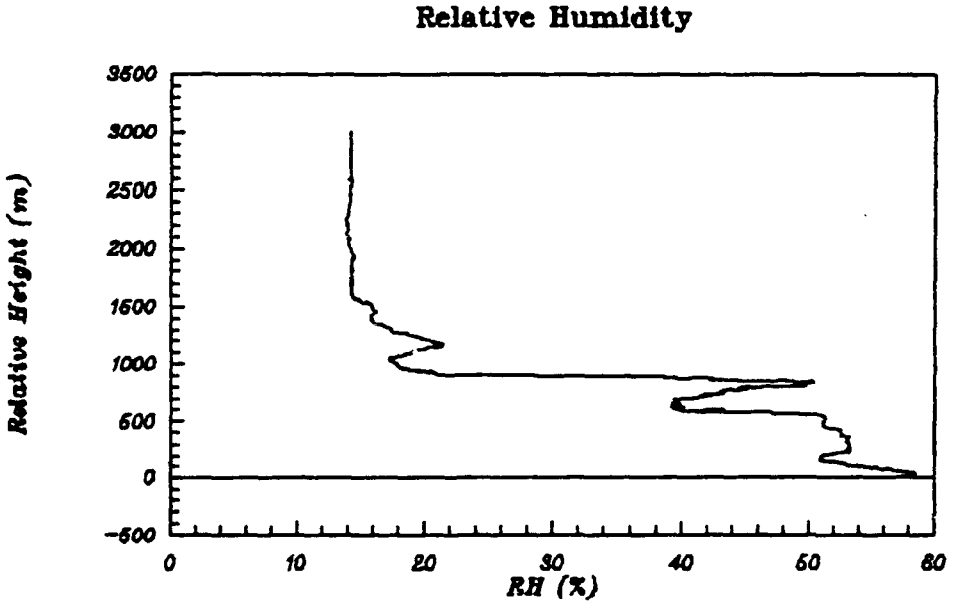

Fig 50. Rawinsonde Profile First 3-km: 89 Sept 21, 0355 MST

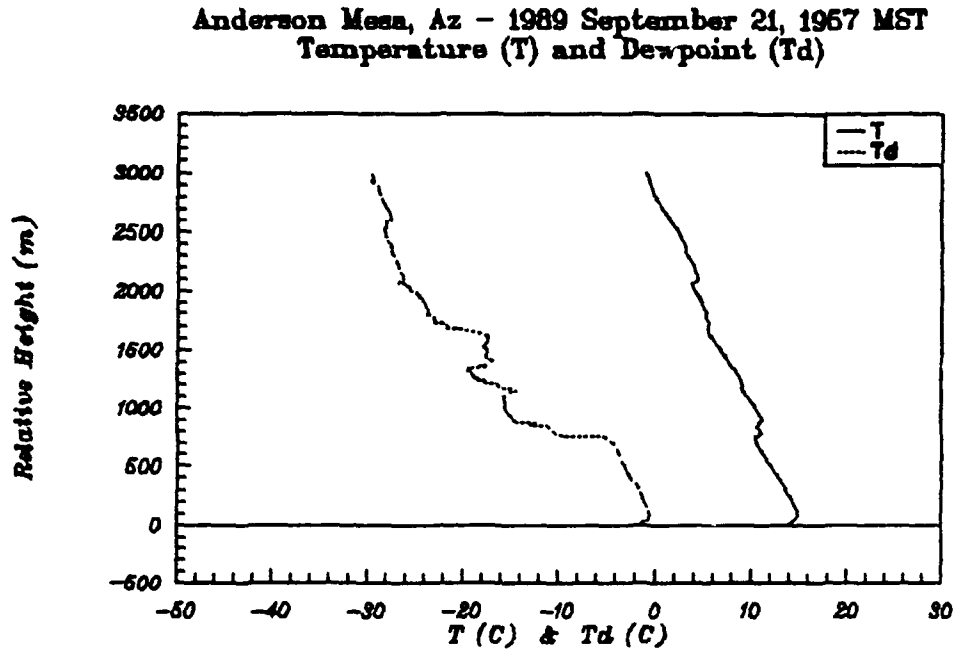

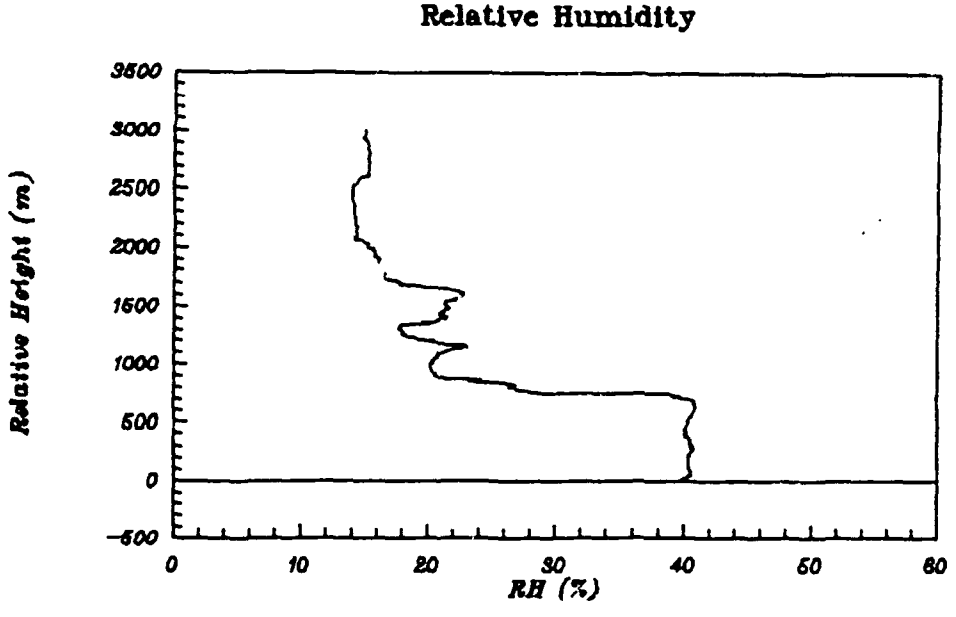

Fig 51. Rawinsonde Profile First 3-km: 89 Sept 21, 1957 MST

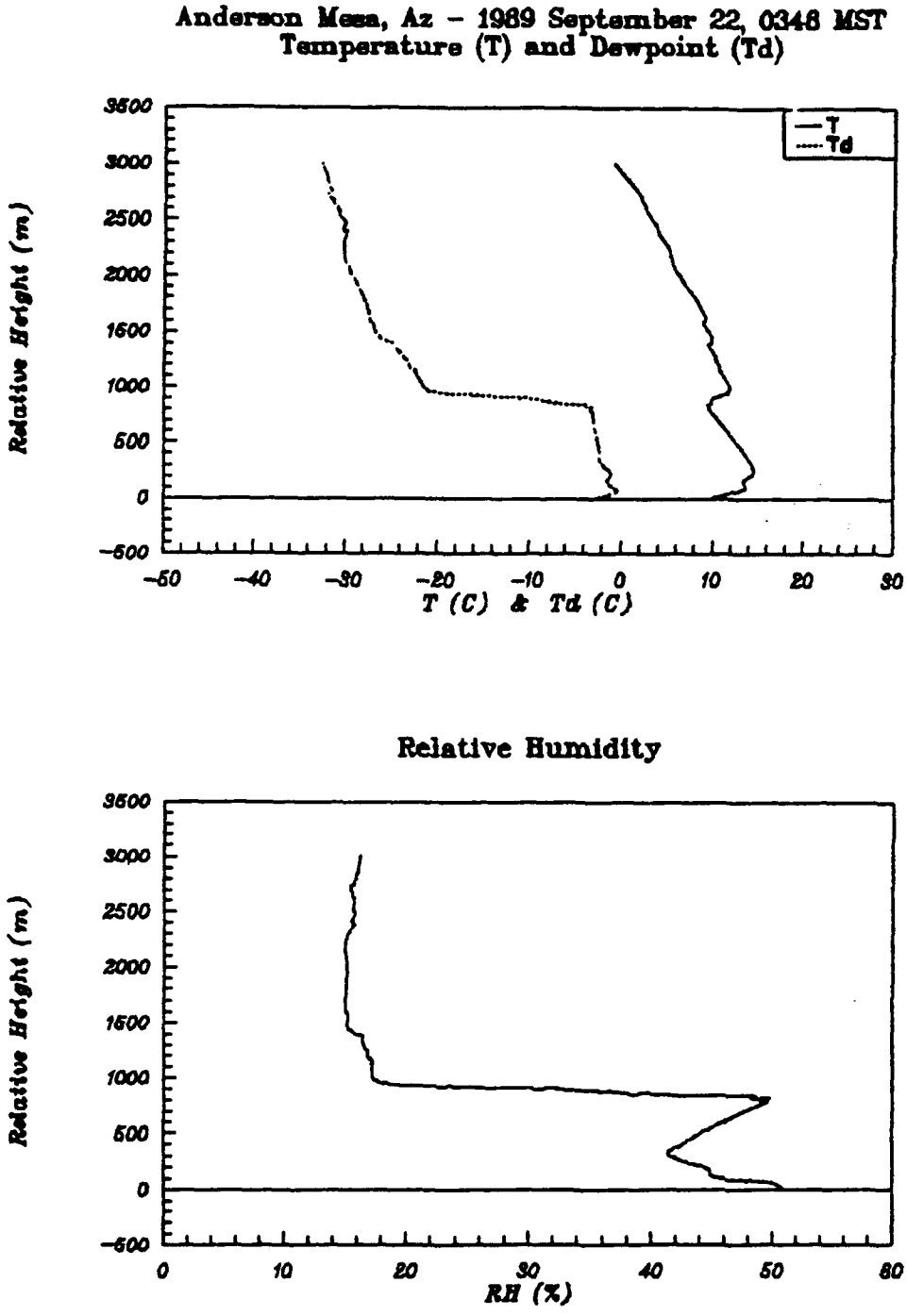

Fig 52. Rawinsonde Profile First 3-km: 89 Sept 22, 0348 MST

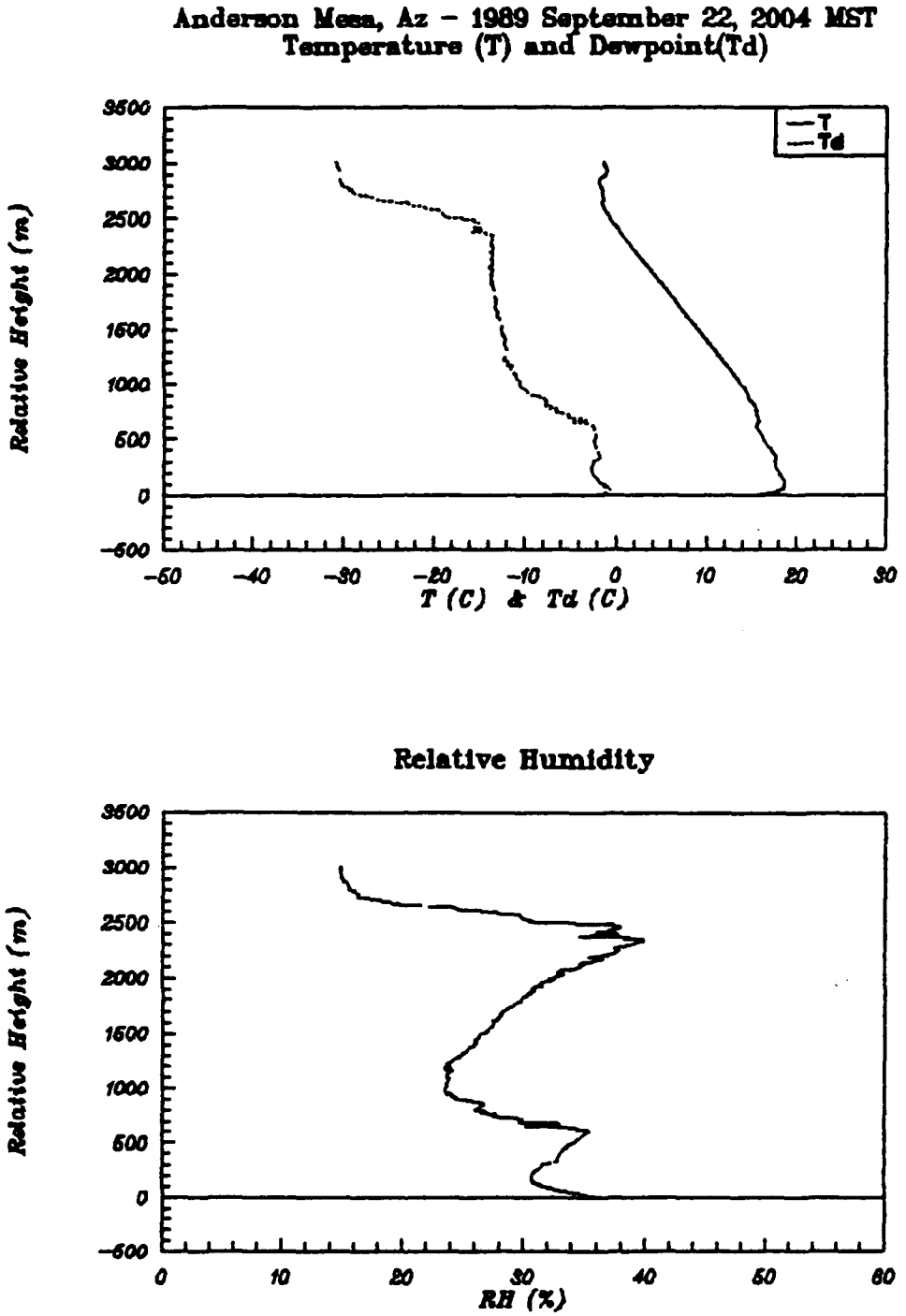

Fig 53. Rawinsonde Profile First 3-km: 89 Sept 22, 2004 MST

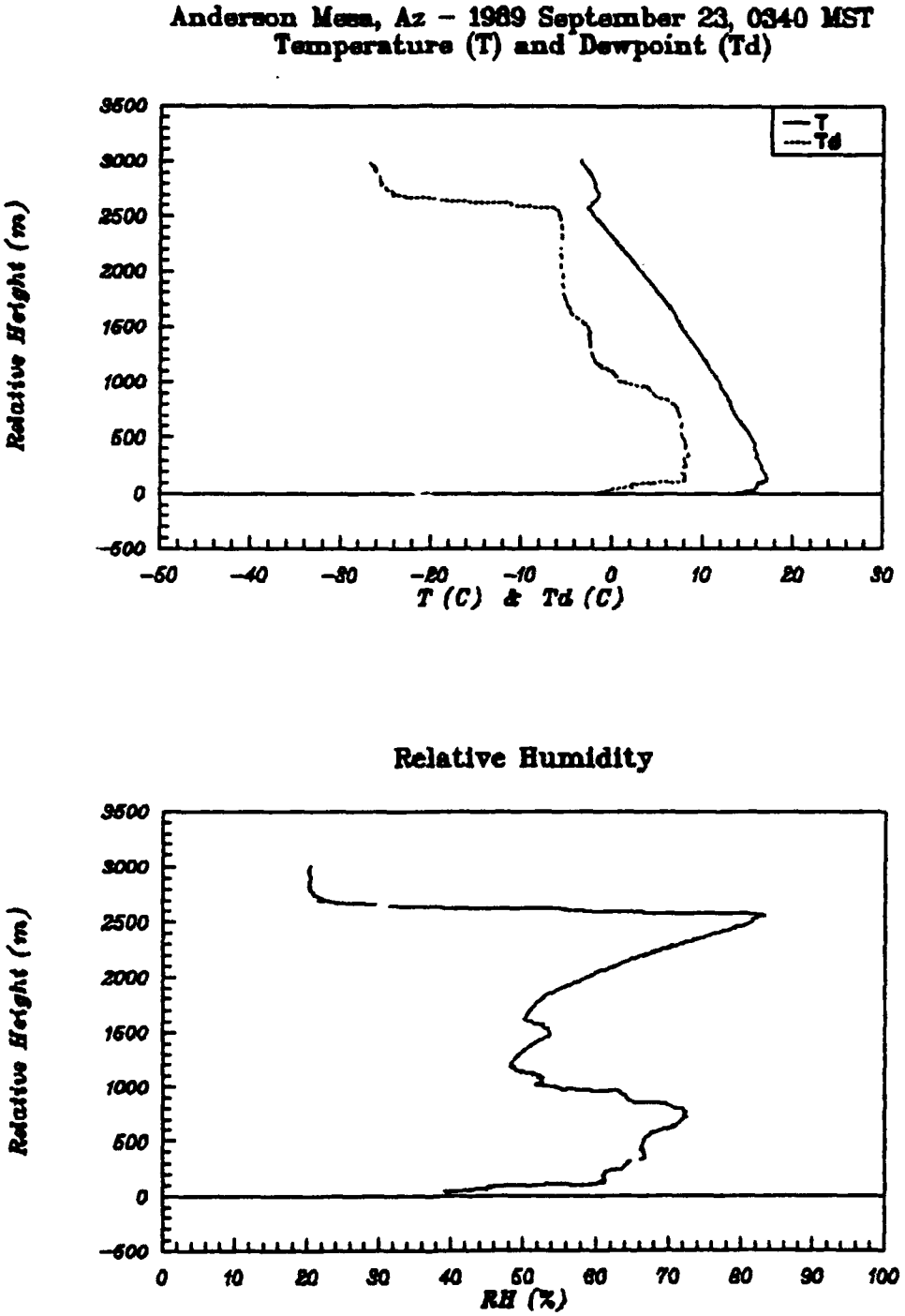

Fig 54. Rawinsonde Profile First 3-km: 89 Sept 23, 0340 MST

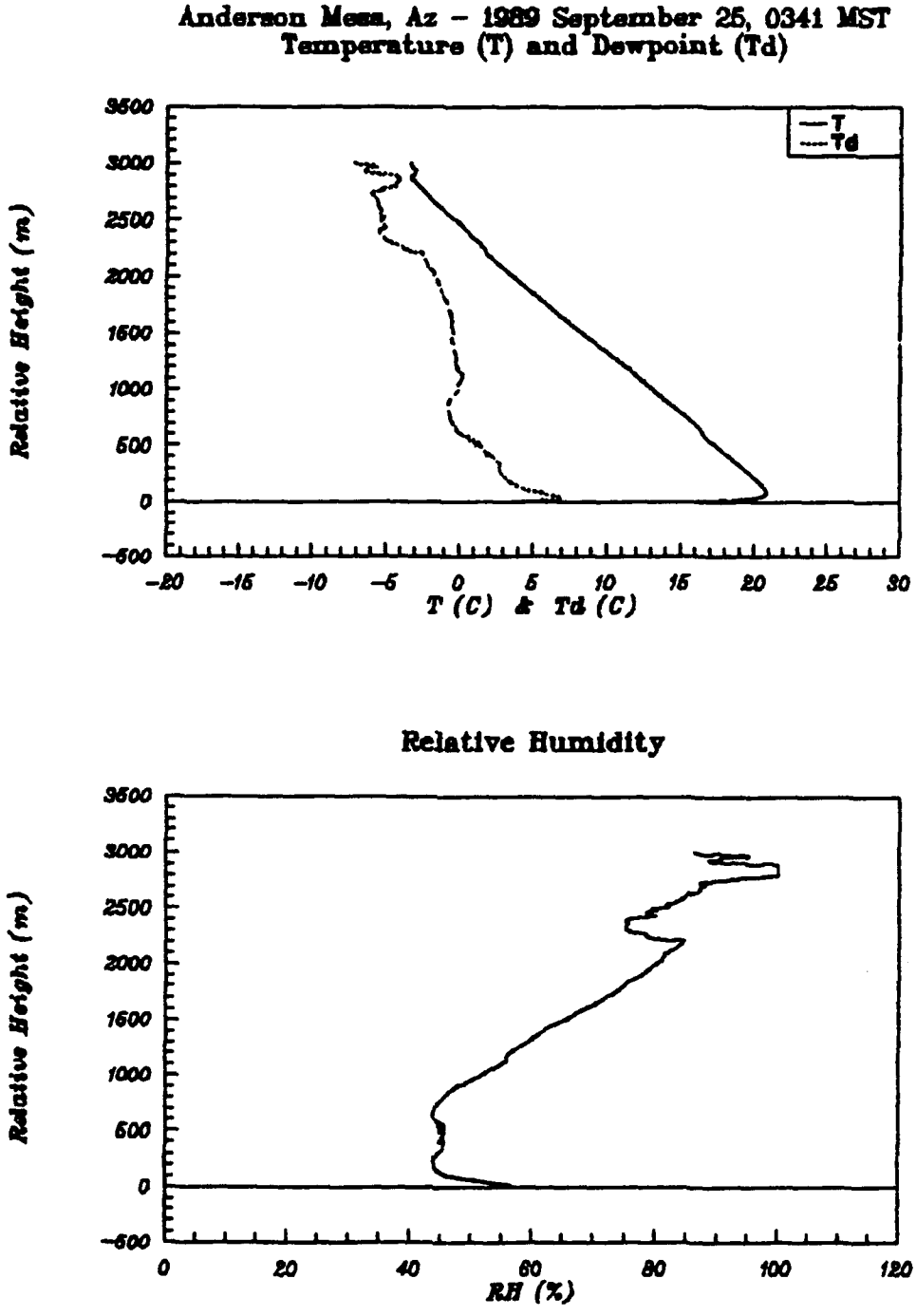

Fig 55. Rawinsonde Profile First 3-km: 89 Sept 25, 0341 MST

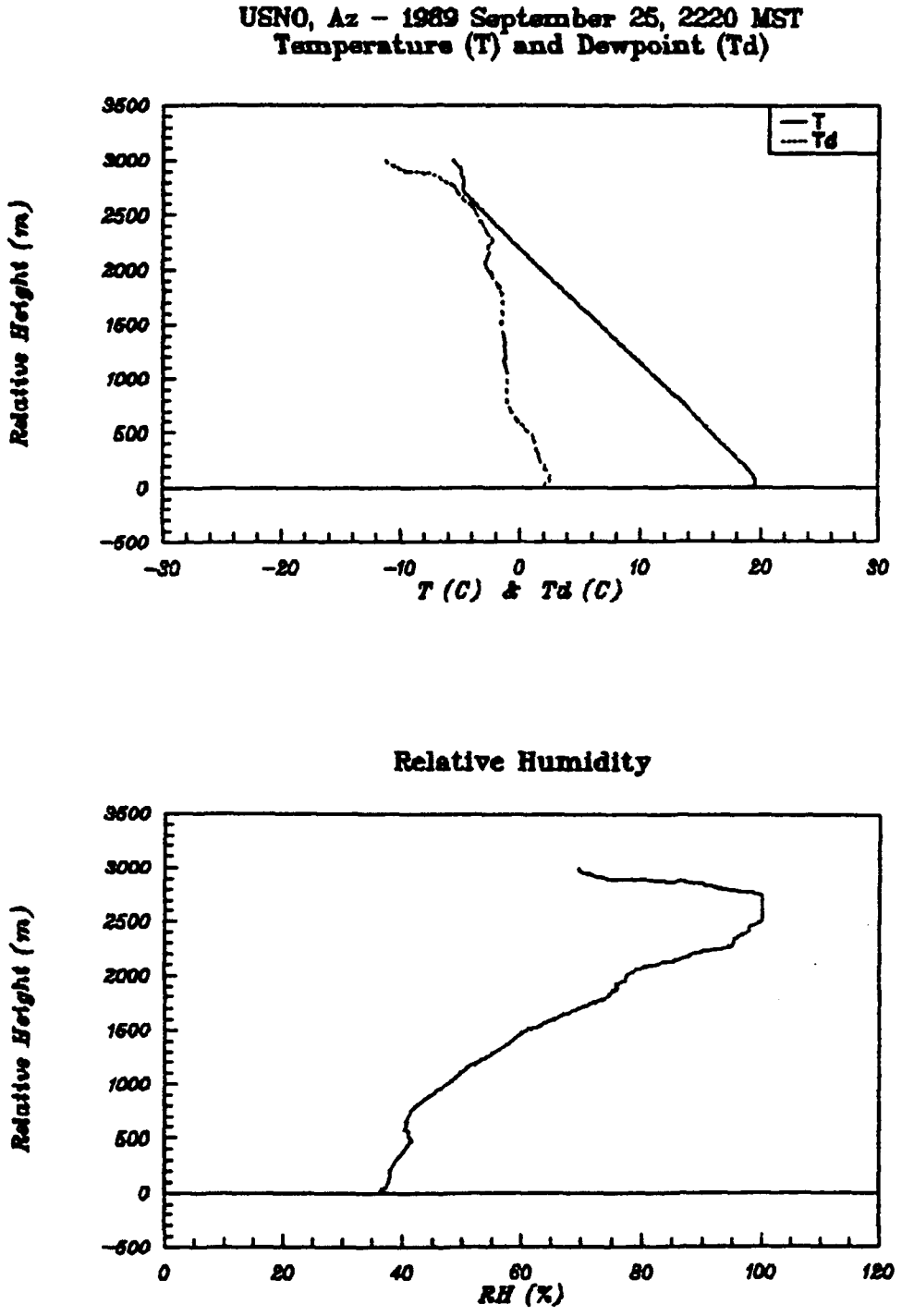

Fig 56. Rawinsonde Profile First 3-km: 89 Sept 25, 2220 MST

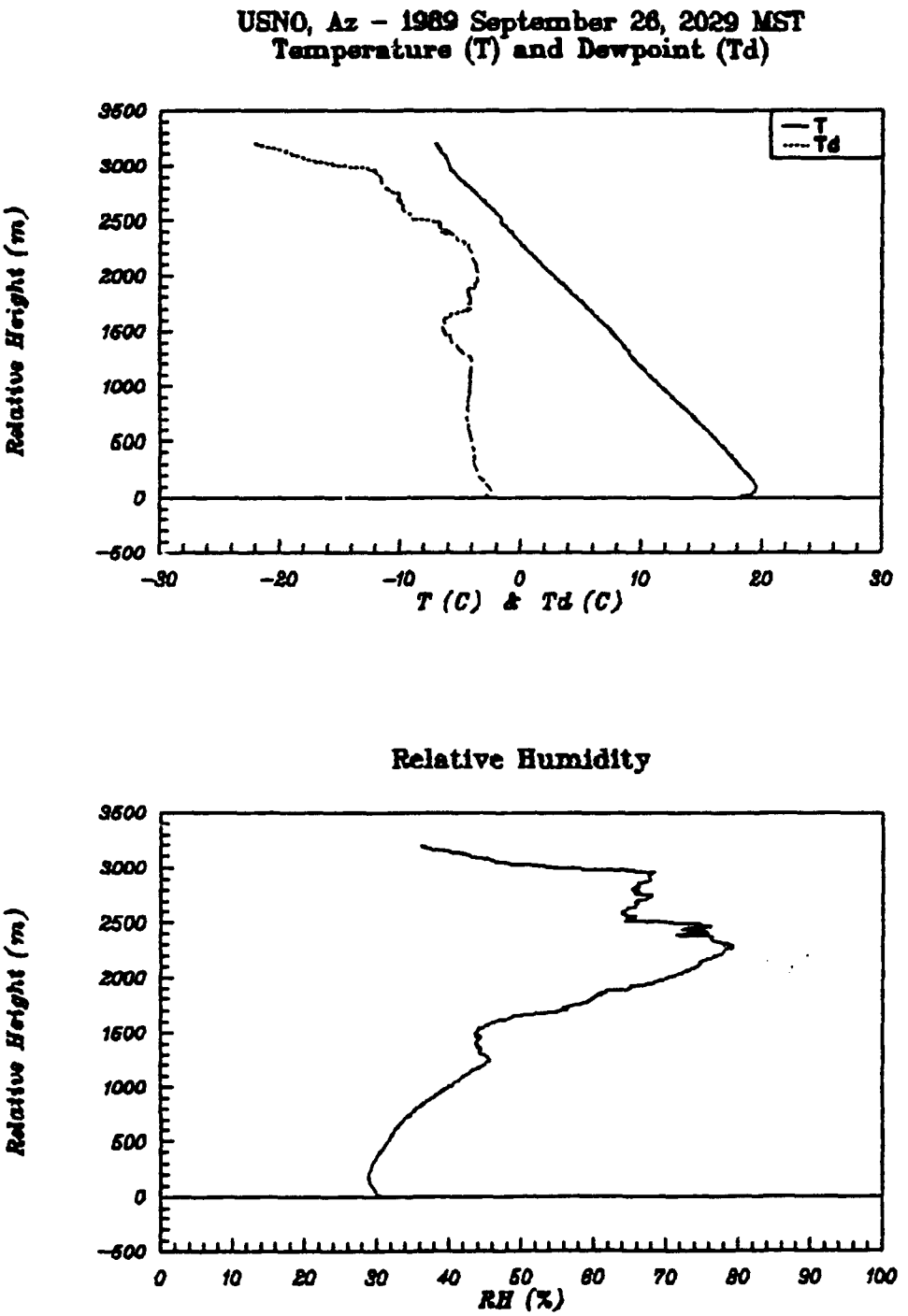

Fig 57. Rawinsonde Profile First 3-km: 89 Sept 26, 2029 MST

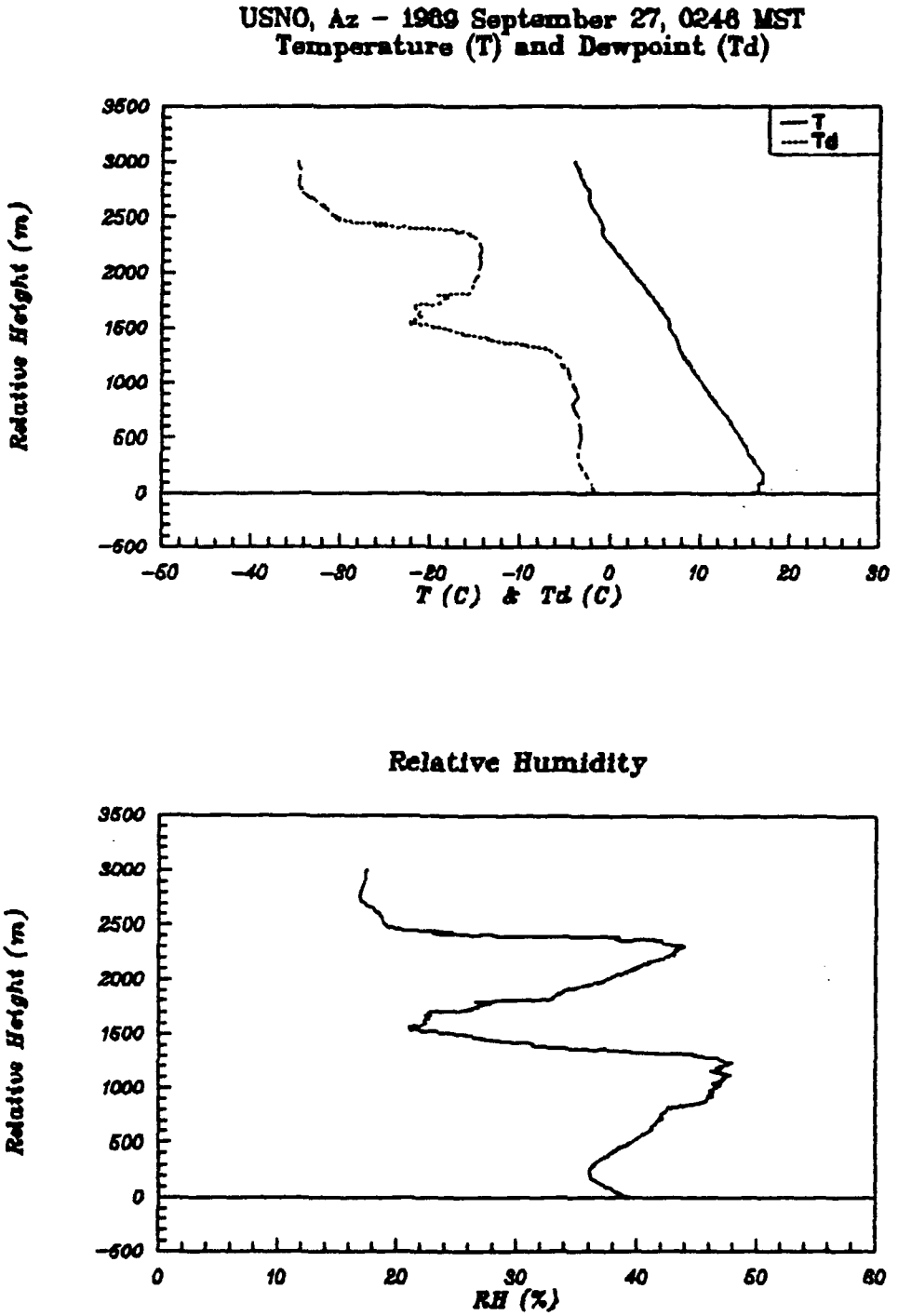

Fig 58. Rawinsonde Profile First 3-km: 89 Sept 27, 0246 MST

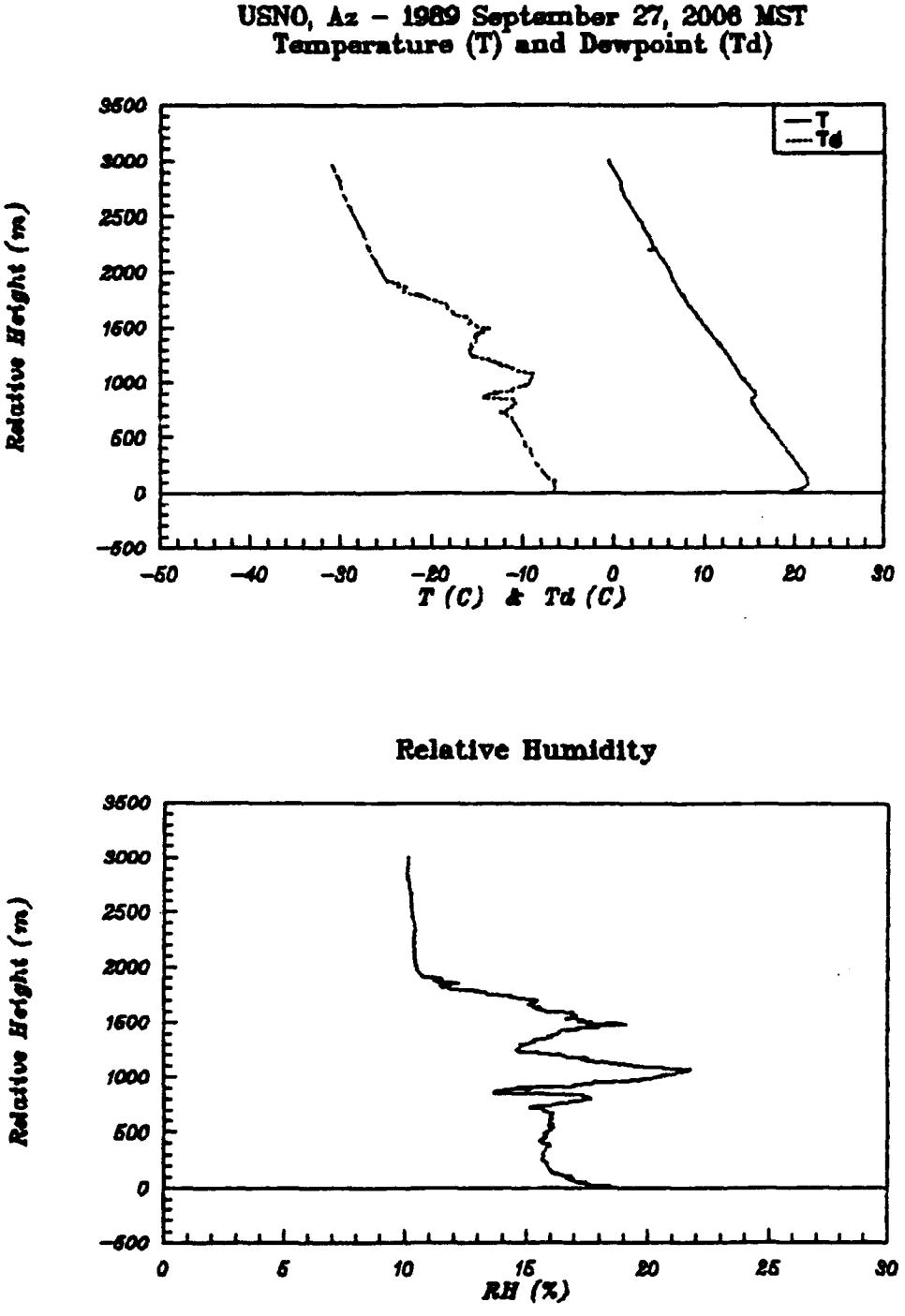

Fig 59. Rawinsonde Profile First 3-km: 89 Sept 27, 2006 MST

LIST OF REFERENCES

Bell, Scott, 1989: Private Communication (VIZ).

Stevens, K.B., 1985: Remote Measurement of the Atmospheric Isoplanatic Angle and Determination of Refractive Turbulence Profiles by Direct Inversion of the Scintillation Amplitude Covariance Function with Tikhonov Regularization, Ph.D. Dissertation, Naval Postgraduate School, Monterey, CA, 170 pp.

Vaucher, G. Tirrell, 1989: Correlation of Atmospheric Optical Turbulence and Meteorological Measurements, M.S., Naval Postgraduate School, Monterey, CA, 145 pp.

Walters, D.L., Favier, D.L., and Hines, J.R., 1979: Vertical Path Atmospheric MTF Measurements. J. Opt. Soc. Am., v. 69, 829.

WeatherMeasure WEATHERtronics, 1987: 1987-1988 Catalog, Geophysical Instruments and Systems, Division of QUALIMETRICS, INC., Sacramento, CA, 323 pp.

INITIAL DISTRIBUTION LIST

	No. Copies
Library, Code 0142 Naval Postgraduate School Monterey, CA 93943-5002	2
Gail Tirrell Vaucher, Code PH Department of Physics Naval Postgraduate School Monterey, CA 93943-5000	4
Christopher Vaucher, Code PH USRA Visiting Scientist Department of Physics Naval Postgraduate School Monterey, CA 93943-5000	4
Professor Donald L. Walters, Code PH/WE Naval Postgraduate School Monterey, CA 93943-5000	6
Dr. Ken Johnston, Code 4130 Naval Research Laboratory Washington, D.C. 20375	2
Lowell Observatory Attn: Dr. Bob Millis, Dr. Nat White Mars Hill Rd, 1400 West Flagstaff, AZ 86001	2
United States Naval Observatory Attn: Dr. Harold Ables, Dr. Jeff Pier P.O. Box 1149 Flagstaff, AZ 86002	2
Dr. Gart Westerhout, Scientific Director United States Naval Observatory 34 Massachusetts Ave, NW Washington, D.C. 20392	1

Dr. Frank Kerr 1
Universities Space Research Association
Mail Stop 610.3
Goddard Space Flight Center
Greenbelt, Maryland 20771

Ms. Nancy Alexander 1
Technical and Business Systems
859 Second St.
Santa Rosa, CA 95404

Research Administrative Dept, Code 012 1
Naval Postgraduate School
Monterey, CA 93943-5000

Library Acquisitions 1
National Center for Atmospheric Research
P.O. Box 3000
Boulder, CO 80307

Department of Physics, Code PH 1
Naval Postgraduate School
Monterey, CA 93943-5000